Chapter 4
Epithermal Deposits of Turkey

Tolga Oyman

Abstract In Europe and Middle East, Turkey is currently positioned as the largest producer of gold with a 2015 production of 27.5 t from predominantly porphyry and epithermal deposits. Although exploration for gold by advanced geochemical methods started in 1980s, Turkey entered into hard-rock mining based on cyanide process for extracting gold from low-grade ore in 2001. Before that, apart from placer mining, gold was sold in concentrate ore as by product in some deposits chiefly mined for base metals. Epithermal deposits are high-grade deposits dominated by open-space textures generally formed at depths of ~2 km with temperatures of < 400 °C. Due to their shallow-depth location, it is regarded that they represent easily mineable source of gold. This chapter is designed to focus attention on the geology of important epithermal gold mineralisation in Turkey with the aim to understand the basic regional and local geological setting and mineralogical and geochemical properties setting for the mineralisation. In the chapter the brief summary of selected epithermal deposits is emphasized the principal characteristics of important epithermal mineralisation all over Turkey including low, intermediate and high sulphidation types without taken into account their major economic element content on the base of reports from government and private companies and published or unpublished studies. Up to date, although literature on epithermal mineralisation in Turkey has been increasing with significant exploration and published data, still numerous questions remain unanswered and provide a source for future research.

4.1 Introduction

Mining in Anatolia dates back to nearly 3200 BC with the archaeological evidence showing that many of the epithermal deposits in western Anatolia and surroundings were exploited. The gold mining industry has a long history with its roots reaching ancient times in Anatolia, called also as Asia Minor. Around 550 BC, the first gold

T. Oyman (✉)
Department of Geological Engineering, Dokuz Eylül University, İzmir, Turkey
e-mail: tolga.oyman@deu.edu.tr

© Springer Nature Switzerland AG 2019

F. Pirajno et al. (eds.), *Mineral Resources of Turkey*, Modern Approaches in Solid Earth Sciences 16, https://doi.org/10.1007/978-3-030-02950-0_4

coin was minted in Salihli (West Anatolia) which had been known in antiquity as Sardis capital of Lydian Kingdom. Alacahöyük located at the junction of three trade routes: to Mesopotamia, to the Black Sea, and to the Aegean Sea was the most important civilisation in the production of gold artefacts in the Bronze age. Alacahöyük near the modern Turkish city Çorum (Central Anatolia), is regarded as the wealtiest city of pre-Hittite times. Due to its coarser gold grain size ranging up to visible gold and shallow emplacement, epithermal vein systems were the main targets for the Romans who had experienced mining methods from the different nations they had conquered and accumulated considerable experience which had been acquired in the course of centuries by many different ethnic groups. The Romans and their descendants mined on a large scale throughout Europe and Africa.

Gold is one of the most important items in Turkish economy both as investment instrument and raw material for the jewellery sector. As the world's fourth largest consumer of gold Turkey is in second place behind India in the production of gold jewellery. The Turkish gold mining industry is small when compared with giant gold producing countries but it is growing rapidly. Gold mining and extraction with cyanide-leach methods started in 2001 with the Ovacık gold mine by Newmont. Increasing gold production almost every year since 2001, growing from 2 tonnes to almost 35 tonnes in 2015 promotes Turkey as Europe's largest gold producer. More than 200 tonnes of gold were being produced between 2001 and 2014 and the Turkish Gold Miners Association estimates c.US$ 700 million has been spent on exploration by foreign companies in the past 25 years. Since a peak was reached in 2012–2013, the number of foreign companies with active exploration projects has decreased somewhat and this is partly due to the reduction of exploration budgets globally. Gold was produced as a by products or coproduct from base-metal and silver mines. Aegean, Black Sea and Central-East Anatolia are the leading gold-producing regions of Turkey. The scientific study on ore deposits in Turkey using modern methods of mineralogy and geochemistry started in the early 2000s. Most of these studies were focused on the deposits of Western Anatolia. In this chapter, on the basis of our studies and the cited published literature, we summarize and describe the principal geological, mineralogical and geochemical characteristics of selected epithermal deposits in Turkey.

The term "epithermal" was first defined by Lindgren (1933) according to the mineralogy, textures, alteration, and temperature and depth of ore formation. In the beginning of 1980s paragenesis based nomenclature has been started to identify the certain type epithermal deposit owing to its high sulphidation state sulphides and characteristic acid-sulphate alteration mineral assemblages (Ashley 1982; Bethke 1984; Bonham 1984, 1986; Berger 1986; Heald et al. 1987; Berger and Henley 1989). Between 1987 and 2003 epithermal deposits have been divided into two groups as high-sulphidation (acid-sulphate, quartz-alunite) and low-sulphidation (adularia-sericite) types, by different workers on the base of their position relative to the magmatic hydrothermal system which is responsible for the associated metal contents and hydrothermal alteration (Henley 1985; Heald et al. 1987; White and Hedenquist 1990; Cooke and Simmons 2000; Hedenquist et al. 1996, 2000). More recently on the base of tectonic setting and volcanic associations, the nature of fluids

involved and the mineral assemblages of epithermal deposits are subdivided into low (LSEM: Low Sulphidation Epithermal Mineralisation), intermediate (ISEM: Intermediate Sulphidation Epithermal Mineralisation), and high (HSEM: High Sulphidation Epithermal Mineralisation) sulphidation subtypes (Sillitoe and Hedenquist 2003). Intermediate sulphidation deposits correspond to "carbonate base metal deposits" of Corbett and Leach (1998). For this review, we use the widely accepted classification scheme of high-sulphidation low-sulphidation type deposits and intermediate sulphidation and the term "intermediate sulphidation" will be used to describe both sulphidation state and a separate sub-type for "carbonate base metal deposits" of Corbett and Leach (1998).

4.2 Tectonic Settings and Ages of Mineralisation

The Tethyan Orogenic Belt is one of the most complex tectonically active regions of the Earth's crust. Turkey encompasses several continental fragments of the super-continents, Gondwana and Laurasia which were sutured during the closing of the Tethyan oceanic basins during the late Paleozoic to Cenozoic period (Şengör and Yılmaz 1981; Şengör et al. 1984). The Izmir-Ankara-Erzincan suture (IAES) (Brinkmann 1966), representing by the closure of the northern branch of the Neo-Tethys along a northern-dipping subduction and the following continental collision between Laurasia and Gondwana during in the Late Cretaceous-Eocene is accepted as the main structure in the tectonic framework of Turkey (Ketin 1966; Okay and Tüysüz 1999). The IAES zone extending nearly 1500 km between Rhodope-Stranca in the west and Caucasus in the east separates the Sakarya Zone of Pontides (Laurasia) from the Anatolide-Tauride Platform (Gondwana) (Şengör and Yılmaz 1981; Okay et al. 1996).

In the West of Anatolia IAES separates the Sakarya Zone of Pontides from the Bornova Flysch and Afyon and Tavşanlı Zones which were derived from deeply buried northern edge of the Anatolide-Tauride Platform. In the east however, IAES zone represents northward subduction of the northern branch of the Neotethys beneath the southern margin of the Laurasia and continental collision between Eastern Taurides and Pontides. This subduction generated well-developed Cretaceous arc magmatism which is known as the Pontide arc. The Intra-Pontide Suture which is accepted as a small oceanic branch within the Neotethyan system separates the Istanbul and Sakarya fragments in northwest Turkey. Furthermore, the existence of another suture zone, Inner Tauride Suture, is still controversial. In many studies, this suture zone is placed between Central Anatolian Crystalline complex (CACC) which is accepted as an isolated microcontinent rifted from northern margin of Gondwana during the Triassic time and eastward continuation of the Afyon zone (Okay and Tüysüz 1999). This oceanic branch is assumed to have closed along northward subduction beneath the CACC during the Late Cretaceous (Pourteau et al. 2010).

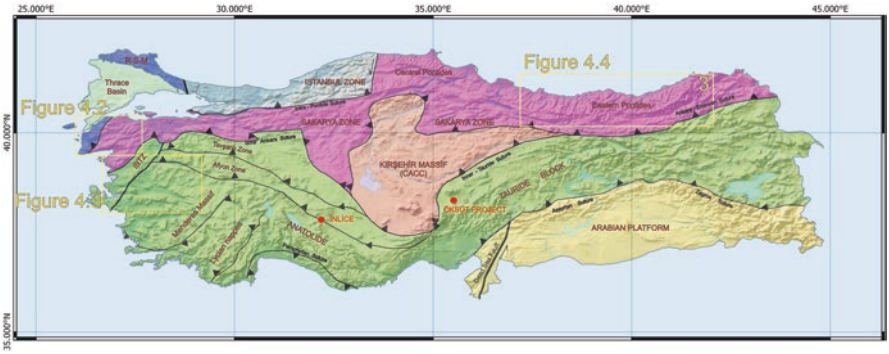

Fig. 4.1 Tectonic framework of Turkey showing the major sutures and continental blocks. (Modified after, Okay and Tüysüz 1999)

Within this tectonic framework epithermal gold deposits occur mainly in three regions: Western Anatolia, Central Anatolia and Eastern Black Sea. These regions are separated from each other with distinct geodynamic evolution and associated magma generations with different geochemical character reflecting spatial and temporal variations (Fig. 4.1).

4.3 Distribution and Geological Features of Epithermal Deposits of Turkey

4.3.1 Western Anatolia Volcanic and Extensional Province (WAVEP) in Western Turkey

The province consists of several NE-trending structural domes composed of metamorphosed Palaeozoic and Mesozoic rocks, volcanic piles and intrusive complexes, and intervening east to northeast trending extensional basins filled with Paleogene and younger volcanoclastic sequences (Fig. 4.2). WAVEP hosts metallogenic province in the Biga Peninsula (NW Anatolia-Turkey) covering an area both in the Sakarya block and a slice of Rhodope Massif. Pre-Jurassic basement rocks, including the Kazdağ metamorphic core complex and numerous exhumed igneous bodies with coeval volcanic rocks (e.g. Okay et al. 1991; Bonev and Beccaletto 2007; Cavazza et al. 2009) can be found throughout the Sakarya block. Northward subduction of northern branch of Neo-Tethyan Ocean initiated the magmatism in the Biga Peninsula during the Late Cretaceous to Eocene. The Late Eocene-Early Oligocene ages (e.g. Kozak and Eybek plutons) may record the subduction related magmatism and the initiation of continental collision. Magma generation during Late Oligocene and Early Miocene is strongly associated with astenospheric uplift in an extended continental crust due to the slab roll-back and/or break-off the

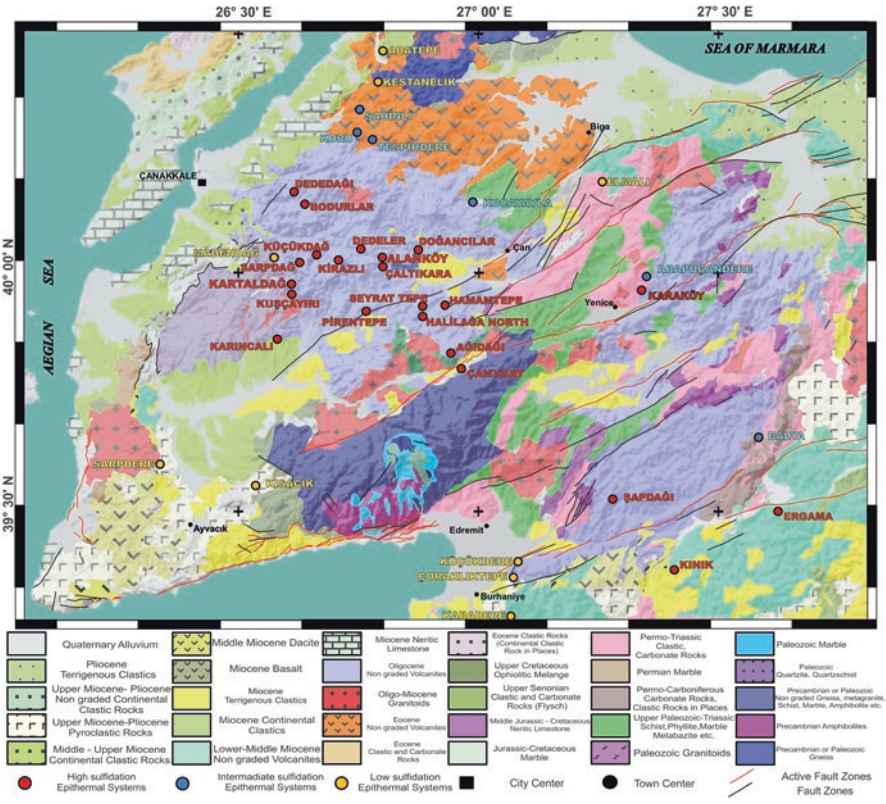

Fig. 4.2 Regional geological map of Biga Peninsula and spatial distribution of significant epithermal mineralisation. (Geology modified from MTA Emre et al. 2013; Akbaş et al. 2017)

subducted slabs (Altunkaynak et al. 2012, Black et al. 2013; Aysal 2015). Recent Sr and Nd isotope results from plutons North of Yenice (Çanakkale) indicate that intrusions were generated by magmatic assimilation and fractional crystallization and formed during large-scale lithospheric thinning during the Late Oligocene (Çiçek et al. 2017).

In Biga Peninsula, world class epithermal gold deposits and prospects are mainly hosted and spatially associated with Cenozoic volcanic rocks (Pirajno 2009). The Cenozoic volcanic rock associations in Biga Peninsula can be divided into three main groups based on their geochemical features and ages. The Eocene volcanic rocks, known as Balıklıçeşme volcanics in the Biga Peninsula, include andesitic and basaltic lavas with medium- to high-K in character which are interlayered with shallow marine sedimentary rocks towards the upper part of the volcanic sequence (Ercan et al. 1995; Altunkaynak et al. 2012; Gülmez et al. 2013). The K-Ar dating of these volcanic rocks yields 52–34 Ma (Dönmez et al. 2005; Kürkçüoğlu et al. 2008; Gülmez et al. 2013). Widespread high-K calc-alkaline volcanism took place during the Late Oligocene to Early Miocene and comprise andesite, dacite and

trachyandesite with large amounts of dacitic-rhyolitic ignimbrite, pyroclastic and tuffaceous rocks (Ercan et al. 1995; Chakrabarti et al. 2012). The Oligocene-Miocene volcanic associations comprise the Oligocene Çan volcanics (34.3 ± 1.2 and 29.2 ± 0.6 Ma), Kirazlı volcanics (31.1 ± 0.7 and 27.6 ± 0.6 Ma) and Early-Middle Miocene Behram volcanics (21.5–6.8 Ma) in the Biga Peninsula (Ercan et al. 1995). Continuation of Cenozoic volcanic activity to the late Miocene is represented by Na-alkaline volcanism including basaltic-trachyandesitic lavas and dykes. They are known as Ezine volcanics in northern Anatolia and yield an Upper Miocene age ranging from 11.68 ± 0.25 to 6.47 ± 0.47 Ma (Ercan et al. 1995; Aldanmaz 2002). In the North and around Kozak Pluton the volcanic association comprises lavas and pyroclastic rocks of nearly equal proportions. The compositions range from dacite-rhyolite to basaltic andesites (Altunkaynak and Yılmaz 1998). In the south Dikili group is Early-Middle Miocene in age and consists mainly of pyroclastic rocks, andesitic-dacitic lavas, lava breccia, lahar flows and associated sedimentary rocks. The Çandarlı group consists of Upper Miocene-Pliocene lavas and sediments. The volcanic rocks consist mainly of rhyolitic domes and basaltic trachyandesite-basaltic andesite lavas erupted along the NW–SE and NE–SW trending fault systems; the faults controlled the development of the Çandarlı depression (Karacık et al. 2007).

4.3.2 Epithermal Systems In Biga Peninsula

The Biga Peninsula located in northwestern Anatolia, represents one of the important Turkish metallogenic province, which has been divided into several tectonic zones separated by suture zones. This area is one of the most widely recognised metallogenic provinces in terms of precious and base metal potential in the world due to the diversity in metallogeny and abundance of mineral occurrences with >50 hydrothermal Pb-Zn-Cu ± Ag ± Au and Au-Ag deposits (e.g., Koru, Tesbihdere, Balya, Arapuçandere, Kalkım-Handeresi, Küçükdere) and ongoing projects (e.g., Şahinli, Kartaldağ, Kestanelik, Çataltepe, Kirazlı, Ağı Dağı, TV Tower), (Fig. 4.2). Until the early 2000s the importance of this metallogenic province had not been fully understood, but has since emerged in the spotlight of geological studies with modern analytical techniques (Bozkaya and Gökçe 2001, 2009; Bozkaya 2009; Yılmaz et al. 2010; Yalçınkaya 2010; Çiçek et al. 2012; Yiğit 2012; Çiçek 2013; Bozkaya et al. 2014; Çiçek and Oyman 2016). Among the most essential and debatable problems regarding the genesis of the base metal ± silver ± gold and gold ± silver deposits in Biga Peninsula can be given as the origin of the fluids, spatial and temporal relationship between volcanism and ore-forming hydrothermal activity.

4.3.2.1 TV Tower

The TV Tower prospect is located in the central part of Biga Peninsula. The basement rocks of the TV Tower property is composed of metamorphic basement rocks of Paleozoic and Early Mesozoic mainly including various schists and phyllite. The basement is intruded by the Eocene (~43 Ma) calc-alkali Kuşçayırı pluton composed of feldspar-hornblende-biotite porphyritic monzonite (Yiğit 2012) at the southern end of the property. Both basement and intrusive rocks are overlain by a thick pile of volcanic rocks including rhyodacitic to basaltic-andesite lavas. The volcanic rocks are overlain by crystal lapilli tuffs and sedimentary rocks with a wide grain size spectrum from mud to conglomerates. The property covers an area of 67 km^2 and contains nine targets including Küçükdağ, Kayalı/Nacak, Karaayı/K2, Sarp/Columbaz, Valley, Kestanecik, Gümüşlük, Tesbihçukuru and Kartaldağ West. Küçükdağ target that is hosting the third largest silver resources in Turkey, is characterized characterised by a high sulphidation gold-pyrite-enargite assemblage and associated silicification and advanced argillic alteration. Many of the targets, except Gümüşlük and Kestanecik which are low-sulphidation epithermal gold targets, are characterised by high-sulphidation ore assemblages in TV Tower property. These targets are in association with lithocaps which are spatially, temporarily and genetically linked to shallow seated mineralised porphyritic intrusions.

The Küçükdağ target is one of the most important project among nine target areas in TV Tower property (Fig. 4.2). Tuff and volcaniclastic rocks are ideal hosts for structure controlled mineralisation due to their high permeability in Küçükdağ. Gold is predominantly found in the permeable lithic lapilli tuffs and epiclastic rocks with lesser amounts in andesitic breccias and welded lithic lapilli tuff. Copper is mainly associated with Au in the sedimentary sequence and volcaniclastic rocks respectively. In the upper oxide zone gold mineralisation is associated with massive to weakly vuggy quartz alteration with hematitic breccias, WNW- and NS-striking shears, and fracture infills in rhyodacitic crystal and lapilli tuff (Smith et al. 2014). The lower gold zone is largely hosted in dacitic tuff with different subtypes of ore formation styles that can be divided into three subzones including (a) Stratiform gold in zones of dark grey to black vuggy quartz (b) ESE-WNW trending gold-sulphide veins with varying amounts of quartz, (c) Au-Ag breccia (Smith et al. 2014). The silver-rich zone is primarily hosted in the fluvial-lacustrine sequence and overlying andesitic breccia and gold-copper mineralisation. Characteristic sulphide minerals and sulphosalts of high-sulphidation systems represented by enargite which is precipitated in veins and breccia zones. Tetrahedrite-tennantite, famatinite, bournonite, seligmannite, pyrite, marcasite, chalcopyrite, covellite are the main sulphide and sulphosalt minerals (Ross 2013a, b). While principal sulphide minerals associated with pyrite-marcasite which are banded and very fine grained along main silver mineralisation. Alunite, barite, dickite and kaolinite are widespread clay minerals associated with ore in veins and breccia zones.

4.3.2.2 Ağı Dağı

Similar to worldwide HSEM hosted volcanic sequences, the Ağı Dağı deposit formed in the Oligo-Miocene volcanic suite composed of andesitic, dacitic and rhyolitic rocks. Igneous rocks of intermediate composition formed either as porphyritic intrusions or porphyritic andesite lavas at the bottom of the sequence, whereas the dacite-rhyolite facies are located at the top. The entire volcanic sequence is cut by mushroom shape pipes of phreatic and phreatomagmatic breccias. Although gold mineralisation is present in five zones including the Baba, Ayı Tepe, Fire Tower, Ihlamur and Deli Zones, resources will only be exploited at Baba, Deli and Fire Tower zones. The Ağı Dağ north-east trending silica cap and associated alteration occupies a discontinuous zone of 4 × 2 km extent characterised by a massive vuggy silica core. The Baba, Fire Tower and Deli zones occur along the east side of the NE-SW trending mountain ridge, characterised by silicified dacite and phreatic breccia that fills a paleo-basin in dacite and feldspar porphyritic andesite. Alteration assemblages including massive silica, vuggy silica, advanced-argillic, argillic, propylitic, and sericitic facies indicate the role of hot acidic fluid and vapour phases associated with a deeper intrusion related hydrothermal system. As a result of leaching by the hot acidic fluid and vapour phases both vuggy and massive silica formed in the core of the high sulphidation system. The gold is associated mainly with pyrite in the intense silicic alteration comprising both massive and vuggy silica.

Çamyurt is located about 3.5 km southeast of Ağı Dağı. It is a silica ridge lying along 1.5 km at NE-SW direction. Main lithological unit at Çamyurt is andesite which is locally cut by phreatic breccia. Dacite is shown only at northern area. Gold mineralisation is mostly in andesite which is covering the largest part of the area and less in phreatic breccia. The main alteration trend is NE to SW along the main structure trend. Silica alteration, advanced argillic, argillic and propylitic alterations are the main alteration types at Çamyurt. Gold mineralisation is associated with silica alteration which has NE-SW trend along the main structure. Çamyurt has a higher contained Au grade than both Kirazlı and the Ağı Dağı deposits.

4.3.2.3 Kirazlı

Kirazlı is situated 25 km to the northwest of Ağı Dağı mineralisation and 10 km east of TV Tower property (Fig. 4.2). Çamlıca Metamorphics of Lower-Middle Triassic Karakaya Complex are exposed as basement rocks. Various schists and ultramafic rocks of Çamlıca Metamorphics are overlain by andesitic tuffs of Oligocene Çan Volcanics. Mineralisation consists of gold-silver-copper bearing veins and veinlets, hydrothermal breccia, phreatic and phreatomagmatic breccias hosted in dacitic-andesitic volcanic rocks. The sequence is cut by gold-hosted heterolithic, phreatic and phreatomagmatic breccias that were emplaced as mushroom-shaped pipes. The root zones of mushroom-shaped breccia pipes were intersected at a vertical depth of 400 m. Multistage generation of silicification is represented by grey massive and vuggy silica, chalcedonic to opaline silica, grey quartz with a high pyrite content

and fracture-filling crystalline silica is the most prominent alteration type with advanced argillic alteration. Silica ledges and their sub-vertical roots are surrounded by advanced argillic alteration. Degassing of hot acidic magmatic vapour prompted intense leaching of volcanic rocks to form vuggy quartz texture of the silica ledges and the associated advanced argillic alteration around it. Vuggy silica derived as a residual product of acid leaching which is characteristic texture of silicification with massive and sugary silica. Hydrothermal breccia with vuggy silica, advanced argillic and silicic alterations are the prominent alteration facies in association with high grades of gold and silver. In advanced argillic alteration the main minerals in association with silica are alunite, dickite and pyrophyllite. Well developed, multiphase silicification is the most common and widespread alteration in association with phreatic and hydrothermal breccias. Earlier argillic and later advanced argillic alterations formed around the margins of phreatic breccia pipes due to induced secondary porosity and permeability. Propylitic alteration which has been intersected in deeper levels seems earlier than the argillic alteration. Based on spatial and temporal relationship with breccia pipes, sulphide and gangue paragenesis, alteration assemblages this mineralisation is classified as high-sulphidation epithermal gold deposit (Alamosgold company report 2012).

4.3.2.4 Kartaldağ

The Kartaldağ gold mine is located 55 km southwest of Çanakkale. The Kartaldağ gold mine as similar to many epithermal deposits, the gold in Kartaldağ has been exploited since ancient times. Kartaldağ property was subjected to an exploration program including trenching, tunnelling and drilling by MTA during 1960–1962. The mine was reopened by Çanakkale Mining Co. in the late 1980s. The Kartaldağ epithermal vein system is hosted by Middle Miocene dacite porphyry which is the volcanic equivalent of granodioritic intrusions in the area. Kartaldağ fault is the most prominent structure in the area which acts as a conduit for the ore-forming hydrothermal fluids. In the early phase of silicification, vuggy quartz is accompanied by massive silicification. Vuggy texture formed due to leaching of the phenocrysts (e.g., plagioclase and hornblende) of the host dacitic volcanic rocks by acidic hydrothermal fluids. The Au mineralisation is in association with intensive pinkish coloured hypogene quartz-alunite and vuggy quartz assemblages. The late phase of silicification is represented by coarse to medium grained, banded, comb, sometimes colloform, and generally zoned quartz crystals truncating early phase massive silicification. Leaching of the host volcanic rocks was followed by the development of argillic alteration dominated by quartz-alunite-pyrophyllite and quartz-kaolinite from core to rim. Quartz-kaolinite alteration is the most widespread type of alteration, enveloping the quartz-alunite-pyrophyllite±kaolinite assemblage extending to the NW. Chlorite/smectite–illite±kaolinite form the propylitic alteration zone.

The spatial association of the alteration and ore minerals, dominated by pyrophyllite, kaolinite, and alunite, vuggy quartz texture, enargite, and covellite, pyrite, and light coloured sphalerite (indicating high Fe^{3+}/Fe^{2+}) support the formation of the

Kartaldağ epithermal gold mineralisation under the control of low pH-oxidising fluid typical of high sulphidation type epithermal deposits (Ünal-İmer et al. 2013; Einaudi et al. 2003; Sillitoe and Hedenquist 2003). Although homogenisation temperatures from vein quartz are distributed in a wide range, they are scattered mainly between two intervals; 190–290 °C and 300–370 °C (Vural 2006). Vural (2006) ascertained that the quartz crystallisation in association with gold precipitation started to occur at 370 °C and it lasts till about 190 °C. Based on fluid inclusion studies of quartz samples, primary fluid inclusions from late quartz exhibit with relatively low homogenisation temperatures (245–285 °C) and low salinities (<1.7 wt.% NaCl eq.) indicating that a significant amount of meteoric water interacted with the hydrothermal system. The formation of pyrophyllite, kaolinite, alunite-bearing alterations and pyrite alteration and vuggy quartz were generated by leaching under oxidising conditions. Enargite also formed in relatively oxidising conditions. Combined petrographic and geochemical studies suggest that, gold mineralisation at/below the boiling level might have occurred at temperatures greater than 285 °C. The Kartaldağ epithermal gold mineralisation was formed under low pH-oxidising fluids typical of high-sulphidation type epithermal deposits (Ünal-İmer et al. 2013).

4.3.2.5 Madendağ

The Madendağ gold deposit is located nearly 20 km northwest of the Kartaldağ mine and 50 km southwest of Çanakkale (Fig. 4.2). Mining in this deposit was first recorded in the beginning of the last century. An exploration program including trenching, tunnelling and drilling was conducted by MTA during 1960–1962. The deposit is hosted by quartz-mica schists of Paleozoic Çamlıca formation, (Okay et al. 1991) which is overlain and intruded by Middle Miocene to Late Oligocene volcanic rocks including andesite and dacite flows and domes. The Çamlıca formation comprises mainly of quartz-mica schists and calc-mica schists. Both mica schists and dacitic, andesitic volcanic rocks display widespread argillic alteration. The main mineralisation is hosted in the two main silicified structures trending E-W to WNW-ESE and almost parallel to each other with southward dip. In the vein zone multi-stages of ore deposition including network of quartz veins, brecciation and intensive alteration are observed.

Detailed studies by Ünal (2010) and Ünal-İmer et al. (2013) reveal that mineralogy of argillic alteration around mineralisation in Madendağ is controlled both by host rock composition and the distance from the quartz veins. Although the main mineralisation is sulphide poor, in places pyrite disseminations are associated with low grade gold. The gold quartz-cemented breccias have values ranging from 0.27 to 20.60 ppm Au. The low homogenisation temperatures mostly in the range between 235 and 255 °C and low salinities (0.0–0.7 wt.% NaCl eq.) combined with paragenetic and stable isotope characteristics indicate that Madendağ could be regarded as “Low Sulphidation” epithermal deposit (Ünal-İmer et al. 2013).

4.3.2.6 Kestanelik (Şahinli)

The Kestanelik gold deposit is located 35 km NE of the regional centre of Çanakkale, 4 km west of Şahinli village on the Biga Peninsula. Traces of small-scale historical mining activities are observed around the epithermal quartz veins. Low sulphidation epithermal veins hosted within Paleozoic metamorphic rocks and Lutetian quartz-feldspar-hornblende porphyry stock (Ünal-İmer et al. 2013). Kestanelik property consists of a series of low sulphidation style epithermal quartz vein zones namely Karatepe, Karakovan (KK1, KK2 KK3), K (K1, K2, K3, KS and KW) and Meydan zone from north to south respectively. NE-SW and E-W trending vein systems exposed over a strike length up to 400 m and vary in width from 1 to 13.6 m. Veins are dipping as moderately to shallow towards southeast and south respectively. The Meydan Zone, which lies in the southern part of the porphyry intrusion, is characterised as a zone of silicification rather than representing discrete quartz vein zone. However, the gold tenor is generally much less then major quartz veins. The majority of gold-silver mineralisation is in association with multiple episodes of fluid flow. At Kestanelik epithermal system, the degree of erosion can be inferred from near surface high-grade zones in combination with variety of textures including cockade, hydrothermal brecciated, colloform-crustiform banding. At Kestanelik recent studies show that, structural locations along pathways such as vein bends are more favourable than replacement processes for gold precipitation (Gülyüz et al. 2017). Pyrite is the only sulphide mineral associated with the gold mineralisation. It is not particularly widespread and is usually finely disseminated in the breccia matrix and some of the quartz veins. The dominant alteration that appears to be associated with the mineralisation is clay in the form of illite-smectite. An alteration halo of clays is common around the veins.

The Scoping Study Update assumes processing of approximately 844,000 tonnes of ore per year, at an average grade of approximately 2.53 g/t gold and 1.9 g/t silver for life of mine production averaging 63,000 oz of gold and 38,000 oz of silver per year. The Scoping Study Update has a proposed mine life of 8 years (Chesser Resources, news release 2013). It is planned that first gold production will commence at the end of 2017.

4.3.2.7 Koru and Tesbihdere

The Koru and Tesbihdere mining districts in the Biga Peninsula, consist of twelve deposits covering approximately 12 km^2. Early-Oligocene basaltic andesite lavas and dacitic lava and tuffs in the south and Late-Oligocene rhyolitic tuff-lava domes and late stage andesite dykes of Çan Volcanics are the main volcanic units around the Koru and Tesbihdere mining districts (Siyako et al. 1989; Ercan et al. 1995, 1998). Mineralisation in the Koru and Tesbihdere mining districts are mainly hosted by rhyolitic lava-domes and tuffs. While the NW-trending fault system between domes and tuffs hosts the Au-Ag enriched base metal epithermal veins, hanging wall rocks of the vein system host brecciated, stockworks and disseminated ore

(Beşir 2003; Yalçınkaya 2010; Çiçek et al. 2012; Çiçek 2013; Çiçek and Oyman 2016). Çiçek and Oyman (2016), focused on seven mineral systems in the Koru and Tesbihdere districts, which show a complex paragenetic sequences and mineral zonations. On the basis of the paragenetic sequence, hydrothermal alteration assemblages, and the nature of the ore-forming fluids, the Au-Ag enriched base metal epithermal deposits in the Koru and Tesbihdere districts are classified as volcanic-hosted intermediate-sulphidation epithermal deposit (Çiçek and Oyman 2016). In the Koru district, galena is the dominant ore mineral in barite-quartz veins containing sphalerite, chalcopyrite, pyrite, bornite, enargite and tennantite can be subdivided into sphalerite-galena dominated Tesbihdere mineralisation and chalcopyrite-pyrite dominated Bakır and Kuyu mineralisation. The Ag/Au ratio is high in Ag showing assays of up to few hundreds of ppm associated with small quantities of gold with maximum 3.14 g/t Au values either as free grains in quartz or as micro inclusions in pyrite and galena. The most widespread silver minerals are polybasite, pearceite, argentite and native silver, which commonly occur as replacements of galena, sphalerite and pyrite, and other sulphides, or as fillings of microfractures in sulphides and quartz. Isotopic composition indicates a progressive dilution of ore forming fluids as a result of increasing input of meteoric water during transportation along fluid flow path from the Koru to Tesbihdere mining district. The intensity of boiling in the area may also show a decrease with distance away from the Koru mining district and an increase in δ^{18} O in the residual liquid, which probably resulted by steam separation during boiling (Çiçek and Oyman 2016).

4.3.2.8 Arapuçandere

Arapuçandere Pb-Zn-Cu (Au-Ag) ISEM is located in the northeastern part of Yenice (Çanakkale-Biga Peninsula), and is hosted by Triassic metasandstones and metadiabase dykes of the Hodul unit of the Karakaya Complex (Fig. 4.2). The first studies at Arapuçandere were conducted by MTA (i.e. Mineral Research and Exploration Institute of Turkey) as part of a research project in the 1970s. The deposit contains a total reserve of 4 Mt at 16.4% Pb, 12.1% Zn and 2.2% Cu averaging of 4 g/t Au and 260 g/t Ag (MTA 1993a, b). The highest gold grade is obtained from upper part of the deposit (308 m asl) which reaches up to 20 g/t Au, while low-grade gold is observed in deeper levels where Au assayed up to 4 g/t in massive ore. The Arapuçandere mining area contains five sets of mineralised veins parallel to each other in the east-west trending structural zones and these veins were numbered I to V, from NW to SE (Bozkaya et al. 2008; Bozkaya 2011; Yiğit 2012). After intermittent mining operations in the early 1980s, I, II and III veins have been closed because of the uneconomic ore contents. At present, Nesco mining company is actively operating the ore production from IV and V veins. These two veins systems show a close genetic relationship as suggested by their temporal and spatial relationships. Both veins show an E-W strike with steep dips 70–80°S at the surface, however the dips of these veins tend to decrease (approximately 40–50°S) downward and the

veins crosscut at an elevation of 120 m above sea level (asl). The IV and V veins extending to lower level are vary from 0.6 to 17 m in width and mining by conventional underground techniques from 6 different production levels show that they are about 200 m length and extend to a depth of 120 m (asl). The veins (IV and V) and associated stockworks at Arapuçandere show various textures including crustiform, colloform, bladed and brecciated. Ore paragenesis within the veins display a similar assemblage, in order of abundance, comprising mainly galena, sphalerite, chalcopyrite, pyrite, Ag-sulphosalts and minor amount of tennantite-tetrahedrite, magnetite, hematite and chalcosite-covelline. Gangue minerals in both veins exhibit a zonation pattern represented by decrease in quartz and increase in calcite with locally minor barite towards deeper levels of the deposit. Silver mainly occurs as Ag-sulphosalts which fills fractures and cavities within the earliest sulphides.

4.3.2.9 Kısacık

The Kısacık gold deposit is a characteristic multi-stage gold mineralisation within the Ayvacık-Karabiga tectonic zone of the Biga Peninsula (Fig. 4.2). The property was discovered by MTA during 2008 exploration program by defining two old adits and at least four small pits which are suspected to represent gold mining operations (Özpinar et al. 2012). Deposit area is underlain by basement rocks of the Paleozoic Kazdağ Metamorphic Group, which is unconformably overlie younger Upper Cretaceous Çetmi Ophiolitic Melange. Mid-Miocene volcanic rocks including ignimbrites, rhyolite, rhyolitic tuffs and lapilli tuffs mainly host the gold mineralization and has angular disconformity over pre-Tertiary rocks. The Pliocene conglomerates, sandstones and siltstones unconformably overlie older rock units.

Gold mineralisation at Kısacık property is controlled by structure and lithology. Gold occurs as two different type of mineralisation. The first one is relatively high grade gold ore associated with quartz-sulphide veins within pumice and low grade disseminated gold mineralisation within thick layers of pyroclastic rocks. NE-SW trending quartz-sulphide veins at the centre are surrounded by illite-sericite and chlorite-carbonate clay alterations from inner to outer respectively. Based on the MTA's resource estimations, property comprises 56.5 Mt (proven+probable+possible) grading 0.5 g/t Au mineralisation (Özpinar et al. 2012).

4.3.3 Epithermal Systems in the South of Biga Peninsula

4.3.3.1 Küçükdere and Çoraklık Tepe

The Küçükdere deposit is a fracture-filling vein-type formed in extensional tectonic settings (Fig. 4.2). Well developed tension fracture systems and normal faults are the major components of the extensional tectonic settings. The vein zone

is associated with the main fault which extends in a SW to NE direction. The vein system consists of two main segments with different inclinations. The main vein extends east to northeast and dip towards the south with an inclination varying between 60 and 90°. The vein system is traced over approximately 5000 m strike length and few tens of metres down plunge from surface with a different thickness varies between 1 and 50 m. A subhorizontal vein formed as a branch of the main vein and outcrops in the east and south east of Germe vein. It strikes east to northeast and dips 0–30° to the northwest. Ore and gangue minerals precipitated as episodic open-space filling with various internal textures including colloform-crustiform, cockade, brecciated, drusy, comb and bladed textures. Intense brecciation and stockworking occur in the hanging wall and are closely associated with the main fault zone. Among the four mineralisation centres namely Germe, Karayanık, Çoraklık, Çengel in the Küçükdere, the abundance and variations of sulphide minerals are significant in Germe pit. While higher gold grades are controlled by sulphide-rich assemblages (>5% Py) in Germe, textural control plays a far greater role in Karayanık and Çoraklık, such as bladed and brecciated-cockade without the significant sulphide assemblage. The total amount of sulphide minerals in Germe, did not exceed 10% of the total vein minerals. The ore minerals include: pyrite, sphalerite, galena, chalcopyrite as the major phases with minor amounts of tetrahedrite, bornite, hessite, argentite, electrum and native gold with supergene phases. Combined fluid inclusion and stable isotope analysis in Germe and Karayanık suggests that precious metal mineralisation most likely occurs in a wide range of vertical depth.

In Çoraklık pit, from NE to SW the vein curves to E-W and slightly to WNW along its strike while the dip ranges between 47 and 50° to N. Textural variation along the open pit walls indicates that the vein cross cut and are displaced vertically by normal faults. The Çoraklık vein and associated silicified zone are enveloped by a mushroom-shaped argillic alteration and both hosted by propylitic altered andesitic rock. Along the contact between the vein and the hanging-wall disseminated and stockwork ore is hosted extensively by an argillic alteration zone in the hanging wall. The propylitic assemblage consists of chlorite, calcite with lesser amounts of epidote and pyrite. In addition, amorphous silica, crustiform-colloform, cockade and breccia, bladed, comb and carbonate replacement textures were identified macroscopically in Çoraklık. Jigsaw, plumose and spherulitic textures were identified in thin section. In the boiling zone gold mineralisation is strongly related to sulphides including chalcopyrite, pyrite, sphalerite and galena. According to our preliminary fluid inclusion measurements, fluids responsible for Çoraklık Tepe mineralisation showed that the fluid was a low T, low salinity, H_2O-NaCI-$CaCI_2$-$MgCI_2$ brine. Inclusions from the Çoraklık open pit are two-phase, liquid-rich inclusions and occur in coarse quartz crystal with a cockade texture. The final melting of the ice occurred with a final temperature range of −0.4 to −0.9 °C which yielded salinities between 0.7 and 1.6% wt. NaCl equivalent.

4.3.3.2 Kubaşlar

The Kubaşlar property is located on the northwest margin of Kozak Caldera of the Kozak Plutonic Complex (Fig. 4.3). The district also contains the Ovacık and Küçükdere mines and a number of other exploration prospects including Karadere and Gömeç. A low sulphidation quartz vein and associated multi-stage breccia structures 200 m in width and 1400 m in length extends NW-SE between Cenozoic volcanic-plutonic rocks and meta-sedimentary rocks of the Kınık Formation.

Good examples of flamboyant, feathery, plumose, colloform banded plumose textures have been identified in the vein system. This texture is regarded as a typical recrystallisation texture related to boiling and thought to develop after the amorphous silica phase and before the later crystalline quartz phase. Clast supported breccia composed mainly of quartz and rock fragments supported by microcryptocrystalline quartz and opaque minerals (Tezer 2006). Fragments with well-developed colloform banded, colloform-crustiform, plumose jigsaw textures with amorphous and crystalline quartz phases indicate repeated episodes of sealing and fracturing during the lifetime of the shallow hydrothermal system. Opaque minerals are pyrite and marcasite in outcrop samples. Since the acquisition in 2008 by Koza Gold, exploration included drilling programs in 2011 and 2012 as well as surface

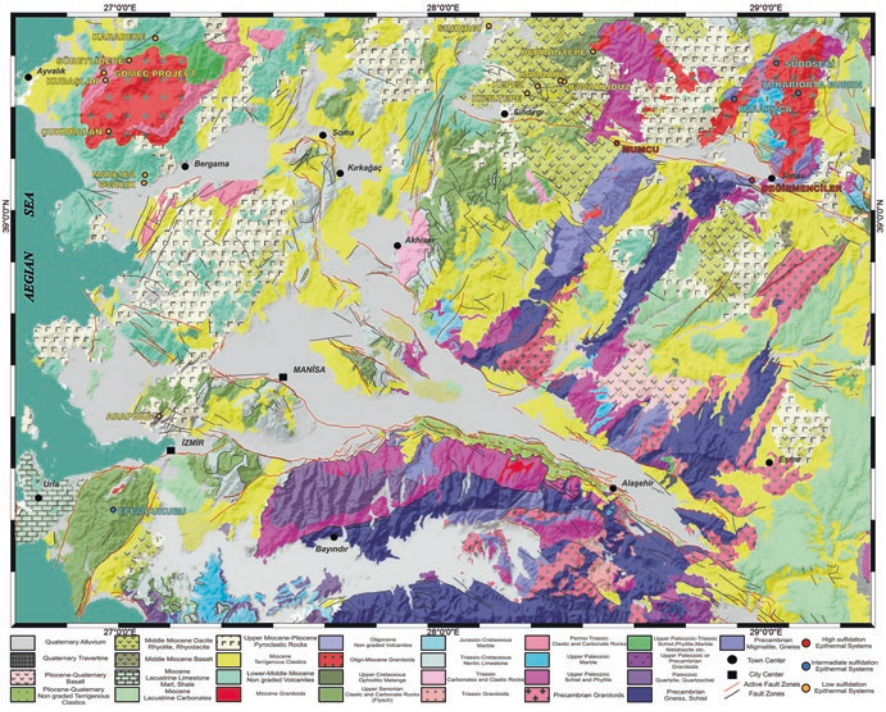

Fig. 4.3 Regional geological map of Inner-west Anatolia and spatial distribution of significant epithermal mineralisation. (Geology modified from MTA Emre et al. 2013; Akbaş et al. 2017)

sampling, geophysics, geochemistry and resource modelling. Kubaşlar deposit has 70.000 oz grading 2.31 g/t Au and 14.53 g/t Ag.

4.3.3.3 Gömeç

The Gömeç Project comprises five contiguous exploration licenses and is an early-stage gold exploration project located 35 km northwest of Ovacık and 20 km southwest of the Havran-Küçükdere gold deposit and 1 km south of Koza Gold's Kubaşlar low-sulphidation gold Project (Fig. 4.3). The Gömeç project was acquired through government tender by Royal Road's JV-Partner, Oremine Madencilik Sanayi ve Ticaret Inc. ("Oremine") in 2008. Soil geochemistry within the Samantaşı and Oremine's Kubaşlar (Kubaşlar East) licences indicated anomalous gold values in excess of 0.5 ppm up to 6 ppm Au which are interpreted to reflect gold-bearing zones. Soil anomalies are fault-controlled and extending E-W in Kubaşlar. At Gömeç 4494 m of combined reverse circulation and diamond drilling was conducted in two separate drilling campaigns during 2014 and 2015. In 2016, a new drilling program was started. The Kocakıran prospect is represented by both outcrop and sub-crop of low-sulphidation epithermal veining and silicified fault systems which extend north-west along strike for approximately 1 km. Mineralisation in Kocakıran consists of silica veins and associated quartz breccia bodies within silicified and altered volcanic rocks in an area of 100–200 m in width. The silica veins with a low sulphide content, display characteristic epithermal textures such as colloform and crustiform silica with banding of quartz-pseudomorphs with bladed calcite and multiphase episodic hydrothermal breccias.

The fragments of the hydrothermal breccia are angular to sub-angular in shape ranging up to few centimetres down to micron scale. The fragments mainly comprise micro-crystalline quartz crystals with irregular and interpenetrating grain boundaries. The clasts of the breccia are supported by dark-coloured, sulphide dominated cryptocrystalline quartz matrix. Disseminated pyrite and marcasite are the most widespread sulphide minerals in the hydrothermal breccia with lesser chalcopyrite, galena and sphalerite. Gold and silver sulphosalts including pyrargyrite were identified either as disseminated individual crystals or adjacent crystals.

4.3.3.4 Karadere

At the Karadere low-sulphidation prospect, five different rock units are recognised; from oldest to youngest these are metamorphic rocks, intrusive rocks, and volcanic-volcanoclastic sequences consisting of agglomerate, volcanic breccia, andesitic flow-dome complexes and basaltic andesite. Gold and silver mineralisation are hosted by quartz veins confined to high to moderate angle normal faults traversing the andesitic domes, and overlying agglomerate-volcanic breccia. The veins are confined to a structural corridor bounded on the south by a NE-trending low-angle

normal fault, and on the north by a high angle normal fault. The structures within this corridor appear to be sub-parallel faults trending in N45–50E direction. The mineralised veins are enclosed within quartz-clay-sericite alteration, sericite being closer to the veins (Aluç et al. 2014). PIMA (Portable Infrared Mineral Analyzer) analyses show three alteration zones: Chlorite-epidote, illite-sericite, and quartz stockworks. The low-sulphidation mineralised veins are composed predominantly of sugary quartz with occasional bladed to brecciated textures. No significant vertical zoning with respect to ore-vein texture association is observed throughout the veins. Based on the geographical distribution, five different main ore zones are recognised in Karadere: South Ore zone, Ballık Ore zone, Kabak Ore zone, Kartaldere Ore zone and Göktepe Ore zone.

4.3.3.5 Ovacık

The Ovacık gold-silver mine is located in West Anatolia about 100 km north of İzmir near the historical city of Pergamon (Fig. 4.3). The cyanide leaching method was first used in the Ovacık mine in Turkey and the mine has been operating since early June, 2001. The Ovacık gold–silver deposit consists of six epithermal quartz veins. Among them production is still ongoing on M and Z veins by underground operation. Both mineralised and unmineralised epithermal quartz veins are controlled by sinistral faults generally oriented E-W and NW-SE. The high-grade, low-sulphidation quartz veins are dominantly northwest-southeast-trending, with dips ranging from 65 to 85° to N. The veins at Ovacık have six main textural types of ores: (a) crustiform/colloform banded ore, which occurs in both the veins and as breccia clasts; (b) coarse, bladed carbonate, occurring as distinct bands or infilling vugs; (c) clast-supported crackle (shattered) breccia with angular monomictic fragments; (d) matrix-supported fluidised (milled) breccia with angular to subrounded polymictic fragments, in which the clasts consist mainly of quartz and adularia with common crustiform banding and quartz-cemented breccia; (e) cockade texture; formed from clasts of silicified wall rock overgrown by crustiform/colloform bands and cockades of chalcedonic quartz and adularia; and (f) a hanging wall zone of silicified porphyritic andesite and sheeted quartz veinlets. High grade gold values up to 100 ppm occur in crustiform/colloform banded quartz-adularia veins and late stage crackle breccia and silicified wall-rock hydrobreccia. Sulphide content is low (<2%) and is dominated by pyrite with traces of chalcopyrite arsenopyrite, acanthite, argentite, pyrargyrite, stibnite, galena and bornite. Alteration minerals are smectite, mixed layer illite/smectite, quartz, adularia and calcite. Fluid inclusion data from the Ovacık Au deposit suggest that the ore-forming fluids were low salinity (<2 wt.% NaCl equiv.) and low temperature ranging from 150 to 250 °C, with most below 200 °C. $^{40}Ar/^{39}Ar$ dating of adularia from gold-bearing quartz veins indicates an age of mineralisation of about 18.2 ± 0.2 Ma. $\delta^{18}O$, $\delta^{18}O_{H2O}$ and δD values suggest that mineralising solutions were a mixture of meteoric and magmatic waters. The $\delta^{34}S_{\Sigma sulphide}$ data at Ovacık and Narlıca range from −2.1 to 5.3‰

(average: +1.7) and from −4.6 to +2.7‰ (average: −0.36), respectively. These $\delta^{34}S_{\Sigma sulphide}$ values are consistent with a magmatic source for S (Yılmaz et al. 2007).

4.3.3.6 Efemçukuru

Efemçukuru is an outstanding example among the epithermal deposits in western Anatolia with its gold and /or silver rich assemblages with diverse gangue minerals, and structural control on vein formation. Efemçukuru shows characteristics of both low and intermediate sulphidation epithermal deposits. Physical and mineralogical properties of the wall rock, erosion level of the different segments of the vein, direction of the hydrothermal fluid path and the distance from the heat source are the main controls on three dimensional zonations of the veins. Along the strike of the veins, there is also a zonation characterised by both ore and gangue mineral distribution and base and precious metal geochemistry in Kestanebeleni vein from South (South Ore Shoot) through middle part (Middle Ore Shoot) to North (North Ore Shoot) respectively. There are several lines of evidence for multiple stages (or pulses) of ore formation. In different levels and in different sectors of the Kestanebeleni vein, more than one generation of sulphide crystallisation (e.g., galena, sphalerite and pyrite) is present. The hydrothermal gangue minerals (mainly quartz and rhodonite, but also axinite, rhodochrosite ± adularia) are crosscut by sulphide assemblage in some core samples (e.g., in North Ore Shoot). Extensive crosscutting relationship among the different hydrothermal gangue phases also indicates distinct pulses of gangue mineral generation. Change in either strike and dip of the vein system reflects the changing volume of the space for the precipitation of gold from boiling hydrothermal fluid. On the base of this approach it has been stated that, most NW-oriented and steepest segments correlate to areas of elevated gold mineralisation. The spaces formed at the joints of two different fracture system are the site of gold rich zones. The Kestanebeleni hydrothermal system produced a sequence of vein textures and breccias in different stages during its evolution. On the basis of a recent study by Boucher et al. (2016) veins in different stages have different mineral assemblages and internal textures such as;

Stage I. Calc-Silicate (qtz-chl-act-ep-py veinlets), Stage II. Quartz-Rhodochrosite Breccia (qtz-rdn-rds), Stage III. Quartz-Rhodochrosite (colloformbanded qtz-rds-rdn±py), Stage IV. Quartz-Sulphide (colloform-crustiform, cockade qtz-rds-py-gn-sp), Stage V. Base Metal Sulphide (massive to colloformbanded gn-sp-py-qtz-cpy), Stage VI. Late Quartz-Carbonate (stringers of qtz-cal±rds). Gold occurs as inclusions in galena and pyrite of Stage IV and V, and as electrum in Stage III and IV. The fluid inclusions clearly indicate that a complex geothermal system existed.

4.3.3.7 Ergama (Gokceyazi)

Ergama Property is situated 35 km West of Balıkesir city centre. The property involves a HSEM gold deposit within a large area of propylitic and argillic alteration. The project area consists of a complex Late Oligocene volcanic structure developed on a slightly metamorphosed basement of Permian age. High grade gold mineralisation is mostly associated with tectonic controlled brecciation and silicification. Silicified zones at higher elevations are represented by fine sugary and drusy cavities and thin breccia zones composed by vein quartz fragments in gossanous matrix. Alunite, pyrophyllite, dickite, kaolinite, diaspore are the main clay minerals along advanced argillic alterations while illite-sericite, smectite are common along argillic alterations. Chlorite dominant propylitic alteration surround all clay minerals at the outer part of the system. Property also comprises high-level porphyry mineralisation zone represented by sheeted or stockwork type dark greyish quartz veinlets and quartz-sericite alterations towards the northern margins of the HSEM.

Recent drilling by Sandstorm Gold Co. (formerly Mariana Resources) intersected long intervals of gold-bearing, porphyry-style quartz (pyrite-chalcopyrite) stockwork mineralisation. Best intersections up to date, 141 m @ 0.23 g/t Au and 156.4 m @ 0.25 g/t Au including 56.4 m @ 0.33 g/t Au and 0.12% Cu (Mariana Resources, News Release, 2017).

4.3.4 Kütahya-Afyon-Uşak Region

The Menderes Massif is a well-studied metamorphic complex, which is made up of a polymetamorphic Precambrian basement which is dominated by orthogneisses and unconformably overlying Paleozoic to Early Tertiary cover series consisting of metaclastic and platform-type metacarbonates (Başarır 1970; Şengör et al. 1984; Dora et al. 2001; Candan et al. 2011). E–W trending active graben systems, dividing the Menderes Massif into submassifs and associated detachment faults are the main structures that give to the Menderes Massif its present structure. In the northernmost area the prominent structure in the Simav region is the Simav detachment fault that is characterised by mylonites in core rocks. They consist of migmatitic-banded gneiss, orthogneiss, biotite gneiss, high-grade schist, amphibolite, and marble and separates so-called mylonitic core rocks of the northern Menderes Massif in the footwall from the Akdere Basin in the hanging-wall (Işık and Tekeli 2001; Bozkurt et al. 2011).

The Eğrigöz pluton is one of the largest (approximately 550 km^2) exhumed granitoid body coexisting with the Koyunoba and Alaçam plutons in Western Anatolia (Fig. 4.3). The pluton is assumed to be a syn-extension following the subduction of African/Arabian Plate beneath Anatolide-Tauride block (Catlos et al. 2012). These syn-extensional granitoid plutons intrude pre-existing regionally metamorphosed basement in the footwall (e.g., Akay et al. 2011; Ring and Collins 2005; Thomson and Ring 2006; Özgenç and İlbeyli 2008; Erkül 2010; Hasözbek et al. 2010; Catlos

et al. 2012). The plutons are surrounded by contact-metamorphic aureoles of pyroxene hornfels and hornblende hornfels facies that grade from the pluton to greenschist facies rocks. Zircon crystals from southern, central and northern portions of the Eğrigöz pluton yield $^{238}U/^{206}$ Pb ages of 20.4 ± 0.5 Ma, 20.8 ± 0.4 Ma and 20.8 ± 0.4 Ma (weighted mean) respectively. Similar to Eğrigöz pluton, zircon crystals from the southern, centre and northern flanks of the Karakoca pluton yield $^{238}U/^{206}$ Pb ages of 26.0 ± 0.6 Ma, 20.6 ± 0.8 Ma and 24.1 ± 0.5 Ma respectively (Catlos et al. 2012). These ages are in agreement with U-Pb zircon ages reported from Hasözbek et al. (2010) and SIMS U–Th–Pb zircon ages by Ring and Collins (2005), which are 19.4 ± 4.4 and 20.7 ± 0.6 Ma, respectively.

The Kalkan Formation is the lowermost unit that is crosscut by the Eğrigöz Pluton and mainly consists of banded migmatites, gneiss, and marble lenses of the Menderes Massif. It is assumed that these high-grade rocks are unconformably overlain by low-grade Simav Metamorphics representing the cover series of the Menderes Massif (Akdeniz and Konak 1979). The Simav metamorphic rocks are made up biotite-muscovite schist, muscovite-quartz schist, biotite-muscovite-chlorite schist, garnet schist, quartzite, chlorite-bearing calc schist (Akdeniz and Konak 1979). The Balıkbaşı Formation conformably overlies the Simav Metamorphic rocks and consists of locally dolomitized marbles derived from neritic limestones. The Balıkbaşı formation is unconformably overlain by Upper Paleozoic-Lower Triassic Sarıcasu Formation consisting of low-grade schist, phyllite, quartzite and marble intercalations. The Sarıcasu Formation is overlain by the Arıkaya Formation. The age of the Arıkaya Formation is thought to be Permian, based either on lithological similarities with the fossiliferous Permian limestone or boundary with overlying fossiliferous Middle-Upper Triassic rocks. The Arıkaya Formation is composed mainly of crystalline limestone, which is obscured by dolomitization in places (Akdeniz and Konak 1979).

The Karakoca and Sudöşeği Pb-Zn-(Cu-Ag) mineralisation are good examples of intra-plutonic epithermal vein type base-metal deposits in the Inner Western Anatolia. They are hosted by Koyunoba and Eğrigöz Plutonic Complex (EPG) respectively (Fig. 4.3). Although there are a number of iron skarns occur in the contact zone between the plutons and carbonate rocks of the Afyon Zone and Menderes Massif, vein type Pb-Zn (Cu-Ag) mineralisation similar to the Karakoca and Sudöşeği have been rarely recognised.

4.3.4.1 Karakoca

The intra-plutonic Karakoca vein, hosted by Karakoca pluton, strikes NW discontinuously for 1400 m and dips 60° to SW. The true thickness of the vein is variable, in a range between a few cm to 2–3 m. Mining operations in Karakoca were only carried out for 1 year in 1960 with the production of ore containing 11% Pb, 3–4% Zn and 2–3% Cu. High grade massive ore with colloform-crustiform texture passes gradually to brecciated and stockwork ore in the hangingwall of the vein zone. The ore paragenesis is represented by pyrite, galena, sphalerite and chalcopyrite with

lesser tetrahedrite-tennantite, bornite and hematite. In the oxidation stage, chalcocite, covellite, goethite, malachite and cerussite replace the hypogene ore minerals. Primary two phases (liquid-rich) inclusions from quartz samples have yielded homogenisation temperatures (T_h), ranging between 250.2 and 322.7 °C (avg. 283 °C with 51 measurements) (unpublished data). Corresponding salinity based on final ice melting (T_{mice}) temperatures are clustered in a wide range of area in between 0.4 and 15.3 wt.% NaCl equivalent (avg. 4.72 wt.% NaCl eq.) The first ice melting (T_{mf}) measurements are 29–63 °C, indicating NaCl, $CaCl_2$, $MgCl_2$ and KCl (Li and Br free) dominated fluids are responsible for the quartz crystallisation in association with mineralisation. Sulphur isotope results close to zero ($\delta^{34}S$ ‰) from sphalerite, pyrite and galena indicate a major contribution of magmatic fluids (unpublished data). The characteristics of Karakoca vein in terms of its texture, composition, ore mineralogy and ore-forming fluid correspond to intermediate sulphidation epithermal veins.

4.3.4.2 Su Döşeği

Similar to Karakoca, Su Döşeği is another example of intra-plutonic vein system which crops out along a NE-SW fracture-fault system in the Eğrigöz Plutonic Complex. High-grade ore is found in the hanging wall of the vein system, showing clear colloform-crustiform texture, while some stockwork and brecciated ore are found in the footwall. Although, there is no recorded mining activity in Sudöşeği, small excavations and some dumped floats were found during our field study, suggesting that short-lived operations took place.

Ore mineralisation consists of a sulphide mineral assemblage containing galena, sphalerite and chalcopyrite in colloform-crustiform and stockwork zones. Galena and sphalerite with subordinate chalcopyrite are more common in colloform-crustiform banded zones, while pyrite, quartz and carbonate gangue are more abundant in stockworks and brecciated zones. The oxidation stage is characterised by goethite, limonite, siderite, cerussite, azurite, malachite and chalcocite-covellite. Fluid inclusion assemblages in quartz yielded T_h between 211 and 349 °C (avg. 269 °C with 32 measurements) with salinities between 0.7 and 9 wt.% NaCl equivalent (mean 4.5 wt.% NaCl eq.). The first ice melting (Tmf) measurements are 29–63 °C, indicating NaCl, $CaCl_2$, $MgCl_2$ and KCl (Li and Br free) dominated fluids are responsible for quartz crystallisation. Similar to Karakoca, sulphur isotope results ($\delta^{34}S$ ‰) close to zero from sphalerite, pyrite and galena indicate magmatic origin for the fluids are responsible in ore generation (unpublished data).

4.3.4.3 Yukarı Ortaburun (Katrandağ)

Katrandağ Pb-Ag (Au) is a complex epithermal and associated skarn type mineralisation, hosted by a roof pendant of dolomitic limestone of Balıkbaşı formation, Simav Metamorphics and Eğrigöz pluton. Epithermal veins extend along N-NE/SW

striking faults. Although there has been some manganese mining in vicinity of Katrandağ, no mining activity has occurred in the area.

The upper part of the system is thought to occur at the interface between the water table and the overlying surficial zone, based on the occurrences of silica cap, oxidation and supergene alteration. The hydrothermal mineralisation occurs in silica cap including silica-rich veins and silicified dolomitic limestone (Balıkbaşı formation), which hosts a Ag-Au rich zone for approximately 6–6.5 m at the uppermost section. Below the Ag-Au rich ore, massive galena, barite with lesser amounts of sphalerite and pyrite are observed. At further depths, the contact zone of Eğrigöz pluton with Balıkbaşı formation and Simav Metamorphics show distal and proximal skarn zone with about 1–1.5 m thickness in average. Based on core samples, the copper-rich distal skarn zone is thinner and characterised by chalcopyrite, bornite and pyrite association, while the iron dominated proximal skarn zone is represented by abundant magnetite, sphalerite, pyrite, chalcopyrite and galena with a thickness up to 4.5 m. Additionally, veinlets of 50–55 mm width in stockworks and stringer zones are observed in the interior of the pluton, which shows roughly % 1–2 sulphide mineralisation including chalcopyrite, galena and pyrite.

4.3.4.4 Mumcu

Mumcu is a poorly studied epithermal system, cropping out along N-S transfer faults linked with the Simav Graben. It is situated within Paleozoic Metamorphics and Miocene andesitic volcanics. The mineral system is associated with silicified, brecciated and opal bearing zones and surrounding argillic alteration mineral assemblages including kaolinite, montmorillonite and cristobalite. The ore minerals including cinnabar, arsenopyrite, electrum and low grade gold (500 and 340 ppb from Hg bearing opal and pyrite samples) are found in opal-rich zones (Oygür 1997). Since there are no core samples, the data from Mumcu epithermal system is only limited to surface observations. However, the presence of arsenopyrite, wall rock alteration and gold anomalies point to the outlying section corresponding to an upper parts of an epithermal system, which also means that higher ore grades might be found at depth.

4.3.4.5 Değirmenciler

The Değirmenciler is an antimony bearing epithermal deposit, hosted in silica replaced limestone lenses of Paleozoic metamorphic rocks. The silicified host rocks show colloform-crustiform texture and jasperoid alteration as a result of calcite-silica replacement. Argillic and advanced argillic alteration represented by montmorillonite, smectite, quartz, opal, cristobalite and dickite surround this epithermal system. Hydrothermal breccia with dark grey silica and abundant pyrite is associated with high grade ore. Lesser amount of galena, chalcopyrite, molybdenite, bismuth, gold and silver accompany to the main ore.

4.3.4.6 Kaymaz

Kaymaz Gold Mine situated at the Kaymaz village near Sivrihisar town of Eskişehir city. Kaymaz is located in the Tavşanlı Zone of the Anatolide-Tauride Block, that was subjected to high pressure-low temperature metamorphism during the Cretaceous. Paleozoic and Mesozoic metamorphic rocks of the Tavşanlı Zone were intruded by the Eocene dykes. Under the influence of these granite dykes, three styles of mineralisation are evident; manto-type mineralisation, quartz stockworks and veinlets and episodic brecciation adjacent to the granite dyke. Mineralisation is hosted mainly in the serpentinites and quartz schists at Damdamca, Karakaya, Küçük Mermerlik and Kızılağıl districts (Yavuz 2013).

Among these, the Damdamca and Main Zone are the two most important districts because of their reserves and exploration activities. The vein in Damdamca has been traced along its N-S strike for over 220 m and dips 45–60° to the east. Similar to Damdamca the vein in the Main Zone has been traced for a length of 1100 m along a N-S strike dipping 45–60° S. Early hydrothermal ore assemblage is composed mainly of magnetite, millerite, pentlandite, nickeline, arsenopyrite, marcasite, pyrite-I, bravoite, gold and silver. Late hydrothermal ore assemblage is composed of pyrite-II and supergene hematite, pyrolusite, goethite, limonite, lepidocrocite and rarely chalcocite-covellite (Yavuz 2013). Quartz, serpentine, ankerite, and dolomite are the main gangue minerals. Homogenisation temperatures for liquid-rich inclusions in quartz, range from 240 to 390 ° C with salinities between 0.3 and 14 NaCl wt.% (Yavuz 2013). On the basis of field relations, petrography and fluid inclusion studies, the Kaymaz gold mineralisation can be considered as listwanite type deposit which formed under epithermal conditions.

4.3.4.7 Red Rabbit (Kızıltepe)

The epithermal mineralisation at Kızıltepe is hosted within the Sındırgı Volcanic Complex, which comprises a sequence of dacitic and rhyolitic intrusions, lava flows and pyroclastic rocks. The Sındırgı Volcanic Complex is considered to be of Miocene age on the basis of K-Ar ages of 19.0 ± 0.4 and 20.2 ± 0.5 (Erkül et al. 2005). Dating of the lower ignimbrite host-rocks also yielded a comparable 40Ar/39Ar plateau age of 19.82 ± 0.14 Ma. There are four main epithermal quartz (-adularia) vein swarms located across the region, namely: Kızıltepe, Kepez, Karakavak, and Kızılçukur (listed from SW to NE). Epithermal gold was discovered in the region during a regional bulk leach extractable gold (BLEG) and 180-μm stream-sediment sampling program, carried out by EuroGold (Yılmaz 1992) and TUPRAG in 1990 and 1992 respectively (Yılmaz 1992). At Kızıltepe, low-sulphidation type epithermal veins, including four economically viable veins referred to as Arzu South, Arzu North, Banu and Derya, are controlled by NW and NNW trending structures in the lower ignimbrite sequence. The subparallel and curvilinear Arzu and Banu vein systems dip steeply 75–85° to the NE and 75–80° to the SW respectively. Along their strikes, the total length of the veins reach up to

19.5 km (Şener et al. 2006a, b). The Kızıltepe deposit exhibits characteristics of an adularia-bearing low sulphidation paragenesis with a low total sulphide content and with a simple ore mineralogy. Disseminated pyrite and associated supergene oxides with traces of electrum and acanthite are the main ore minerals.

Crustiform, carbonate replacement and associated bladed, breccia and associated cockade textures are the prominent textures, which yield the highest gold grades ranging from 12 to 32.5 ppm in the Kızıltepe vein system (Yılmaz et al. 2013). The Kızıltepe low sulphidation epithermal system possesses characteristic textures that are directly or indirectly related to boiling hydrothermal fluids. Silver mineralisation is represented by native silver and acanthite and associated with gold in both the mineralised quartz veins and the stockwork envelope around the veins. Overall, a wide range of Ag:Au ratios has been recorded, commonly between 5:1 and 30:1. Detailed fluid inclusion studies were conducted by Yılmaz et al. (2013), on medium-grained quartz from crustiform banding, carbonate replacement and hydrothermal breccia textures of Phase II, which is regarded as the main phase of Au-Ag deposition. These yielded an average homogenisation temperature of 231 °C (number of samples, n = 85) and salinity of 1.1 wt.% NaCl equivalent (n = 85), suggesting that relatively low temperature diluted fluids of mixed origin were responsible for the Phase II mineralisation.

4.3.4.8 İnkaya

The İnkaya Cu–Pb–Zn–(Ag) is an epithermal vein-type ore mineralisation, hosted by Simav Metamorphics and Arıkaya formation. The epithermal veins extend E-W along strike with a thickness of up to 2 m. Galena, sphalerite, chalcopyrite, pyrite and fahlore with lesser amounts of cerussite, anglesite, digenite, enargite, chalcocite-covellite, bornite are the ore minerals within an iron oxide dominated quartz gangue. Grades of Cu, Pb, Zn and Ag are 77,400 ppm, 102,600 ppm, 6843 ppm and 203 ppm, in average respectively. Microthermometry results from quartz range from 235 to 340 °C with salinities, between 0.7 and 4.49 wt.% NaCl equivalent. Based on wide range of homogenisation temperatures and lower salinities, multiple fluid generations from same source is thought to have occurred as a result of meteoric water mixing with magmatic fluids (Özen and Arık 2015).

4.4 The Central Anatolian Province

Tectono-magmatic evolution of Central Anatolia is closely related to multiphase compressional and extensional events following the continental collision of Gondwana and Eurasian plates. As a consequence of this convergence processes, NE to SW trending volcanic arc extended from Konya to Nevşehir developed during Neogene to Quaternary times. Central Anatolian Crystalline Complex (CACC),

which is also known as Kırşehir Block is bounded on the North by the İzmir Ankara Erzincan Suture that separates the Pontides from both CACC and from Anatolide–Tauride (Fig. 4.1).

In the southwest, CACC is separated from Anatolide–Tauride block by the Inner Tauride suture (Görür et al. 1984, 1998; Dilek et al. 1999; Okay and Tüysüz 1999; Andrew and Robertson 2002; Robertson et al. 2009; Pourteau et al. 2010). The Inner Tauride suture is assumed to have been formed by the closure of an oceanic branch located between the Tauride-Anatolide Block and the CACC. On the basis of geochronological data obtained from ophiolites of the metamorphic soles (Parlak et al. 2013) this oceanic basin is suggested to have been consumed as a result of northward subduction which initiated between 95 and 90 Ma. The latest Cretaceous to Early Cenozoic age is envisaged for the complete consumption and following continental collision of this (Parlak et al. 2013).

The Central Anatolian Crystalline Complex experienced high-temperature, medium-pressure (HT-MP) Barrovian metamorphism at 5–6 kbar/>700 °C, dated about 91–84 Ma. The metamorphic rocks of the Kırşehir Block were subjected to regional high-temperature, medium-pressure (HT-MP) conditions and are subdivided into three massifs namely Akdağ, Kırşehir, and Niğde-Ağaçören-Hırkadağ (Lefebvre 2011; Van Hinsbergen et al. 2016) (Fig. 4.1). The ophiolites and the underlying high-grade metamorphic rocks of the metamorphic basements are intruded by granitoids suites range in age from Late Cretaceous to Eocene with a large compositional diversity from calc-alkaline through subalkaline to alkaline as a result of closure of the Inner Tauride Ocean (Akıman et al. 1993; Aydın et al. 1998; Whitney and Dilek 1998; Fayon et al. 2001; Whitney et al. 2001, 2003; Whitney and Hamilton 2004; İlbeyli et al. 2004; İlbeyli 2005; Kadıoğlu et al. 2003, 2006; Köksal et al. 2004; Önal et al. 2005; Boztuğ 1998, 2000; Boztuğ et al. 2007; Kuşçu et al. 2010). The North-west segment is known as "Kırıkkale granitoid belt" and composed of several calc-alkaline granitoid stocks including Sulakyurt, Keskin, Behrekdağ, Çelebi granitoid and alkaline stocks including Buzlukdağ and Baranadağ granitoids. Ağaçören calc-alkaline intrusive suite which can be divided into two bodies as Ağaçören and Ekecikdağ granitoids lie along the arc which is parallel NW–SE trending Tuz Gölü Fault (Kadıoğlu and Güleç 1996; Türeli 1991). Baranadağ and Buzlukdağ stocks are the well-known examples of alkali plutonism in the Kaman-Kırşehir region.

Development of the intensive Neogene-Quaternary volcanism in the Central Anatolian Volcanic Complex is related to subduction and the following continental collision between the Afro-Arabian and Eurasian plates. The main transcurrent faults such as the North Anatolian, the East Anatolian, the Tuz Gölü and the Ecemiş faults were formed in association with compressional and extensional forces during the closure of the Northern branch of Neo-Tethys (McKenzie 1972; Şengör 1979; Şengör and Yılmaz 1981; Pasquare et al. 1988; Toprak and Göncüoğlu 1993). As the largest volcanic province of the central Anatolia, it includes Upper Miocene-Holocene ignimbrites, volcanic ash deposits and lava flows intercalated with fluvio-lacustrine sediments (Çiner et al. 2015). Central Anatolian Volcanic Province hosts

numerous monogenetic volcanoes including Erciyes, Hasandağ and Melendiz main stratovolcanoes which are responsible for the volcanic activities between Miocene to recent. The Melendizdağ Volcanic Complex hosts several high sulphidation mineralisation and comprises Miocene-age coalescing lava domes, flows, vent breccias, and pyroclastic deposits. The Miocene Develidağ volcanic complex is situated at the southeastern end of the Sultansazlığı pull-apart basin and the southern part of the eastern Ecemis fault. Ecemiş and Tuz Gölü Faults create an area of crustal extension resulting in tectonic depressions such as pull apart basins exemplified by Sultansazlığı and Tuz Gölü basins. Tuz gölü and Sultansazlığı basins along with the Ecemiş Fault Zone are active pull apart basin since the Early Quaternary (Dirik and Göncüoğlu 1996). Previous structural studies suggest that Develidağ volcanism was generated prior to and during the extension of the Sultansazlığı pullapart basin (Koçyiğit and Beyhan 1998; Toprak 1998). The common features of the central Anatolian volcanic rocks are abundant tholeiitic and calc-alkaline rocks, followed by alkaline activities at the final stage of the volcanic events. Develidağ eroded stratovolcano is represented mainly by tholeiitic basalts associated with minor calc-alkaline products (Kürkçüoğlu 2010). The CAFZ transform microplate boundary separates Sultansazlığı basin from the Develidağ volcanic system.

Within the Anatolian block, some sedimentary basins are related to these faults (Şengör 1979; Şengör and Yılmaz 1981), such as the Sultansazlığı and Tuz Gölü basins (pull-apart basins, according to Pasquaré et al. 1988). The common features of the central Anatolian volcanic rocks are abundant tholeiitic and calc-alkaline associations, followed by alkaline activities at the final stage of this volcanism. The Develidağ volcanic system is represented mainly by tholeiitic basalts associated with minor calc-alkaline rocks. Melting modelling suggests that basaltic rocks can be derived by partial melting (3–4%) of a spinel peridotite source component, whereas calc-alkaline rocks show minor amount of crustal contribution during differentiation as indicated by LIL/HFS element ratios and supported by AFC modelling. Development of the tholeiitic calc-alkaline associations for Develidağ volcanic system could be related to the activities of the eastern segment of the Ecemiş fault. Tholeiitic and calc-alkaline associations can be explained either by combined development of partial melting of a mantle source and following crustal involvement or by the change in the rate of the melting degree. The lack of alkaline rocks seems to be attributed to either the lack of extensional development or to the poor extension in Central Anatolia before the late Miocene.

Another important volcanic centre Konya Volcanics outcrop along a 60 km, northwest trending zone which is up to 40 km in width, between the cities of Konya and Beyşehir. Permo-Mesozoic autocthon-para autocthon Gökçeyurt Group and allocthonous Ladic Metamorphics are the main components of the metamorphic basement. The basement is overlain unconformably by subduction related calc-alkaline volcanic and volcano-sedimentary rocks of the Late Miocene-Pliocene Konya Volcanics. The Konya Volcanics comprise dykes, lava flows, tuffs, ignimbrites, volcanic breccias and agglomerates in composition vary from rhyolite to andesite. The Konya belt is a recently discovered metallogenic unit defined by at

least 15 alteration zones of gold and/or silver mineralisation including İnlice, Doğanbey and Karacaören in the Central Anatolia of Turkey. Mineralisation is related to a belt of Miocene volcanic rocks, most of which constitute a series of large compound stratovolcanoes of calc-alkaline composition.

4.4.1 Öksüt

Öksüt is a high-sulphidation epithermal gold deposit located in Develidağ Volcanic Complex (DVC) in Central Anatolia (Fig. 4.1). The deposit was discovered by Stratex in early 2007. Develidağ is an eroded stratovolcano represented by tholeiitic basalts and minor calc-alkaline rocks composed mainly of andesites (Kürkçüoğlu 2010). The deposit covers two reasonably well-defined targets, known as Kel Tepe and Güney Tepe, which are characterised by intense silicic alteration and advanced argillic alteration. Keltepe and Güneytepe deposit are both considered to be controlled by NW-SE and NE-SW trending faults.

Intense silicic alteration formed as massive silica and massive silica breccia with lesser vuggy silica. Advanced argillic alteration is characterised by the presence of the mineral assemblage comprising alunite, kaolinite, dickite, pyrophyllite, diaspore, aluminium-phosphate-sulphate minerals (woodhouseite-svanbergite series), zunyite, minamyite, pyrite and enargite.

In Kel Tepe four different types of breccia have been identified on the basis of their clasts, matrix and alteration features. These are massive silica breccia, silica-hematite-limonite breccia, alunite breccia and the quartz-kaolinite ± alunite breccia. Texturally a variety of polymictic breccias and a texturally uniform porphyritic andesite are the main host rock for gold mineralisation (Sillitoe 2012).

Massive to vuggy residual quartz commonly occurred at increasing elevations with a vertical limit of up to 100 m. (Massive to vuggy residual quartz with associated silicification were formed at the higher levels of the system with a vertical extent of up to 100 m. However, quartz-alunite and quartz-kaolinite alteration is encountered at lower levels of the system. These two alteration controlled by NW-SE and NE-SW trending faults are the most prominent alteration types associated with gold mineralisation. The property contains probable reserves of 26.1 Mt at 1.4 g/t gold, containing 1.16 million ounces of gold. The Öksüt feasibility study evaluates a mine plan of two open pits operated over an 8 year mine life (http://sandstormgold.com/news/2016/index.php?&content_id=475).

Mineralisation at Öksüt is believed to be related to the contemporaneous emplacement of a subvolcanic breccia and a porphyritic andesite. A 2012 site visit by Dr. Richard Sillitoe described gold mineralisation as being *"preferentially precipitated in the siliceous ledge and its immediate quartz-alunite halo,"* and having been *"fed by at least one, and probably several steep structures represented by massive silicification."*

4.4.2 İnlice

This prospect was the first of more than twenty hydrothermal alteration zones discovered by Stratex in the Konya Volcanic Belt. The İnlice epithermal gold project is located in the Konya (Erenlerdağ) Volcanic Belt, approximately 40 km northeast of Konya (Fig. 4.1). In the area, Miocene-Pliocene volcanism with calk-alkaline and high-K calk-alkaline affinity is composed mainly of andesitic and dacitic lavas and tuffs. The widespread alteration of the andesitic and dacitic lavas consists mainly of kaolinite, and associated halloysite, alunite, cristobalite, quartz, illite, montmorillonite, and zeolite group minerals (Karakaya et al. 2001).

The İnlice epithermal gold project comprises WNW to NW trending subvertical silica ledges referred to as Ana Zone, Batı Zone and Keşif Zone which are hosted within intensely altered dome-like andesitic body. Silica veins which crosscut the dome-like andesitic body are controlled by oblique-slip normal faults. Ana zone is the widest and longest silica ledge which striking N 50–80° W and dipping 60–70° SW. Alteration typically changes outwards from silica to quartz-alunite and quartz-kaolinite, illite-chlorite and smectite-chlorite respectively, which reflects the decreasing temperature and the increasing pH of the hydrothermal fluid. The vuggy and sugary quartz host the gold mineralisation in the main zone, and show outward transition to advanced-argillic and argillic alteration zones, typical of the outflow path of a high sulphidation epithermal system in which alteration and gold precipitation is controlled by mainly pH and temperature changes. Chalcedony after opal is also present in the eastwards of Ana East section.

Doğanbey alteration zone is located near the side of the eroded stratovolcanoapproximately 15 km NE of İnlice deposit. Doğanbey prospect is believed to have similar potential to İnlice and is in the focus of continuing exploration. The silica alteration is largely represented by opalisation of andesitic and dacitic volcanic rocks that are covered by unaltered rhyodacitic lavas. Beneath the opalised horizon the pyroclastic volcanic rocks in andesitic to dacitic composition were crosscut by structurally controlled quartz-alunite ledges. Kaolinite dominated illite-bearing alteration widespreadly outcrops between the quartz-alunite ledges. Advanced argillic alteration is represented by vuggy quartz with infilling alunite, kaolinite and hematite.

The anomalous gold grades up to 0.6 gr/t encountered at Doğanbey, occur with the network of quartz veinlets with a thickness varies between 1 and 3 mm. Gold is positively corellated with Mo, Sb, Pb, S, As, and S in soil samples and with Mo, Pb, Ag, Hg, Sb, Bi, Cu in rock samples. Further exploration activities including shallow drill programme to test the porphyry and or gold enriched zone are necessary.

4.5 Eastern Black Sea, Pontide Metallogenic Province: Northeastern Turkey

Due to its complex geological dynamics, the Pontide Belt hosts numerous kuroko, porphyry, skarn and epithermal prospects and deposits associated with Late Cretaceous-Mid-Eocene magmatism. The Pontide Belt extends east–west along the Black Sea coast and was formed in the eastern part of Alpine-Himalayan belt between the Rhodopes in the west and the Caucasus in the east. The subduction of the northern branch of the Neo-Tethyan oceanic crust beneath the Eurasian (Laurasian) plate (Okay and Şahintürk 1997; Şengör and Yılmaz 1981; Yılmaz et al. 1997) caused an arc-type magmatism during the Late Mesozoic-Early Cenozoic (e.g., Şengör and Yılmaz 1981; Okay and Şahintürk 1997; Boztuğ et al. 2004, 2006; Rice et al. 2006, 2009; Yılmaz and Boztuğ 1996; Altherr et al. 2008; Çinku et al. 2010; Karslı et al. 2010, 2011, 2012; Meijers et al. 2010; Ustaömer and Robertson 2010; Topuz et al. 2011). This subduction, was followed by collision of the Tauride–Anatolide block with the Pontide and Kırşehir blocks in the Late Paleocene and Early Eocene closing the Ankara–Erzincan branch of the northern Neotethys (Richards 2015). It is also suggested that northward subduction of Paleotethys formed the eastern Pontides orogenic belt during the Paleozoic–Mesozoic (e.g., Adamia et al. 1977, 1981; Dilek et al. 2010; Rice et al. 2009; Ustaömer and Robertson 1997). The Pre-Jurasic basement units are composed mainly of Carboniferous metamorphic rocks, and associated Permocarboniferous granitoids and sedimentary rocks (Topuz et al. 2004, 2007). In this crystalline basement cross-cutting granitoids of the Late Carboniferous age were also recognised previously (e.g., Çoğulu 1975; Dokuz 2011; Kaygusuz et al. 2012; Okay and Şahintürk 1997; Topuz et al. 2010).

Plutonic rocks in Eastern Pontide Belt are dominantly I-type metaluminous, calc-alkaline to high-K and shoshonitic with lesser A-type constituting more than 50% of the present erosion surface of the Eastern Pontides. The emplacement age of these intrusive rocks ranges a time interval from Cretaceous to Paleocene (Delaloye et al. 1972; Giles 1974; Taner 1977; Gedikoğlu 1978; Moore et al. 1980; Jica 1986; Okay and Şahintürk 1997; Yılmaz et al. 2000; Köprübaşı et al. 2000; Yılmaz-Şahin 2005; Boztuğ et al. 2006; Kaygusuz et al. 2008, 2009; Boztuğ 2008; İlbeyli 2008; Kaygusuz and Aydinçakir 2009) and the *Eocene* (Boztuğ et al. 2004; Arslan et al. 2004; Yılmaz-Şahin 2005; Topuz et al. 2005; Karslı et al. 2007).

The Pontide Belt is divided into three zones by Bektaş et al. (1995) and Bektaş et al. (1999) as the northern, southern and axial zones, based on their characteristic tectonic and lithological features. Konak et al. (2009) proposed to divide Eastern Pontides into two zones as northern/outer and southern/inner zones on the basis of geochemical, geochronological and tectono-magmatic features. The Northern zone is characterised dominantly by arc-related igneous rocks of Late Mesozoic and Cenozoic volcanic and volcanoclastic rocks. The occurrences of VMS deposits and some porphyry type mineralisation are usually attributed to the formation of the Late Cretaceous arc related igneous activity in the region. Post-collisional Early to

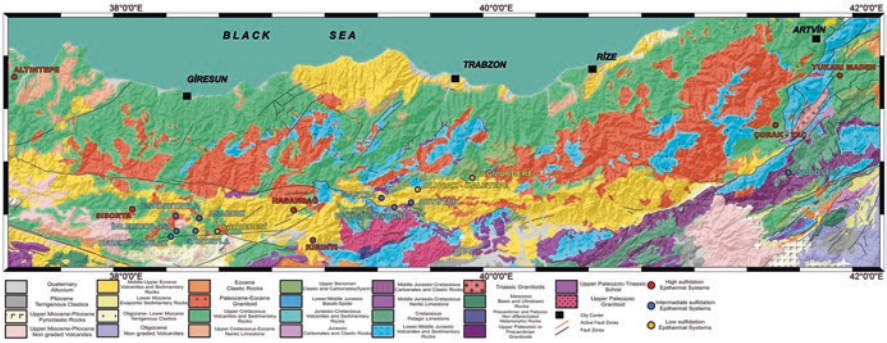

Fig. 4.4 Regional geological map of Eastern Pontides and spatial distribution of significant epithermal mineralisation. (Geology modified from MTA Emre et al. 2013; Akbaş et al. 2017)

Late Eocene volcanic and plutonic rocks are very important in terms of hosting porphyry and epithermal mineralisation and prospects in the Southern Zone of the eastern Pontides orogenic belt (Fig. 4.4) (Akçay and Gündüz 2004; Yiğit 2009; Eyüboğlu et al. 2014; Richards 2015).

The Pontide Belt is considered to be the most important lead-zinc-copper metallogenic province of the Turkey. Porphyry and epithermal deposits are also common, however, just few of them are of economic interest. Below, brief geological data are given on selected epithermal systems (e.g., Mastra, Hasandağ, Sisorta, Arzular, Olucak, Eskine, Etir, Asarcık, İnler) scattered mainly on Southern Zone of the eastern Pontides orogenic belt. The Altıntepe, Bahçecik, Midi, Kırıntı, Aktutan, Taç and Çorak are the other important mineralisation in this belt (Fig. 4.4).

4.5.1 Mastra

The Mastra Gold Mine is located approximately 5 km northwest of Gümüşhane, in the southern zone of East Pontides (Fig. 4.4). Although it has been known since the 1980s, the mine commenced open pit production in May 2007 and underground mining in 2008. The ore production is carried out by open pit and underground mining until the open pit production was terminated at the end of 2013. Porphyritic andesitic lavas and volcanoclastic rocks of Eocene age are the most widespread rocks in the area. Andesitic lavas gradually change to pyroclastic rocks towards the north and to agglomerates towards the south. Andesitic lavas are unconformably overlain by Eocene sedimentary rocks. The ore vein is envelopped by the intense argillic alteration which overprint porphyritic andesites. Outwards from argillic alteration zone, a propylitic alteration zone is present changing gradually to unaltered andesitic volcanics. Mineralisation and associated argillic alteration at Mastra are controlled by NW-SE striking and NE dipping structures. Occurences of barite

and alunite confirm that higher oxidition and sulphidation states are present in the evolutionary history of the deposit (Bilir 2015; Bilir and Kuşçu 2016). In addition to barite and alunite, characteristic minerals of acid-sulphate alteration (e.g., kaolinite, jarosite and gypsum) were found in the alteration assemblage (Tüysüz et al. 1995). However, adularia-sericite were identified as main gangue minerals in the boiling zone with bladed calcite. Mineralisation at the Mastra deposit is divided into two stages. The first stage is represented by galena and sphalerite with lesser chalcopyrite, pyrite, argentite and tetrahedrite-tennantite. The second phase is dominated by native gold, pyite and chalcopyrite. Detailed fluid inclusion studies from two stages of quartz related to gold mineralisation have been realized by Tüysüz et al. 1995. In this study the homogenisation temperatures ranging from 160 to 340 °C with salinities ranging from 4.1 to 10.9 wt.% NaCl equivalent. Similarly more recent fluid inclusion study shows that the ore forming solution varies in temperature between 113 and 390 °C (Aslan and Akçay 2011). Free gold in Mastra was formed in association with quartz predominantly in the native state with lesser amounts as electrum. The ore and alteration mineral assemblages in association with ore textures and fluid inclusion data are consistent with a low-sulphidation epithermal environment.

4.5.2 Hasandağ

The Hasandağ epithermal gold mineralisation located 20 km northeast of Alucra (Giresun) (Fig. 4.4). The Hasandağ mineralisation is hosted in Eocene volcanic rocks including andesite, dacite andesitic tuff, brecciated andesite and andesitic dykes in the southern zone of East Pontides. The volcanic succession is crosscut by intrusions varying in composition from quartz-monzodiorite to syenogranite. The volcanic and intrusive rocks of the area have experienced several stages of intense hydrothermal alteration. It seems like that the intrusions of felsic magma along the fracture zones prompted advanced argillic alteration due to high temperature, acidic fluids and associated diatreme formation. Silicification and argillisation are widespread as the main types of hydrothermal alteration (Acarlıoğlu et al. 2013). Field and paragenetic studies demonstrate that centres of acid-sulphate-altered rock are internally zoned and transition outward from argillic (smectite ± illite) into propylitic zones (chlorite ± epidote ± sericite ± calcite). Vuggy quartz dominated silicification with advanced argillic to argillic alteration which formed due to the leaching of host rocks by hot acidic hydrothermal fluids are indicators of high-sulphidation type mineralisation (Acarlıoğlu et al. 2013). The ore minerals are pyrite, native gold, hematite, goethite-lepidochrosite (Acarlıoğlu et al. 2013; Bilir 2015). Iron oxide alteration dominated by hematite and goethite is associated with higher gold assays indicating gold enrichment via supergene alteration.

4.5.3 Sisorta

The Sisorta epithermal mineralisation is located in 120 km northeast of Sivas and 60 km southwest of Giresun city (Fig. 4.4). Igneous rocks of Eastern Pontide arc varying ages between Late Jurassic to Pliocene with different composition and facies unconformably overlie the metamorphic basement and cover large areas in the region. The calc-alkaline volcanics of Late Cretaceous are characterised by andesitic dacitic lava, agglomerate and tuffs. Andesite and andesitic tuffs are the main volcanic rocks, which host the HSEM and the associated alteration. The volcanic successions are intruded by stock-like intrusions ranging from quartz-monzonitic to monzo-gabbroic in composition.

Sisorta alteration system covers a large area of more than 5 × 5 km and displays typical features of the HSEM systems, including vuggy silica lithocap, underlain by advanced argillic style alteration, high level multi-stage phreatic and hydrothermal breccias and associated intrusions. Gold is enriched at the top of the HSEM system, and is localised within silica cap which is surrounded by the advanced argillic alteration assemblage dominated by alunite, dickite, kaolinite, pyrophyllite and diaspore.

Post-mineral faults are responsible for secondary enrichment of gold and oxide and sulphide assemblages (Bilir 2015). In hydrothermal breccia zone, the silica cap with the significant gold assays comprises pyrite, chalcopyrite, barite and hematite. The lithocap represents the largely oxidised, gold enriched top of the system, and is underlain by less oxidised mineralisation enriched at depth. Petrographic studies indicate that Sisorta deposit includes fine to medium grained pyrite with some chalcopyrite, and tetrahedrite-tennantite group minerals with minor enargite.

$^{40}Ar/^{39}Ar$ age dating is ranging from 78.85 ± 0.94 to 76.59 ± 2.19 Ma as a plateau age and 78.25 ± 0.42 and 75.30 ± 0.90 Ma as an isochron age in K-alunite, 80.44 ± 0.84 in hornblende minerals from unaltered andesitic volcanic rocks. This shows that hydrothermal gold mineralisation was deposited 3 Ma later than the volcanic host rock eruption (Şahin Demir and Uçurum 2016).

4.5.4 Arzular

Arzular is hosted in the Eocene volcanic rocks in the southern part of the Eastern Pontides Orogenic Belt (Fig. 4.3). The Eocene volcanic sequences around the project area are subduction related basaltic-andesitic volcanic and associated pyroclastic rocks. These volcanic sequences are the final products of Early Cenozoic adakitic magmatism and cut by non-adakitic granitoid intrusions. The alteration and associated mineralisation are formed under the control of NE-SW and NW-SE striking fault zones (Akaryalı and Tüysüz 2013; Bilir 2015). The E-W trending fracture zone where the LSEM emplaced in, extends over 400 km along its strike and dips about 70 to the north. The thickness of quartz veins varies from 10 cm or less up to 50 cm. In the early stage of silicification, the quartz-chlorite assemblage is not associated

with significant mineralisation. However, in the later stage of silicification, quartz is formed in association with sulphides dominated by pyrite and gold (Bilir 2015).

Fluid inclusion petrography and vein mineral textures are the indicatives of boiling conditions in an open system (Akaryalı and Tüysüz 2013). The homogenisation temperatures for fluid inclusions from quartz vary from 130 to 295 °C, with an average of 214 °C. Ice melting temperatures ranges from −2.6 to −8.6 °C, and the corresponding salinities of the inclusions are 4.3–12.4 wt.% NaCl eq. Sphalerite crystallisation was achieved at a temperature between 90 and 133 °C from hydrothermal fluids with a salinity in a narrow range between 0.7 and 2.7 wt.% NaCl with a mean of 1.7 wt.% NaCl eq. (Akaryalı and Tüysüz 2013). The O and H isotope compositions of sericite and quartz suggest derivation of hydrothermal fluids from mixed sources including magmatic, metamorphic and meteoric waters.

The main ore minerals are native gold, silver, galena, sphalerite, chalcopyrite, fahlore minerals, pyrite and covelline, and associated gangue minerals are calcite, quartz, clay and gypsum. Gold commonly occurs as native Au intimately associated with chalcopyrite or as isolated grains, and ranges in size from 1 to 15 mm. The Fe content of analysed sphalerite ranges between 0.54 and 1.76 wt.%, corresponding to FeS contents of 0.85–2.77 mol%. The range of FeS content between 0.85 and 2.77 is comparable with those of the lower limit of the ISEM systems ranging from 1 to 20 mol% FeS.

4.5.5 Olucak

This property is situated within the central part of the Eastern Pontides. The property is located approximately 100 km South-southwest of Trabzon and 13 km northeast of Gümüşhane (Fig. 4.4). Silicified zones hosting anomalous gold-silver and associated base metals were originally identified by MTA in 1990 by stream sediment sampling surveys.

The Early to Middle Lutetian basaltic–andesitic lavas and their pyroclastic equivalents widely crop out in the area. The Early to Middle Lutetian volcanic sequence was cut by Late Lutetian non-adakitic granitic intrusions. The vein and veinlet zones are hosted by altered andesitic and dacitic volcanic rocks. Silicified zone extends for 600 m along strike with a thickness up to 50 m until it is covered with overburden. Intermediate argillic alteration is widespread in the andesitic lavas and represented by illite and smectite with lesser kaolinite. Phenocrysts of plagioclase, hornblende and biotite are replaced by clay minerals. The argillic alteration grades outwardly propylitic alteration. Epidotisation is the most prominent alteration with chloritisation in basaltic lavas.

Mineralisation and associated alteration are mainly controlled by sets of NW-SE trending strike slip and oblique faults typically dipping at high-angles between 70 and 90°. Pyrite, chalcopyrite, sphalerite, fahlore group, galena are the major sulphides in gold-bearing veins. Hematite, limonite, bornite, covellite, chalcosite and digenite are observed as supergene enrichment. Quartz, barite, sericite, calcite,

adularia, illite and kaolinite are the main gangue and clay minerals of the veins. Epithermal textures including crustiform banding, comb textures, alteration mineralogy and patterns and geothermometres of fluid inclusion studies are indicative of low sulphidation epithermal system (Bilir 2015).

4.5.6 Eskine Yayla

Granitoid rocks in the Eskine Yayla area (Şebinkarahisar), host polymetallic (Pb, Zn, Cu, U) vein-type mineral deposits (Fig. 4.4). The host granitic rocks belong to the Upper Cretaceous–Middle Eocene metaluminous, subduction-related plutonic rocks composed of quartz syenite, syenite, granite, monzonite and quartz monzonite. The veins are dispersed in an area of about 1 km^2. The strikes of the veins are N 75–85° E with dips of 70–80° SE. The veins extend for about 10–200 m with thicknesses of 10 cm and 3 m. Sphalerite, galena, pyrite and chalcopyrite are the most common ore minerals in the vein paragenesis of Eskine Yayla. Fahlore group minerals, Bi-sulphides and sulphosalts, green and purple fluorites are present in minor amounts. Quartz is the major gangue mineral with fluorite in some veins and with barite in the rest. Some carbonate minerals are also present. Three successive crystallisation stages of quartz are identified during the formation of vein system. Native gold is recorded in between the crystals of stage II quartz. The homogenisation temperatures are in the range of 200–260 °C concentrating between 220 and 240 °C for quartz I and in the range of 100–200 °C concentrating between 120 and 160 °C for quartz II. The homogenisation temperatures on fluid inclusions in green fluorites range from 160 to 330 °C concentrating between 270 and 300 °C for green fluorite I and between 160 and 190 °C for the green fluorite II. The inclusions from purple fluorites homogenise to liquid in the range between 120 and 220 °C concentrating between 140 and 170 °C. Salinities were 9.5–15 wt.% NaCl equivalent for inclusions trapped within quartz II, 5.0–11 wt.% NaCl equivalent for green fluorites and 7–13 wt.% NaCl equivalent for purple fluorites (Ayan 1991).

4.5.7 Etir Yayla

Etir Yayla veins are hosted in andesite and andesitic breccia of the Upper Cretaceous volcanic succession of the region (Fig. 4.4). Three subparallel vein systems strike mainly N 10–40° W and dip about 80–85° to SW. The longest vein has been traced for more than 300 m. Sphalerite is the most common sulphide in the ore paragenesis which also includes pyrite, arsenopyrite, chalcopyrite, Bi-minerals, fahlore group minerals, and galena. Fluorite is the dominant gangue mineral and most of the fluorite veins have thickness of 1–15 cm with some of them exceeding 50 cm. Both green and purple fluorites are common gangue minerals of the Etir Yayla veins formed under a wide range of temperatures between 110 and 290 °C (Ayan 1991).

4.5.8 Asarcık

The Asarcık intermediate sulphidation type vein system is hosted by granitoids composed mainly of syenite, monzonite (Fig. 4.4). Tourmaline is the most prominent gangue phase with lesser quartz in Asarcık vein system, which is controlled by a steeply-dipping, NW–SE strike-slip fault zone. The vein system has lengths of up to 3050 m with thicknesses varying from a few cm up to 4 m. The strike of the vein is N45–50°W, dipping nearly vertically southwest. Three phases of mineral deposition are recorded: early pyrite-pyrrhotite, and arsenopyrite, intermediate arsenopyrite, chalcopyrite, Bi-minerals and base metals. The highest ore-forming temperatures are with the sulphide minerals including pyrrhotite, pyrite and arsenopyrite associated with quartz I which has higher homogenisation temperature interval mainly scattered in between 320 and 360 °C. On the basis of homogenisation temperatures from sphalerite and quartz III, the main base metal mineralisation is formed in the range of between 130 and 160 °C with salinities between 6.5 and 14 wt.% NaCl equivalent (Ayan 1991).

4.5.9 İnler Yaylası

The İnler Yaylası system is hosted in a series of volcanic rocks of rhyolitic, rhyodacitic, andesitic composition, and consists mainly of veins with strike lengths of between 80 and 450 m. Their thickness vary from 0.5 to 2 m and their vertical extension vary between 100 and 300 me. Sphalerite, galena, chalcopyrite and pyrite are the most common ore minerals. Fahlore group minerals, enargite-luzonite are present as accessory minerals. Quartz and minor carbonates and barite are the main gangue minerals. Inclusions in quartz I are primary, two-phase (L+V), liquid-rich, and irregular to negative crystal shaped, and have homogenisation temperatures ranging from 180 to 330 °C (mainly between 240 and 270 °C). Inclusions from sphalerite have yielded homogenisation temperatures of 160–270 °C, and ranging between 190 and 230 °C (Ayan 1991).

4.6 Ore Mineralogy

Well developed mineralised veins of low-sulphidation epithermal systems provide convenient material for advancing our knowledge of the nature of the vein formation systematics. In a typical low and intermediate epithermal system, ore bodies include veins, veinlets, stockwork, stringer, brecciated and disseminated ore. Precipitation of precious minerals and associated sulphide and sulphosalts is a function of diverse factors including temperature, pressure and redox state of the solution oxygen and sulphur fugacity. Although the elemental association is represented by ore elements such as Au, Ag, As, Sb, Hg, Tl, Te, Pb, Zn and Cu, the mineralogy

of sulphide, sulphosalt and associated gangue minerals are rather complex. Characterisation of gold-bearing ore including the distribution of gold in different mineral phases, grain size, and, if present, the distribution and nature of invisible gold is important for the best method of metallurgical recovery. A rather complex system of fluid circulation seems to have been involved in the genesis of the both intermediate and high sulphidation subtypes, which have a more complex mineralogy and metal suite that includes gold, silver, copper, zinc, lead, bismuth sulphides and sulphosalts that tend to be associated with porphyry systems. Correlations between gold, silver and Te-Se sulphosalts in epithermal deposits has not been studied yet in Turkey.

The total sulphide content is negligible or lower than 5 wt% of the whole vein in LSEM. The gold in some LSEM in western Anatolia is associated mainly with pyrite and subsequently with other sulphides such as galena, sphalerite and chalcopyrite. Although sulphide and sulphosalt contents are in trace amounts in the paragenesis of LSEM their composition and paragenetic relationship with gold and silver minerals furnish important data both in exploration and mine development processes. The ISEM sub-type is characterised by the highest content of base-metals among all the sub-types of epithermal deposits. The Ag/Au ratio is also higher than those of LSEM and HSEM. The most common sulphide minerals in both Au-Ag ISEM and base metal ISEM are galena, sphalerite, pyrite and chalcopyrite. Bornite, arsenopyrite, cubanite, chalcocite, marcasite, hessite, native gold, electrum, tellurides occur in different quantities.

4.6.1 Pyrite

Without a depth limit, pyrite is the most common and widespread sulphide in most of the epithermal systems in Turkey. Different grain size, crystal shape and textures of pyrite in epithermal deposits have been documented in Turkey. It occurs in more than one generation and in general one is formed in the early stages of sulphide precipitation. Crystal morphology of the pyrite may be a useful indicator during exploration. Changes in the crystal morphology of the pyrite from cubes through octahedra to gelpyrite, generally coincides with the changes from barren to mineralised systems (e.g., Mauk et al. 1998).

Porous pyrite of early stages in Efemçukuru is an important host for gold mineralisation. Pyrite, particularly arsenian pyrite and arsenopyrite, are the major sulphides that carry significant quantities of invisible gold. The term “invisible” arises from the fact that one cannot distinguish, by conventional microscopy, between gold chemically bound in the mineral and submicroscopic inclusions (Cabri et al. 2000). The laser ablation inductively coupled plasma mass spectrometry (LA-ICP-MS) has been successfully used for in situ determination of gold and trace elements in minerals and their inclusions in last two decades (Cook et al. 2009; Maslennikov et al. 2009; Large et al. 2009; Sung et al. 2009; Thomas et al. 2011; Ye et al. 2011; Zhao et al. 2011; Winderbaum et al. 2012; Zheng et al. 2013). It has

been inferred that the solubility of Au in nonarsenian pyrite does not exceed few ppm, however Au content increases with As-rich compositions in pyrite growth zones (Cook and Chryssoulis 1990; Wells and Mullens 1973; Sha 1993; Arehart et al. 1993; Fleet and Mumin 1997; Simon et al. 1999; Cline 2001; Pals et al. 2003). The quasi-steady arsenian pyrite in Carlin-type and epithermal deposits has abundant Au contents, because those pyrites are formed at low-temperatures (<250° C) in which disequilibrium conditions and surface defects are pervasively developed (Zhu et al. 2011).

Pyrite is abundant in Efemçukuru with variable morphology and grain size from sub-mm, idiomorphic single and clustered grains, making this deposit worthwhile to study the distribution of invisible gold in pyrite. In Küçükdere, pyrite is common however less abundant than Efemçukuru. The pyrite content is increased with the total sulphide content in certain parts of the deposit. Pyrite is the most common sulphide throughout the deposit, with its subhedral to euhedral cubic and pyritohedron crystals. Laser Ablation studies were performed on pyrites of Efemçukuru and Küçükdere to provide analytical data on precious and trace element composition. Laser Ablation data in Efemçukuru show a positive correlation between Au content and As-rich zones (Oyman et al. 2010). Gold concentration in pyrite and arsenopyrite ranges from below one ppm to several hundred ppm. In HSEM of Turkey, pyrite is the most widespread sulphide in association with gold mineralisation.

4.6.2 Sphalerite

In epithermal deposits the common occurrence of sphalerite provides an additional useful measure of sulphidation state. The mol% FeS in sphalerite coexisting with pyrite or pyrrhotite is continuously variable as a function of sulphidation state (Scott and Barnes 1971; Czamanske 1974); 40–20mol % FeS at low sulphidation states, 20–1 at intermediate sulphidation states, 1.0–0.05 at high, and <0.05 at very high. Unfortunately, there are few studies that document sphalerite compositions in any detail and address the question of equilibrium with iron sulphides (Einaudi et al. 2003).

Sphalerite from both Şahinli and Tesbihdere is very poor in iron. The iron content of sphalerite vary between 0.4 and 1 wt.% Fe which corresponds 0.6–1.4 mol% FeS (Yılmaz et al. 2010). Çiçek and Oyman 2016, reported that the Fe content of sphalerite from Tespihdere is 0.89 wt.%, corresponding to FeS content of 1.41 mol% which is consistent with the data of Yılmaz et al. (2010). The highest Fe concentration of sphalerite in the Koru and Tesbihdere mining districts is in the Kuyutaşı mineralisation where it reaches up to 3.09 wt.% Fe content, corresponding to 4.86 mol% FeS. In general, the Fe content of sphalerite from both mining districts is compatible with the values of intermediate sulphidation epithermal base metal-rich deposits ranging from 1 to 20 mol% FeS, while high sulphidation epithermal deposits usually contain <1 mol% FeS (Shikazono 1974, 2003; Watanabe and Soeda 1981; Einaudi et al. 2003; Yılmaz et al. 2010). Early-stage sphalerite in V. Viraj

(Koru Mining district, Çanakkale), which surrounds and postdates early-stage pyrite, commonly occurs as euhedral to subhedral crystals without distinct exsolutions. Contrary, late-stage sphalerite contains exsolutions of chalcopyrite as tiny blebs and replaces other abundant sulphide minerals such as galena, chalcopyrite and pyrite. The Fe content of late-stage sphalerite vary from 0.71 to 1.12 wt.%, corresponding to FeS contents of 1.12–1.76 mol%.

In Efemçukuru, grains of sphalerite with overgrowths were analysed from North Ore Shoot (N2, 9 spots). The data show that the cores have mean concentrations of 13.5 wt.% Fe, with very high Ag (mean 1880 ppm) and are also rich in Cd (mean 8400 ppm), Sn (mean 180 ppm) and Ga (mean 62 ppm) (Oyman et al. 2010).

In Arapuçandere deposit, the ore assemblages and moderate iron content up to 11 mol% of FeS in sphalerite typically refer to the properties of base metal-rich Ag±Au ISEM. The FeS content of sphalerite ($Zn_{0.85–0.98}Fe_{0–0.11}Cu_{0–0.06}Cd_{0–0.02}S_{0.97–1.03}$) displays an increase towards the deeper levels of the mineralisation (Çiçek et al. 2017). In sphalerite of ISEM, it seems like high Cd contents positively correlated with gold assays.

4.6.3 Fahlore Group

The composition and substitution mechanisms of "Fahlore" group minerals have been used as a petrogenetic indicator of ore forming processes in epithermal environments. The composition of fahlores and its evolution could be used as an important guide to follow up the flow pattern and fluid evolution with respect to time and space. Chemical evolution of fahlores from porphyry to epithermal systems is determined in mining districts all over the world.

Such sulphides, including the relatively high-sulphidation state minerals tennantite-tetrahedrite (Barton and Skinner 1979), are typically rare or absent in low-sulphidation deposits. In Turkish LSEM fahlore group minerals are rare and tetrahedrite is the dominant fahlore mineral. Up till now, mineral chemistry on sulphide and sulphosalts including fahlore group minerals are based on SEM and EDS analysis. In Ovacık and Küçükdere LSEM fahlore group minerals are represented by tetrahedrite. Tetrahedrite at Ovacık is associated with chalcopyrite, bornite and gold with lesser galena and sphalerite. At the Ovacık gold deposit, tetrahedrite–tennantite is represented by Sb–Ag-rich tetrahedrite (26.7–29.6 wt.% Sb, 1.3–2.5 wt.% Ag, 29.5–33.9 wt.% Cu, 1.5–2.7 wt.% As), with minor As-rich tennantite (14.6–19.6 wt.% As, 0.4–0.9 wt.% Ag, 33.9–34.8 wt.% Cu, 2.3–3.9 wt.% Sb). It is clear that some paragenetic overlap occurs between bornite and tetrahedrite, since these minerals enclose one another (Yılmaz et al. 2007). In Küçükdere, tetrahedrite (20 wt.% Sb; <5 wt.% As) replaced chalcopyrite both of which are replaced by the late stage sphalerite.

Minerals of tetrahedrite-tennantite solid solution series are more abundant in intermediate sulphidation assemblages in western Turkey. ISEM with fahlore group minerals are more common in accordance with their higher base metal content and

sulphidation state. Fahlore group minerals in ISEM are closely associated with precious metal tellurides and/or gold-silver alloy (e.g., electrum). Fahlore group minerals in Koru, Tesbihdere and Şahinli ISES were studied using SEM in the beginning of 2010s.

It has been inferred that the fahlore group minerals such as goldfieldite, tellurian tennantite and extreme "Cu-excess" tennantite and tetrahedrite are indicative of high-sulphidation, enargite/luzonite-bearing assemblages and a very close association with native gold (Repstock et al. 2015).

4.6.4 Gold and Silver

Native gold and electrum either as free grains within gangue or associated with sulphides, sulphosalts, tellurides and selenides are the main gold phases which have been identified in the epithermal deposits of Turkey. Efemçukuru has a more complex paragenesis due to multiple pulses of fluid in a short period of time with different geochemical character even in the same zone (SOS, MOS or NOS) of the vein system. Although native gold occurs associated with all sulphides, pyrite is the most common gold-host followed by galena, sphalerite, chalcopyrite and arsenopyrite in descending order. In SOS, we observe that gold is tied to galena (notably where relictic galena is present in sphalerite), as droplet-shaped inclusions up to 50 μm in size. In MOS, gold in association with silver minerals is present in pyrite, especially in the porous bands, as sub-rounded to elongate grains, up to 10–20 μm in size (Fig. 4.5a, b). In NOS, native gold is present in arsenopyrite as sub-5 μm-sized grains.

As documented in most of the epithermal systems free gold is present chiefly in pyrite as is the case for the Küçükdere deposit. Pyrite is the main sulphide in Küçükdere including gold and some tellurides dominated by hessite (Fig. 4.5c, d). In Çoraklık, our preliminary petrographic studies show that in high-grade samples, gold is intimately associated with silver minerals and sulphosalts in sulphides including pyrite, chalcopyrite, galena and sphalerite (Fig. 4.5e). Gold distribution and associated fluid flow is well documented in the Ovacık deposit. Both electrum and native gold are associated with sulphides at certain depths below the current topographic level. It seems like that the base metal zone is related to the boiling zone at least along 300 m vertically. Detailed mineralogical studies combined with geochemistry showed that gold is associated with chalcopyrite more than other copper minerals including bornite and tetrahedrite and tennantite in Ovacık (Fig. 4.5f). In the Red Rabbit Project a relatively simple ore mineralogy has been documented by Yılmaz et al. (2013). Pyrite is the essential sulphide where the sulphides are in trace amounts in the vein paragenesis. Gold is commonly found as individual crystals or in association with acanthite.

ISEM are characterised by high Ag:Au ratios and base metal content. Silver mineral assemblage is well documented in the Koru and Tesbihdere mining districts by Çiçek (2013) and Çiçek and Oyman (2016). In Koru, the Kuyutaşı mineralisation

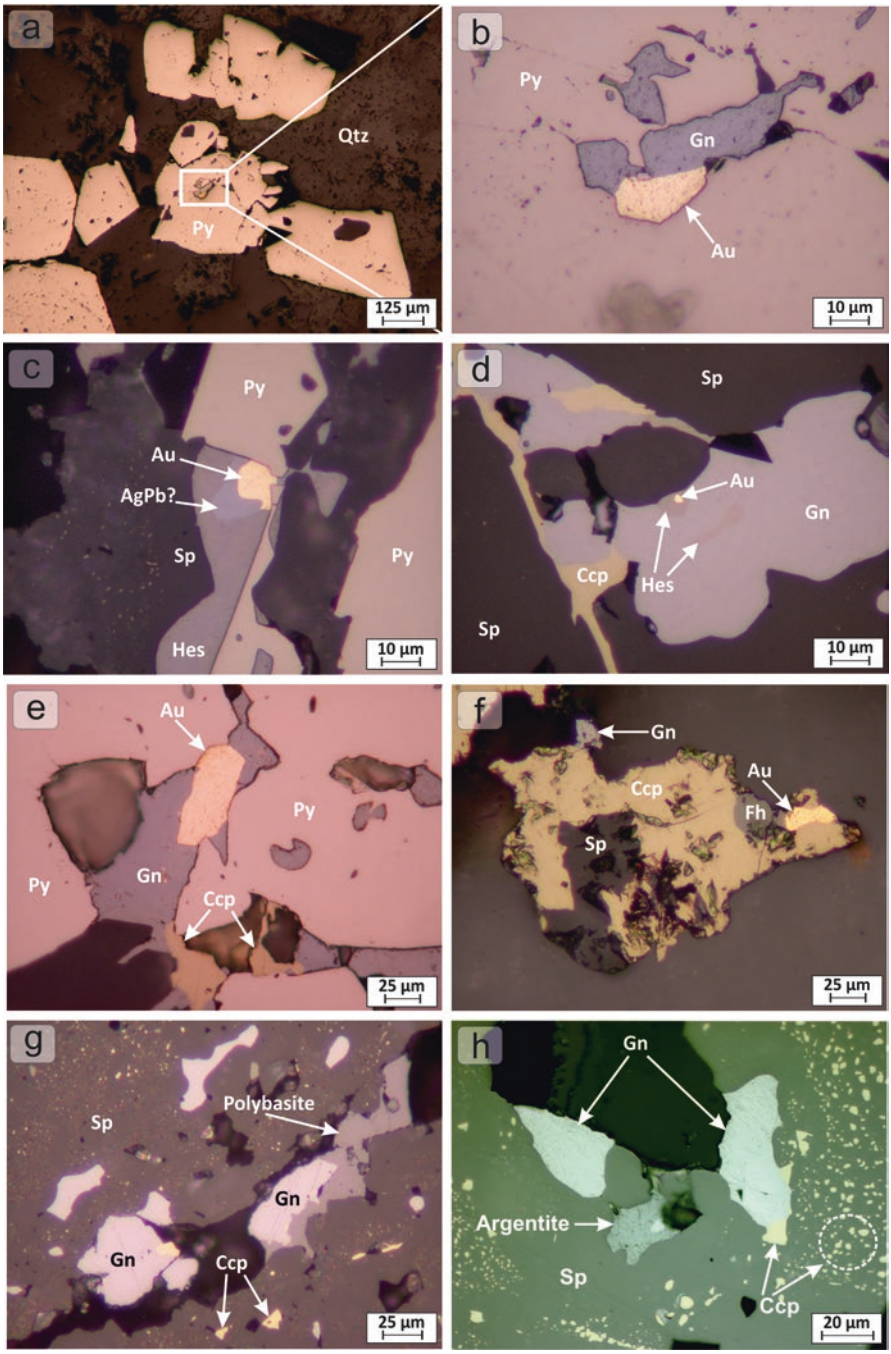

Fig. 4.5 Photomicrographs under reflected light (//N), showing textural relationships between Au-Ag minerals and associated sulphide minerals at the selected epithermal deposits. (**a**, **b**) Gold in association with silver minerals in pyrite (Py) in Middle Ore Shoot of Efemçukuru gold deposit.

commonly contains Ag-sulphosalt, up to 80 μm in size, which occurred as cavity-filling in pyrite in the later stages of the mineralisation. The Kuyutaşı mineralisation comprises pearceite type Ag-sulphosalt, which has lower Sb (0.29 wt.%) and As (4.16 wt.%) contents. Furthermore, fine-grained gold ranging between 1 and 6.5 μm in size is usually found as free grains in association with euhedral quartz. The abundance of gold and silver tends to increase with the increase in copper ore at depth (Çiçek 2013). At Şahinli, economic concentrations of Au occur mainly within quartz-rich veins whereas higher Ag concentrations are associated with base metal-rich quartz veins, particularly those rich in Pb.

Argentite, acanthite, jalpaite, polybasite-pearceite, freibergite and Ag-rich tetrahedrite-tennantite are the most widespread Ag-bearing sulphosalt minerals in the overall Arapuçan vein zone. They are associated with late stage mineralisation, and mainly occur either as fracture-fillings, or as haloes surrounding the early sulphides. Gold occurs as rounded-shaped inclusions within chalcopyrite and galena, and present variable Au and Ag contents. Electron microprobe measurements also have shown that most gold grains are compositionally zoned. Gold grains present a marked variation in their contents in Cu, Fe and S, as a function of their host sulphide and sulphosalt phases (Çiçek et al. 2017).

4.7 Epithermal Textures and Associated Minerals

The recognition and interpretation of textural features of epithermal systems and to be able to determine the physical and chemical environments where the hydrothermal fluids circulate is one of the important approaches in exploration. In epithermal systems, varieties of silica with carbonates are the main gangue minerals. The carbonates mainly consist of calcite with rhodonite, ankerite and siderite. Multiphase calcite generations are found in most of LSEM and ISEM systems in Turkey. While barite is found in some ISEM in Koru Mining district of the Biga Peninsula, fluorite is abundant in epithermal deposits in the Şebinkarahisar area in the Black Sea Region.

Boiling is often temporally and spatially associated with gold and silver mineralisation in epithermal systems and the boiling horizon also outlines a possible precious metal zone in an epithermal system where rising magmatic fluids mix with oxidising near surficial groundwater. Occurrence of hydrothermal breccias is

Fig. 4.5 (continued) (**c**, **d**) Euhedral gold and some tellurides dominated by hessite (Hes) is present chiefly in pyrite as the main sulphide with galena (Gn) and sphalerite (Sp) in Küçükdere. (**e**) Gold and sulphide association after pyrite represented by enclosed gold (Au) in galena in Çoraklık. (**f**) Positive correlation between gold and copper is emphasized by the close relationship between chalcopyrite (Ccp) fahlore (Fh) and native gold (Au) in Ovacık. Galena and sphalerite are the common accompanying sulphides. (**g**) Silver minerals are represented by native silver, acanthite, polybasite and pearceite in Tesbihdere. (**h**) In Arapuçandere argentite is one of the dominated silver minerals in association with galena and sphalerite.

regarded as an evidence of boiling. Hydrothermal breccias are formed when hydrothermal fluid exceeds the lithostatic pressure, resulting in the fracturing of the rock showing typical jig-saw structures. Beside brecciation, quartz veins in the epithermal environment are characterised by multiple generations of chalcedonic, microcrystalline, and comb-textured quartz exhibiting crustiform and colloform bands and cockade overgrowths.

The style of carbonate occurrences in epithermal deposits is discussed broadly in some papers and examples mentioned in economic geology literature. In epithermal systems, carbonates assemblages are composed mainly of calcite with rhodochrosite, ankerite with lesser amounts of siderite. Multistage calcite generations are found in both LSEM and ISEM systems. Either as barren or as boiling-related calcite is a widespread mineral in epithermal systems in western Anatolia. As long as boiling continues, volatiles such as CO_2, H_2S, CH_4, SO_2, SO_4 are lost to the steam phase along the open system up to the paleosurface. Partitioning of CO_2 in the steam phase causes precipitation of calcite and a rise of pH in the remaining solution. Thus the occurrence of bladed calcite is accepted as evidence of boiling in epithermal systems. Microthermometric studies on bladed calcite would guide us to approach the true trapping temperatures. Although calcite is a widespread gangue in LSEM and ISEM bladed-like texture is more likely developed in classic LS epithermal vein deposits. In some epithermal deposits including Küçükdere, Çoraklık, Ovacık, Efemçukuru, Çukuralan and Kepez (Red Rabbit) carbonates are the most common gangue minerals in association with quartz. Küçükdere is one of the best examples of LSEM with its carbonate content and carbonate paragenesis. Calcite, ankerite, rhodochrosite are the most common carbonates in and around the veins. Most of the rhodochrosites are at and near the surface, well developed examples of bladed calcite were found in the Karayanık vein in Küçükdere. Replacements of bladed calcites pseudomorphly by silica were not observed. This observation suggests that bladed calcite formation is the latest hydrothermal event in the mineralisation. Parallel type bladed calcites vary in thickness from 0.3 to 2 mm. Lattice type bladed calcites were formed as thin and discontinuous lamellas. There are at least four stages of calcite precipitation in Karayanık Tepe. Early calcites (Cal I) tend to be thicker, reaching a maximum thickness of 2 mm and range in length from 0.3 to 2 cm (Fig. 4.4a). The early calcites (Cal I and Cal II) show bright blue or yellow colours of the fourth and fifth orders in thin section. The later calcites which form as lattice type bladed crystals range in thickness from 20 μm to about 800 μm. Under the microscope, calcites from the third and fourth generations (Cal III and Cal IV) are pale brown or grey colours. Although not widespread as in Küçükdere and Çoraklık, in Ovacık calcite, ankerite and siderite are the most common carbonates associated with mineralisation. Networks of intersecting blades of calcite were replaced by quartz. Lattice-bladed carbonate replacement texture is well developed in Karadüz area in Kızıltepe vein system (Sındırgı-Balıkesir).

The crustiform texture is usually interpreted to represent episodic rapid nucleation that occurs as a result of intermittent boiling and changes in pressure (Taylor 2009). The crustiform textures in the veins system are represented by rhythmic alternation of bands different mineral proportions dominated by cryptocrystalline

quartz, calcite, manganese-bearing calcite, sulphides, rhodochrosite and rhodonite with lesser amounts of adularia. Crustiform texture is the most widespread texture in Germe Tepe vein. Calcite is the major constituent of some veins (e.g., Germe Tepe and Karayanık Tepe) where it precipitates in different stages of vein formation either as bladed, crustiform or infilling forms. The mineralogy of crustiform textures gives important clues about the formation of precious mineral deposition in epithermal deposits. In the Efemçukuru, complex crustiform texture shows successive bands with different orientations and defined by differences in mineralogy or colour. Calcite is an abundant carbonate with rhodochrosite in concentric and banded vein formations. Calcite bands of the concentric structures are replaced by euhedral crystals of manganaxinite and tinzenite (Oyman et al. 2003). Cockade structures are widespreadly occurred. Drusy quartz is commonly occurring in the cavities, vugs either in breccia or in crustiform bands.

The study of textural features of hydrothermal breccia is one of the requirement to be able to ascertain the chronology, mechanism and classification of ore deposition. Hydrothermal breccias are commonly observed in veins that were formed close to the surface where it is favourable for brittle deformation (Genna et al. 1996). As mentioned a boiling occurs when pressure drops due to fracturing when fluid pressure exceeds lithostatic pressure.

Critical fracturing is related to the destruction of the equilibrium between the pressure of the fluid and the regional stress within a vein (Hobbs 1985). High fluid pressures and the local structural context combine to maintain open the hydrothermal channelways, enabling hydraulic fracturing within the vein (Phillips 1972). Fluid pressure decreases in response to a sudden opening of space generated by rapid slip or by the intersection between different veins. Within the vein system, repeated episodes of brecciation due to cyclic self-sealing and overpressuring could result in the multi-phase enrichment of gold. One of the most diagnostic feature of epithermal breccias is the widespread occurrence of fine grained chalcedonic quartz both as replacement of fragments and a cement between fragments (Sillitoe 1985). Rock-flour is silicified in most of epithermal system-related breccia. The lithology of fragments, rock flour and intensity of silicification of both matrix and fragments are controlled by various factors (e.g., depth of the system, duration of the hydrothermal activity, permeability of surrounding rocks, and inclination of the vein).

The clast-supported breccia is composed mainly of wall-rock fragments in some LSEM and ISEM such as Küçükdere and Efemçukuru. As observed in most LSEM systems (e.g., Ovacık, Red Rabbit, Küçükdere) clasts of vein material, cemented by silica or other materials including sulphides are commonly due to hydraulic fracturing or to multiple generations of quartz. The Ovacık examples of clast-supported crackle (shattered) breccia with monomictic fragments and matrix-supported fluidised (milled) breccia with angular to subrounded polymictic fragments have been well documented in Yılmaz et al. (2007). Examples of cockade breccias are also well documented in Efemçukuru, Red Rabbit, and Küçükdere deposits. The Efemçukuru deposit provides an exceptional example of mineralised breccias, and in particular cockade breccias. The cockade breccias varying in size from few centimetres up to decimetres were observed in various depths in Kestanebeleni vein

system in Efemçukuru. In Efemçukuru, the fragments which formed the nuclei of the breccias are composed mainly of hornfels which formed by the contact metamorphism of pelitic rocks of the Bornova Flysch Formation. Low permeability of the hornfels is diminished in time as a result of repeated silicification during the active period of the Efemçukuru hydrothermal system. The fragments of hornfels are coated by alternating manganaxinite–tinzenite, rhodonite, rhodochrosite, quartz and calcite bands to form cockade textures (Oyman et al. 2003). Significant rotation of clasts was observed.

In Germe Tepe (Küçükdere), cockade textures composed mainly of concentric layers of quartz were formed around the nucleus of the propylitically altered andesite breccia fragments. Gangue minerals are mainly quartz, calcite and Mn-oxides with lesser barite. In Çengel Tepe (Küçükdere), relatively coarse (up to cm in length) crystal aggregates of quartz have a comb-like radial disposition around the nucleus of the phyllic altered andesite breccia fragments. The cockades are interpreted as reflecting the occurrence of hydraulic fracturing within open-space domains (Genna et al. 1996). Matrix or clast-supported hydrothermal breccia with angular-subround monomictic to polymictic fragments is also common. Best examples of hydrothermal breccias were observed in Çoraklık Tepe vein system. In between 50 and 150 m of depth in drillholes well developed matrix-supported breccias are thought to have formed during repeated brecciation. Angular to sub-angular clasts of the breccia composed mainly of calcite and bladed-calcite indicate boiling and related self-sealing.

4.8 Fluid Inclusions

Due the limited space in most of the recent papers on epithermal deposits in Turkey, fluid inclusion studies are not fully considered or represented. The fluid inclusion data from epithermal mineralisation in Turkey are summarized in Table 4.1. Fluid inclusion studies were performed mainly on LS and IS type epithermal systems in Turkey. One of the most crucial features related to boiling hydrothermal fluids are the fluid inclusion assemblages trapped from the boiling horizon to the surface. Coexisting liquid-rich and vapour-rich inclusions of a same paragenetic stage is accepted as one of the most reliable evidence of boiling. It should be taken into account that boiling causes higher homogenisation temperatures than the true trapping temperatures. These coexisting inclusions indicate trapping also in an immiscible fluid environment. As mentioned earlier, the occurrence of platy or bladed calcite is a good indicator of boiling conditions (Browne 1978; Simmons and Christenson 1994), consistent with the occurrences of some coexisting liquid-rich and vapour-rich inclusions (Bodnar et al. 1985). Therefore, it is believed that homogenisation temperatures obtained from calcite represent true trapping temperatures, excluding the need for pressure corrections. The lattice-bladed calcite could

Table 4.1 Selected fluid inclusion data for the epithermal mineralisation in Turkey

Deposits	Type of inclusions	$T_{H\ (°C)}$		$T_{H\ (°C)}$ ort	Salinity (wt.% NaCl)		Salinity ort	Tm_{first}	Minerals	References
Şahinli	Primary	180	321	–	0.5	7.7	–	–	Quartz	Yılmaz et al. (2010)
		229	321	–	2.6	7.6	–	−24.5 to −19.0	Sphalerite	
Alakeçi-Kısacık	Primary	148	389	241.3	0.1	6.5	2.6		Quartz	Vural (2006)
Kuşçayırı	Primary	192	370	294	0	31.2[a]	2.7		Quartz	Vural (2006)
Sındırgı	Primary	150	395	250	0.2	4.8	1.8	−20 to −33	Quartz	Yılmaz et al. (2013)
Ovacık	Primary	147.6	298.3	187.3	0.7	2.1	1.4	–	Quartz	Yılmaz et al. (2007)
Narlıca	Primary	205	303	236	0.1	0.8	–	–	Quartz	Dag (1993) and Ebert (2004)
Kaymaz	Primary	238	389	319.7	0.3	14	–	−72.1 to −49.6	Quartz	Yavuz (2013)
Arzular	Primary	130	295	214	4.3	12.4	8.5	−30.2 to −36.4	Quartz	Akaryalı and Tüysüz (2013)
		90	133	109	0.7	2.7	1.7	−32.4 to −37.2	Sphalerite	
Arapuçandere	Primary	150.2	438	–	0	34.0	–	−37.5 to −10.1	Quartz	Orgun et al. (2005), Bozkaya et al. (2008) and Bozkaya and Banks (2015)
		186	384	–	1.7	29.2	–	−30.8 to −12.4	Sphalerite	
		206.1	321.9	263.6	22.5	29.6	27.1	−31.4 to −20.1	Calcite	
	Secondary	193.7	354.4	278.2	13.6	27.5	22.7	−28.1 to −9.7	Quartz	
		139.8	345.2	279.2	14.3	32.0	22.7	−34.9 to −10.3	Calcite	
Kartaldağ	Primary	135	285	–	0	1.7	–	–	Quartz	Ünal-İmer et al. (2013)
	Secondary-pseudosecondary	93	279	–	0	1.4	–	–	Quartz	
Madendağ	Primary	235	255	–	0	0.4	–	–	Quartz	Ünal-İmer et al. (2013)
	Secondary-pseudosecondary	90	285	–	0	0.7	–	–	Quartz	
İnkaya	Primary	235	340	299.8	0.7	4.5	3.0	−32.9 to −49.6	Quartz	Özen and Arık (2015)
Altınpınar	Primary	170	380	–	2.4	7.3	4.7	—	Quartz	Akaryalı (2016)

(continued)

Table 4.1 (continued)

Deposits	Type of inclusions	$T_{H\ (°C)}$		$T_{H\ (°C)}$ ort	Salinity (wt.% NaCl)		Salinity ort	Tm_{first}	Minerals	References
Mastra	Primary	113	331	213.5	0.4	10.2	4.7	−31 to −17	Quartz	Aslan (2011)
		150	390	280.3	0.7	10.1	3.7	−19.5 to 28.3	Barite	
	Secondary	110	240	159.4	2.4	6.6	4.4	–	Quartz	
		218	267	249.0	–	–	–	–	Barite	
Tesbihdere/ Sarıoluk	Primary	152.0	387.0	–	0.2	10.6	–	−58.0 to −25.0	Quartz	Yılmaz et al. (2010), Bozkaya et al. (2014), and Çiçek and Oyman (2016)
		220.0	342.0	266.5	0.7	6.0	4.3	−46.2 to −19.0	Sphalerite	
	Secondary	177.0	333.0	–	–	–	–	–	Quartz	
Koru	Primary	146.0	358.0	254.5	0.2	6.3	2.1	−51.0 to −32.3	Quartz	Çiçek and Oyman (2016)
		191.2	371.5	277.0	2.1	12.5	6.7	−52.2 to −29.5	Sphalerite	
		160.6	407.0	314.6	0.7	11.6	4.2	−54.0 to −34.0	Barite	
	Primary	129.7	159.3	145.0	2.1	9.9	6.8	−55.0 to −49.5	Sphalerite	Bozkaya and Gökçe (2001)
		54.3	79.8	71.3	6.0	11.1	8.6		Barite	
	Secondary	92.8	224.9	129.0	0.9	9.5	4.3		Barite	
Efemçukuru	Primary	174	328	243.1	0.2	9.9	–	–	Quartz	Oyman et al. (2003)
		185	224	211	2.1	4.0	–	–	Sphalerite	
Balcılar	Primary	70	135	102.3	0.0	1.4	0.7	–	Barite	Özdemir (2011)
		142	187	161.8	0.0	2.1	0.8	–	Sphalerite	
		203	286	250.0	6.3	7.2	6.7	–	Quartz	
		135	198.1	167.6	18.1	20.0	19.2	–	Barite	Bozkaya and Gökçe (2007)
		114.7	277.1	200.7	15.8	26.9	21.9	–	Sphalerite	
		71.2	246.8	–	14.0	22.6	18.6	–	Quartz	

[a]Salt value

be observed as being indicator of boiling throughout a wide range of vertical depth in Germe and Karayanık in Küçükdere deposit. The best examples of lattice-bladed calcite bearing samples, were proved of having higher gold values, thus indicating their relationship with the boiling zone. In Karayanık the fluid inclusion studies on the bladed calcites, indicates similar homogenisation temperatures with the adjacent quartz.

Fluid inclusion data indicate that the low-sulphidation deposits (e.g., Ovacık, Red Rabbit) have very low salinity ore-forming fluids. Low salinity (<2 wt%) fluids are responsible for the gold precipitation of quartz and calcite gangue (Albinson et al. 2001). Such low-salinity fluids were incapable of transporting significant quantities of silver and base metals (Henley 1990), explaining their generally low contents in these ores.

In ISEM systems such as Tesbihdere and Koru, Ag sulphosalt minerals (e.g., polybasite, pearceite) are precipitated by saline fluids with about >10 wt% NaCl equiv (Bozkaya et al. 2014; Çiçek and Oyman 2016). In Arapuçandere there are at least two episodes of quartz precipitation. Petrographical studies indicate that euhedral quartz crystals of an early generation were surrounded by sulphide dominant ore minerals representing the main ore phase. Fluid inclusion assemblages in these quartz crystals are good examples of primary fluid inclusions which form when fluid is trapped on the active growth surfaces of a crystal (Bozkaya and Banks 2015). Fluid inclusion data of Orgun et al. (2005) indicate that these veins were deposited at temperatures ranging from 242 to 438 °C with an average of 303 °C in quartz and from 229 to 384 °C with an average of 295 °C in sphalerite. Although salinity of the fluid inclusions had not been measured because of the low salinity and small size of the inclusions, the salinity was estimated between 1.7 and 18.5 wt.% NaCI equivalent by using the temperature-depth diagram. The fluid inclusion measurements of Bozkaya et al. (2008) were performed on primary and secondary inclusions within sphalerite, quartz and calcite, which represent the early and late stage deposition at Arapuçandere. The homogenisation temperatures in sphalerite range from 276.3 to 319.7 °C with an average of 301.4 °C and salinity varying from 16.3 to 29.2 wt.% NaCI equivalent with an average of 18.3 wt.% NaCI equivalent (Bozkaya et al. 2008). These high homogenisation temperature and intermediate salinity were interpreted to indicate sulphide precipitation during the early stage of mineralisation. The later stages are represented by a slightly decreasing homogenisation temperature with increasing salinity which reflects multiple precipitation of quartz (an average of: Th = 240.2 °C and salinity = 25.3 wt.% NaCI equiv.) and calcite (an average of: Th = 263.6 °C and salinity = 27.1 wt.% NaCI equiv.) (Bozkaya et al. 2008). Recent fluid inclusion data of Bozkaya and Banks (2015) shows that fluid inclusions in quartz have very low salinity values varying from 1.7 to 0 wt.% NaCI equivalent and wide ranges of homogenisation temperatures from 360 to 160 °C.

In Efemçukuru the fluid inclusion data indicate a broad range in T_h from about 200 to 300 °C and range in salinity from near zero to about 9 eq. wt.% NaCl. The higher salinities are more common at depth with no apparent difference in T_h with depth (Oyman et al. 2003). Fluid inclusion assemblages in high grade plunges from Kestanebeleni and Kokarpınar contain coexisting liquid-rich and vapour-rich

inclusions with a high varying liquid/vapour ratios indicating the boiling of fluids. Higher homogenisation temperatures (over 300 °C) and moderate salinities (>10 eq. wt.% NaCl) in coexisting liquid-rich and vapour-rich inclusions in Kokarpınar indicating relatively higher temperatures for the boiling and associated gold precipitation in Kokarpınar vein (unpublished data).

Up till now, there no published data are available on fluid inclusions from HSEM in Turkey. Fine grain size of the quartz in such systems is one of the main reasons for the Kartaldağ HSEM homogenisation temperatures associated with mineralisation being in the range of 245–285 °C. The salinities calculated from these fluid inclusions are low.

4.9 Stable Isotopes

In Turkey sulphur isotopes have been widely applied for the study of ore deposits to determine the formation temperatures of sulphide assemblages and the origin of the sulphur in the epithermal deposits. Characteristic intervals of sulphur isotope compositions of some geological environments are given in Fig. 4.6. The $\delta^{34}S$ values of sulphide minerals from various epithermal deposits in Turkey are distributed in the interval of $\delta^{34}S$ values of granitic rocks (Fig. 4.6). Caution should be taken in the use of sulphur isotopes to distinguish between ore deposits originating in sedimentary (e.g., sea water) and igneous environments due to the extensive overlap of $\delta^{34}S$ values (Fig. 4.6). ISEM and HSEM tend to have greater variation in the sulphur isotope composition of ore minerals because of the precipitation of significant quantities of both sulphide and sulphate from the hydrothermal fluids at the time of mineralisation. Low-Fe sphalerite is a characteristic mineral of intermediate sulphidation state with sulphide-rich Ag-Au bearing base-metal veins containing chalcopyrite, pyrite, galena and fahlore group minerals. In most base metal rich ISEM, galena is a common sulphide mineral together with sphalerite. They precipitate contemporaneously in similar conditions in at least one of the ore deposition stage of an individual deposit, implying that the galena-sphalerite pair is a reliable geothermometer. In epithermal systems, pyrite is the most common sulphide which tends to precipitate at different stages and at different temperatures of ore deposition. Similar to pyrite, more than one generation of sphalerite and/or galena precipitation could be responsible for the widely scattered $\delta^{34}S$ values in epithermal deposits. Additionally, in most ISEM systems the broad distribution of sulphide $^{\delta 34}S$ values suggests either a mixture of several sulphur sources or disequilibrium mineralisation in an open system.

Oxygen isotopes have been widely used since the 1970s to determine the nature and source of the fluids associated with oxygen-bearing gangue minerals, alteration and ore minerals in ore deposits. In Turkey since the 2000s some papers including contributions to O and D isotope compositions of ore forming hydrothermal fluids have been published (e.g., Yılmaz et al. 2007, 2010; Çiçek and Oyman 2016). In the final analysis, O and D isotope systematics of hydrothermal fluids can only be

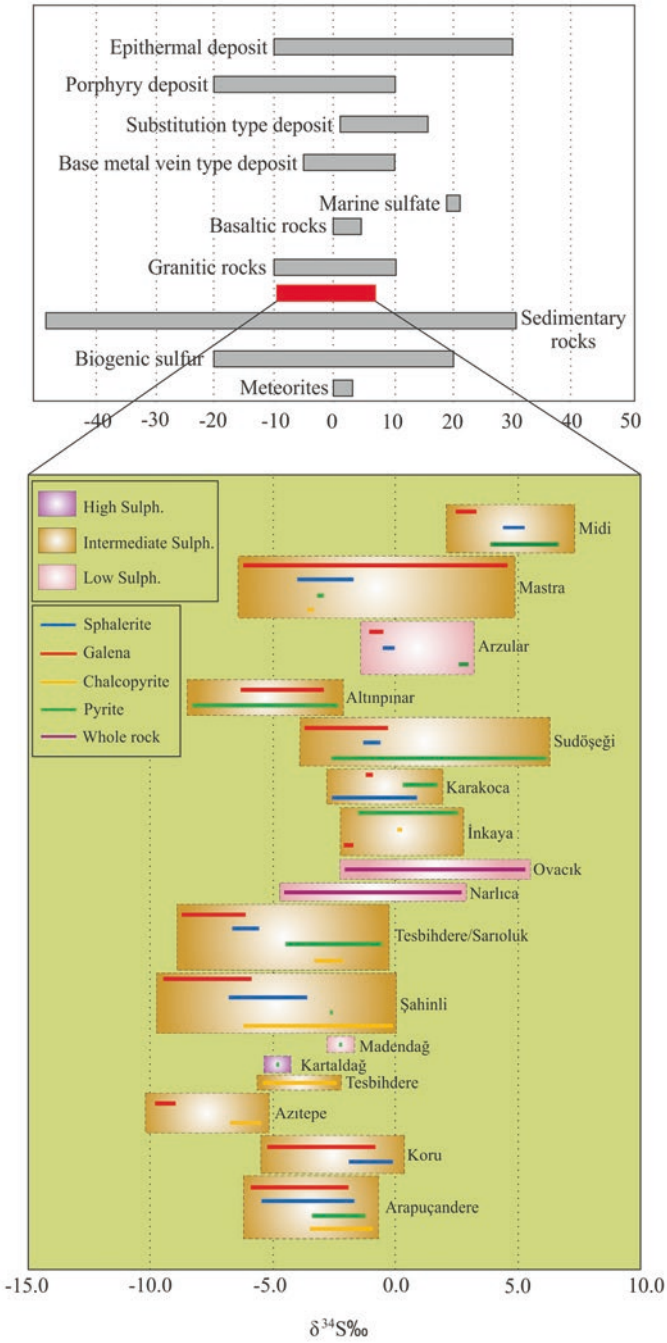

Fig. 4.6 Sulphur isotope composition diagram for different environments and some epithermal deposits in Turkey

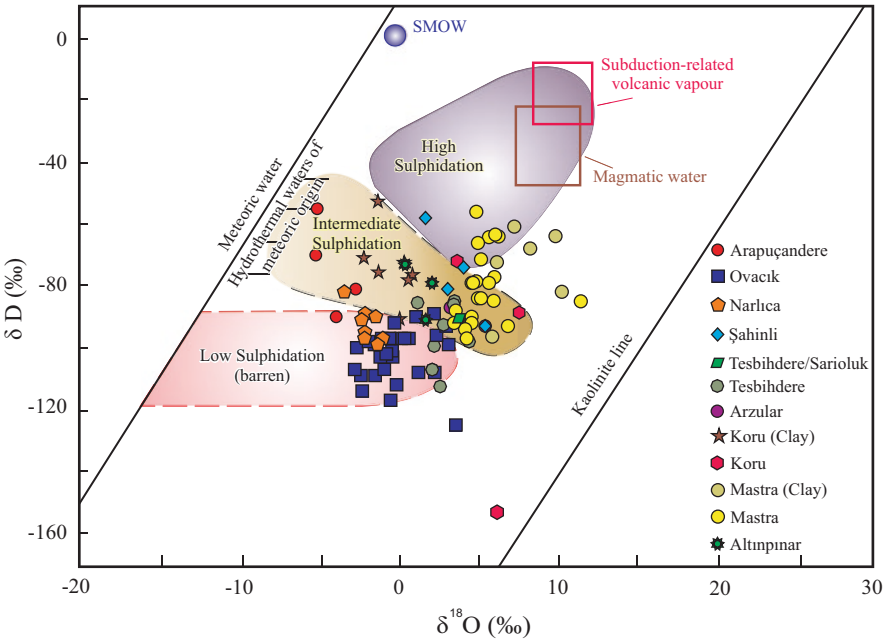

Fig. 4.7 Summary diagram showing the variation in $\delta^{18}O_{H2O}$ and δD isotopic compositions of hydrothermal fluids in the selected epithermal deposits in Turkey

realistically evaluated in conjunction with other data, including fluid inclusion measurements, petrography and, importantly, field relations (Pirajno 2009).

The D and O isotopic data for the ore fluids obtained from quartz and clay samples indicates varying degrees of $\delta^{18}O_{water}$ enrichment relative to the meteoric water line (Fig. 4.7). The wide range in the ^{18}O values of the LSEM systems can be interpreted by different degrees of mixing and/or boiling in an individual hydrothermal system. Most of the quartz samples plot in the low sulphidation area through the O-shift (black arrow), which represents the effect of isotope exchange between meteoric water, magmatic water, wall-rock and the formation waters. This trend can also be explained by isotopic exchange as a result of the interaction between deep circulating meteoric fluid and the wall-rock (Taylor 1979). However, clay samples from varying depths associated with mineralisation plot on the mixing field which exhibits an involvement of magmatic fluid. In most of the epithermal systems the early hydrothermal fluids, associated with the main Au mineralisation, have oxygen and hydrogen isotope compositions that plot in a field close to waters which are associated with magmatic ore deposits and felsic magmas, but they are displaced slightly towards values of present-day meteoric water. One of the effects of boiling on fluid chemistry might be relative enrichment and depletion in isotope compositions. In most of LSEM in western Anatolia the D and O data for the ore fluids obtained from the quartz samples exhibit a trend emphasized by the relative

enrichment of the $\delta^{18}O_{water}$ combined with a relative depletion in D. This trend could have occurred due to vapour separation due to boiling.

There can be some problems with the quartz from epithermal systems regarding the source of fluid. It should be considered that the O and D isotopic composition of water from fluid inclusions reflects the possible mixture of late stage meteoric dominated water mixing, depending on the amount of secondary fluid inclusion in the analysed quartz. The D and O data for ore fluids obtained from quartz identified by their low salinity and temperature, indicates varying degrees of $\delta^{18}O_{water}$ enrichment relative to the local meteoric water. This is the result produced by the exchange of igneous or metamorphic rocks at relatively shallow levels of formation (b1.0 kbar): the classic ^{18}O-shift (Criss and Taylor 1983; Larson and Taylor 1986; Larson and Zimmerman 1991).

Although it is not suitable quantitative comparison of O and D isotope values yielded with different techniques, we have plotted some data from epithermal deposits on a O versus D diagram. Conventional fluorination techniques involve sample heating between 500 and 700 °C (Clayton and Mayeda 1963) using an external furnace whereas the new generation laser-fluorination technique use IR or UV laser for localised heating of the samples (Mattey and Macpherson 1993; Young et al. 1998; Sharp 1990; Elsenheimer and Valley 1992). Recently, the fluorination based IRMS is a preferred technique producing data with high precision better than 0.1%.

4.10 Conclusions

Anatolia (Turkey) is part of the Tethyan orogenic belt, which formed by the amalgamation of microcontinental blocks as a result of evolution through complex tectonic periods from the Late Paleozoic to the late Cenozoic. The epithermal gold provinces of Turkey occupy three main tectonic domains including Western Anatolian Extensional Province, Pontides and Central Anatolian Volcanic Complex. Epithermal deposits of Turkey are hosted essentially in poorly eroded volcanic terrains which are genetically linked with relatively younger or active subduction zones.

In the Late Paleocene–Early Eocene, the Anatolide-Tauride block began to subduct northwards beneath the Pontides of Eurasian Plate, resulting widespread igneous activity, strike-slip faulting and the following extensional tectonic regime in Oligo-Miocene. The porphyry and epithermal deposits of the Black Sea Region are genetically linked with back arc extension which follows the collision between Pontide and Anatolide-Tauride blocks. The ore deposits in Black Sea Region are related to Late Cretaceous arc-magmatism in association with subduction and post collisional extension related Eocene magmatism. Late Cretaceous volcanic, volcano-sedimentary rocks in Eastern Pontide metallogenic belt has been known as the host lithological assemblage mainly for the Kuroko type VMS (e.g., Murgul, Çayeli and Lahanos). Early Cretaceous epithermal systems were preserved in the

Jurassic-Late Cretaceous Banatitic Metallogenic Belt in the western extension and Lesser Causcasus in the eastern extension of Pontide belt. Due to the intimate linkage between the Eastern Pontides with these two belts, Eastern Pontide should be tested for the buried epithermal systems in association with Late Cretaceous arc type volcanism.

Currently active dextral North Anatolian Fault zone becomes wider from east to west and splits in to dextral strike-slip fault branches covering almost whole of the Biga Peninsula. The pull-apart–originated basins of various sizes along North Anatolian Fault System have been recorded. In Biga Peninsula, the epithermal systems are associated spatially and temporally with the NE-SE trending pull-apart basins and volcano-tectonic depressions or calderas (e.g., TV Tower, Kirazlı, Arapuçan). In the Aegean Region NNE-SSW directed continental extension and associated graben development resulted from the combination of Anatolian extrusion and Hellenic subduction roll-back. The graben systems (e.g., Bergama, Edremit, Simav grabens) and associated extensional structures are the conduits for both the calcalkaline igneous activity and the circulation of the hydrothermal fluids between Late Miocene and Late Pliocene.

Epithermal systems are closely related to extensional deformation and magmatism during the Oligocene-Miocene interval in Biga, Eocene in Black Sea, Miocene in South Central Turkey. Epithermal deposits in Black sea region are hosted by Eocene volcanic suits associated with lavas and pyroclastic rocks of volcanic complexes that show mainly andesitic compositions with dacite in lesser amounts. There is only few epithermal mineralisation has been recognised in Late Cretaceous-Paleocene volcanic rocks, which developed due to the arc-type magmatism during the Late Mesozoic-Early Cenozoic.

In Biga Peninsula, epithermal deposits are hosted by Paleogene to Neogene (Oligo-Miocene) volcanic association that records bimodal, calc–alkaline, high-K calc-alkaline shoshonitic and midly alkaline volcanism at several discrete volcanic centres. The epithermal mineralisation and prospects in the Kütahya region are hosted by the Eğrigöz and Koyunoba plutons and their sedimentary roof pendants.

The epithermal deposits in South-central Anatolia are hosted in volcanic rocks with ages ranging from Miocene to Pliocene, of which the Messinian volcanic sequences are the most important. Formation of HSEM systems is associated with the subvolcanic-volcanic systems including stratovolcanos, calderas, phreatomagmatic breccia pipes and fracture systems. In the central Anatolia, HSEM are hosted in stratovolcanos comprising the lava flows and pyroclastic units in andesitic to rhyolitic compositions (e.g., Öksüt, İnlice, Doğanbey). Spatial and temporal distribution of ore in some HSEM were controlled by caldera structures and geometry of related faults systems (e.g., Kirazlı and Kartaldağ). Large scale phreatomagmatic brecciation which caused by the contact of the magma with groundwater is the one of most characteristic indicator for HSEM systems in Biga Peninsula (e.g. Kirazlı, Ağıdağı). Flow dome complexes are important volcanic edifices for vein type and associated stockwork, disseminated and replacement type epithermal mineralisation. In western Anatolia, post-dome vein type epithermal mineralisation is hosted

in rhyolitic to dacitic flow-dome complexes (e.g., Koru, Tesbihdere, Ağı Dağı, Kirazlı, Kuşçayırı, TV Tower prospects).

Host-rock rheology as a function of mineralogical compositions of the host rocks is one of the key issues on the control of the permeability and open spaces for the circulating hydrothermal fluids and volatiles. Andesite like intermediate volcanic rocks is reactive lithologies permitting to develop different hydrothermal alteration types. Fractures that are path for the ascending ore-bearing fluids are better developed in silicified host rocks than shales or phyllites. Unlike HSEM, the vein zones of LSEM and ISEM systems are mostly associated with narrow alteration haloes dominated by clay alteration giving illite, smectite, illite-smectite mixed layers and kaolinite (e.g., Red Rabbit, Ovacık, Küçükdere, Efemçukuru, Tesbihdere and Koru). Both LSEM and ISEM systems have appreciable carbonate contents, however the amount and the minerals of carbonates are different.

Well-developed hypogene advanced argillic alteration related to the low pH and oxidised volatiles and fluids are characteristic for HSEM systems. In this context, it seems like oxidised zones characterised by hematite-rich iron-oxides after sulphides are one of the exploration keys for HSEM. Whereas lath-like and/or fibrous hypogene hematite crystals in subordinate amounts are characteristic for ISEM systems. However, it should be taken in to consideration there are also post mineralisation barren porphyritic intrusions particularly in Biga region.

References

Acarlioğlu S, Kadir S, Abdioğlu E, Arslan M (2013) Epithermal-alteration geology, mineralogy and geochemistry of Eocene volcanic rocks in the Hasandağ (Giresun) area, eastern Pontides, NE Turkey. N Jb Mineral Abh 190(1):79–99

Adamia SA, Lordkipanidze MB, Zakariadze GS (1977) Evolution of an active continental margin as exemplified by the Alpine history of the Caucasus. Tectonophysics 40:183–199

Adamia SA, Chkhotua T, Kekelia M, Lordkipanidze MB, Shavishvili I, Zakariadze G (1981) Tectonics of the Caucasus and adjoining regions – implications for the evolution of the Tethys Ocean. J Struct Geol 3(4):437–447

Akaryalı E (2016) Geochemical, fluid inclusion and isotopic (O, H and S) constraints on the origin of Pb–Zn ± au vein-type mineralizations in the Eastern Pontides Orogenic Belt (NE Turkey). Ore Geol Rev 74:1–14

Akaryalı E, Tüysüz N (2013) The genesis of the slab window-related Arzular low-sulphidation epithermal gold mineralisation (eastern Pontides, NE Turkey). Geosci Front 4–4:409–421

Akay E, Işintek İ, Erdoğan B, Hasözbek A (2011) Stratigraphy of the Afyon Zone around Emet (Kütahya, NW Anatolia) and geochemical characteristics of the Triassic volcanism along the northern Menderes Massif. Neu Jb Mineral Abh 188(3):297–316

Akbaş B, Akdeniz N, Aksay A, Altun İ, Balcı V, Bilginer E, Bilgiç T, Duru M, Ercan T, Gedik İ, Günay Y, Güven İH, Hakyemez HY, Konak N, Papak İ, Pehlivan Ş, Sevin M, Şenel M, Tarhan N, Turhan N, Türkecan A, Ulu Ü, Uğuz MF, Yurtsever A (2017) Geological map of Turkey, General Directorate of Mineral Research and Exploration Publication. Ankara Türkiye

Akçay M, Gündüz O (2004) Porphyry Cu–Au mineralisation associated with a multiphase intrusion, and related replacement fronts in limestones in an island arc setting near the Gümüşhane village (Artvin) in the Eastern Black Sea Province (Turkey). Chem Erde 64:359–383

Akdeniz N, Konak N (1979) The rock units of the Simav region of Menderes Massif and the situation of metabasic and metaultramafic rocks. Bull Geol Soc Turk 22(2):175–183 (in Turkish with English abstract)

Akıman O, Erler A, Göncüoğlu MC, Güleç N, Geven A, Türeli TK, Kadioğlu YK (1993) Geochemical characteristics of granitoids along the western margin of the central Anatolian Crystalline Complex and their tectonic implications. Geol J 28:371–382

Albinson T, Norman DI, Cole D, Chomiak B (2001) Controls on formation of low sulphidation epithermal deposits in Mexico: constraints from fluid inclusion and stable isotope data. In: Albinson FT, Nelson CE (eds) New mines and discoveries in Mexico and Central America. Soc Econ Geol Spec Publ 8:1–32

Aldanmaz E (2002) Mantle source characteristics of alkali basalts and basanites in an extensional intracontinental plate setting, western Anatolia, Turkey: implications for multi-stage melting. Int Geol Rev 44:440–457

Altherr R, Topuz G, Siebel W, Şen C, Meyer H-P, Satır M (2008) Geochemical and Sr–Nd–Pb isotopic characteristics of Paleocene plagioleucitites from the Eastern Pontides (NE Turkey). Lithos 105:149–161

Altunkaynak Ş, Yılmaz Y (1998) The Mount Kozak magmatic complex, Western Anatolia. J Volcanol Geotherm Res 85(1–4):211–231

Altunkaynak Ş, Dilek Y, Genç CS, Sunal G, Gertisser R, Furnes H, Foland K, Yang J (2012) Spatial, temporal and geochemical evolution of Oligo-Miocene granitoid magmatism in western Anatolia, Turkey. Gondwana Res 21:961–986

Aluç A, Gürler Z, Kuşcu İ, Aydoğan S (2014) A new low sulphidation epithermal Au – Ag mineralisation within Biga Peninsula: Karadere (Burhaniye, Balıkesir, Turkey). 8th International Symposium on Eastern Mediterranean Geology, Muğla-Turkey, p 32

Andrew T, Robertson AHF (2002) The Beyşehir-Hoyran-Hadim Nappes: genesis and emplacement of Mesozoic marginal and oceanic units of the northern Neotethys in southern Turkey. J Geol Soc 159:529–543

Arehart GB, Chryssoulis SL, Kesler SE (1993) Gold and arsenic in iron sulphides from sediment-hosted disseminated gold deposits; implications for depositional processes. Econ Geol 88:171–185

Arslan M, Kolaylı H, Temizel İ (2004) Petrographical, geochemical and petrological characteristics of the Güre (Giresun, NE Turkey) Granitoid. Bull Earth Scis Appl Res Cent Hacet Univ 30:1–21

Ashley RP (1982) Occurrence model for enargite-gold deposits. In: Erickson RL (ed) Characteristics of mineral deposit occurrences. United States Geological Survey, Open-File Report 82–795:144–147

Aslan N (2011) Mastra (Gümüşhane) Yatağı'nın jeolojik, mineralojik ve jeokimyasal özellikleri. Master's Thesis, Karadeniz Technical University, Trabzon, pp 190 (unpublished)

Aslan N, Akçay M (2011) Mastra (Gümüşhane) Au-Ag yatağının jeolojik, minerolojik ve jeokimyasal özellikleri [Geologic, minerologic and geochemical characteristics of Au-Ag deposits in Mastra (Gümüşhane)]. 64th Geological Congress of Turkey, Proceedings book, 25–29 April 2011, Ankara, p 181–182

Ayan Z (1991) Şebinkarahisar (Giresun) Kuzeybatısındaki Pb-Zn-Cu Cevherleşmelerinin Mineralojik-Jeokimyasal İncelenmesi ve Kökensel Yorumu [Petrogeologic and Mineralogical-geochemical investigation and genetic interpretation of Pb-Zn-Cu mineralizations in northwest of Şebinkarahisarın (Giresun)]. PhD Thesis Dokuz Eylul Universty, Izmir (In Turkish, unpublished)

Aydın NS, Göncüoğlu MC, Erler A (1998) Latest Cretaceous magmatism in the central Anatolian crystalline complex: review of field, petrographic and geochemical features. Turk J Earth Sci 7:259–268

Aysal N (2015) Mineral chemistry, crystallization conditions and geodynamic implications of the Oligo–Miocene granitoids in the Biga Peninsula, Northwest Turkey. Asian J Earth Sci 105:68–84

Barton PB, Jr Skinner BJ (1979) Sulphide mineral stabilities. In: Barnes HL (ed) Geochemistry of hydrothermal ore deposits, 2nd edn. Wiley, New York, pp 278–403

Başarır E (1970) Bafa gölü doğusunda kalan Menderes masifi güney kanadının jeolojisi ve petrografisi. [The petrology and geology of the southern flank of the Menderes Massif east of the Bafa Lake]. Scientific Reports of the Faculty of Science, Ege University No. 102 (in Turkish with English abstract)

Bektaş O, Yılmaz C, Taslı K, Akdağ K, Özgür S (1995) Cretaceous rifting of the eastern Pontide carbonate platform (NE Turkey): the formation of carbonates breccias and turbidites as evidences of a drowned platform. Giorn Geol 57:233–244

Bektaş O, Şen C, Atıcı Y, Köprübaşı N (1999) Migration of the upper cretaceous subduction-related volcanism towards the back-arc basin of the Eastern Pontide magmatic arc (NE Turkey). Geol J 34:95–106

Berger BR (1986) Descriptive model of epithermal quartz-alunite Au. In: Cox DP, Singer DA (eds) Mineral deposit models. USGS Bull 1693:158

Berger BR, Henley RW (1989) Advances in understanding of epithermal gold-silver deposits, with special reference to the western United States. Econ Geol Monogr 6:405–423

Beşir D (2003) Koru Köyü (Lapseki-Çanakkale) Pb-Zn-Ag Yatağının Jenetik İncelenmesi. [Genetic Investigation of the Koru Village (Lapseki-Çanakkale) Pb-Zn-Ag Deposit]. Master's thesis, Dokuz Eylul University (In Turkish, unpublished)

Bethke PM (1984) Controls on base and precious metal mineralisation in deeper epithermal environments. United States Geological Survey, Open-File Report 84890:40

Bilir ME (2015) Geochemical and geochronological characterization of the early-middle Eocene magmatism and related epithermal systems of the Eastern Pontides, Turkey. Master's thesis, Muğla Sıtkı Koçman University, pp 138 (unpublished)

Bilir E, Kuşcu, İ (2016) Geochemical and geochronological characterization of the early-middle Eocene magmatism and related epithermal systems of the Eastern Pontides, Turkey. SEG 2016 Conference

Black KN, Catlos EJ, Oyman T, Demirbilek M (2013) Timing Aegean extension: evidence from in situ U–Pb geochronology and cathodoluminescence imaging of granitoids from NW Turkey. Lithos 180–181:92–108

Bodnar RJ, Reynolds TJ, Kuehn CA (1985) Fluid inclusion systematics in epithermal systems. In: Berger BR, Bethke PM (eds) Geology and geochemistry of epithermal systems. Rev Econ Geol 2:73–98

Bonev N, Beccaletto L (2007) From syn-to post-orogenic Tertiary extension in the north Aegean region: constraints on the kinematics in the eastern Rhodope Thrace, Bulgaria Greece and the Biga Peninsula, NW Turkey. In: Taymaz T, Yılmaz Y, Dilek Y (eds) The Geodynamics of the Aegean and Anatolia. Geol Soci Lond Spec Publ 291:113–142

Bonham HF Jr (1984) Three major types of epithermal precious metal deposits. Geol Soc Am Abstr Programs 16:449

Bonham HF Jr (1986) Models for volcanic-hosted epithermal precious metal deposits; a review. Int Volcanol Congr N Z Proc Symp 5:13–17

Boucher K, Misković A, Sánchez M, Baker T, Hart CRJ (2016) Structural and hydrothermal fluid evolution at the Efemçukuru epithermal Au deposit, Western Turkey. Mineral exploration roundup 2016. Association for Mineral Exploration British Columbia, p 9

Bozkaya G (2009) Fluid inclusion and stable isotope (O, H and S) evidence for the origin of the Balcılar vein type barite-galena mineralisation in Çanakkale, Biga Peninsula, NW Turkey. J Geochem Explor 101:1–8

Bozkaya G (2011) Sulphur- and lead-isotope geochemistry of the Arapuçandere (Karaköy-Yenice, Çanakkale) Pb-Zn-Cu deposit, Biga Peninsula, NW Turkey. Int Geol Rev 53:116–129

Bozkaya G, Banks DA (2015) Physico-chemical controls on ore deposition in the Arapuçandere Pb–Zn–Cu-precious metal deposit, Biga Peninsula, NW Turkey. Ore Geol Rev 66:65–81

Bozkaya G, Gökçe A (2001) Geology, ore petrography and fluid inclusion characteristics of the Koru (Çanakkale) Pb-Zn deposits. Eng Fac Bull Cumhuriyet Univ Earth Sci 18–1:55–70 (in Turkish with English abstract)

Bozkaya G, Gökce A (2007) Fluid inclusion and isotope geochemistry studies of the galena-barite veins in Balcılar (Lapseki-Çanakkale) area. Abstract of 60th Geological Congress of Turkey, 188–190

Bozkaya G, Gökçe A (2009) Lead and sulphur isotope studies of the Koru (Çanakkale, Turkey) lead–zinc deposits. Turk J Earth Sci 18:127–137

Bozkaya G, Gökçe A, Grassineau NV (2008) Fluid-inclusion and stable-isotope characteristics of the Arapuçandere Pb-Zn-Cu deposits, NW Turkey. Int Geol Rev 50:848–862

Bozkaya G, Banks DA, Özbaş F, Wallington J (2014) Fluid processes in the Tesbihdere base metal-Au deposit: implications for epithermal mineralisation in the Biga Peninsula, NW Turkey. Cent Eur J Geosci 6:148–169

Bozkurt E, Satır M, Buğdaycıoğlu C (2011) Surprisingly young Rb/Sr ages from the Simav extensional detachment fault zone, northern Menderes Massif, Turkey. J Geodyn 52(5):406–431

Boztuğ D (1998) Post-collisional Central Anatolian alkaline plutonism, Turkey. Turk J Earth Sci 7:145–165

Boztuğ D (2000) S-I-A type intrusive associations: geodynamic significance of synchronism between metamorphism and magmatism in Central Anatolia, Turkey. In: Bozkurt E, Winchester JA, Piper JAD (eds) Tectonics and magmatism in Turkey and the surrounding area. Geol Soc Lond Spec Publ 173:441–458

Boztuğ D (2008) Petrogenesis of the Kösedağ Pluton, Suşehri-NE Sivas, east-central Pontides, Turkey. Turk J Earth Sci 17:241–262

Boztuğ D, Jonckheere R, Wagner GA, Yeğingil Z (2004) Slow Senonian and fast Palaeocene-Early Eocene uplift of the granitoids in the Central Eastern Pontides, Turkey: apatite fission-track results. Tectonophysics 382:213–228

Boztuğ D, Erçin I, Kuruçelik MK, Göç D, Kömür I, İskenderoğlu A (2006) Geochemical characteristics of the composite Kaçkar batholith generated in a Neo-Tethyan convergence system, Eastern Pontides, Turkey. Asian J Earth Sci 27:286–302

Boztuğ D, Harlavan Y, Arehart GB, Satır M, Avci N (2007) K–Ar age, whole-rock and isotope geochemistry of A-type granitoids in the Divrigi-Sivas region, eastern-central Anatolia, Turkey. Lithos 97:193–218

Brinkmann R (1966) Geotektonische gliederung von West-Anatolien. N Jb Geol Paläont 10:603–618

Browne PRL (1978) Hydrothermal alteration in active geothermal fields. Annu Rev Earth Planet Sci 6:229–250

Cabri LJ, Newville M, Gordon RA, Crozier ED, Sutton SR, Mcmahon G, Jiang DT (2000) Chemical speciation of gold in arsenopyrite. Can Miner 38:1265–1281

Candan O, Koralay OE, Akal C, Kaya O, Oberhänsli R, Dora OÖ, Konak N, Chen F (2011) Supra-Pan-African unconformity between core and cover series of the Menderes Massif/Turkey and its geological implications. Precambrian Res 184:1–23

Catlos E, Jacob L, Oyman T, Sorensen S (2012) Long-term exhumation of an Aegean metamorphic core complex granitoids in the northern Menderes Massif, Western Turkey. Am J Sci 312:534–571

Cavazza W, Okay AI, Zattin M (2009) Rapid early-middle Miocene exhumation of the Kazdağ Massif (Western Anatolia). Int J Earth Sci 98:1935–1947

Chakrabarti R, Basu AR, Ghatak A (2012) Chemical geodynamics of Western Anatolia. Int Geol Rev 54:227–248

Çiçek M (2013) Koru ve Tesbihdere (Lapseki-Çanakkale) epitermal Pb-Zn-Cu+-Au+-Ag yataklarına ait hidrotermal akışkanların kökeni ve evrimi [Origin and Evolution of Hydrothermal Fluids in Koru and Tesbihdere (Lapseki-Çanakkale) Epithermal Pb-Zn-Cu ± Ag ± Au Deposits] MSc thesis, Dokuz Eylul University (In Turkish, unpublished)

Çiçek M, Oyman T (2016) Origin and evolution of hydrothermal fluids in epithermal Pb-Zn-Cu ± Au ± Ag deposits at Koru and Tesbihdere mining districts, Çanakkale, Biga Peninsula, NW Turkey. Ore Geol Rev 78:176–195

Çiçek M, Oyman T, Özgenc I, Akbulut M (2012) Fluid evolution of the Koru Pb-Zn deposit, Çanakkale (NW-Turkey). International Earth Science Colloquium on the Aegean Region, IESCA-2012 Abstract Book, 1–5 Oct, p. 158

Çiçek M, Oyman T, Kaliwoda M, Hochleitner R (2017) Mineralogy and mineral chemistry of the Arapuçandere Pb-Zn-Cu (Ag-Au) mineralization in the Northeast of Yenice (Çanakkale), Biga Peninsula, NW Turkey. In: International Workshop on Subduction Related Ore Deposit, 23–23 Sept 2017, Karadeniz Technical University, Trabzon-Turkey, p 18

Çiner A, Doğan U, Yıldırım C, Akçar N, Ivy-Ochs S, Alfimov V, Kubik PW, Schlüchter C (2015) Quaternary uplift rates of the Central Anatolian Plateau, Turkey: insights from cosmogenic isochron-burial nuclide dating of the Kızılırmak River terraces. Quat Sci Rev 107:81–97

Çinku MC, Ustaömer T, Hirt AM, Hisarli ZM, Heler F, Orbay N (2010) Southward migration of arc magmatism during latest Cretaceous associated with slab steepening, East Pontides, N Turkey: new paleomagnetic data from the Amasya region. Phys Earth Planet Inter 182:8–29

Clayton RN, Mayeda TK (1963) The use of bromine pentafluoride in the extraction of oxygen from oxides and silicates for isotopic analysis. Geochim Cosmochim Acta 27:43–52

Cline JS (2001) Timing of gold and arsenic sulphide mineral deposition at the Getchell Carlin-type gold deposit, north-central Nevada. Econ Geol 96:75–89

Çoğulu E (1975) Gümüşhane ve Rize Granitik Plutonlarının Mukayeseli Petrojeolojik ve Jeokronolojik Etüdü. [Petrogeologic and Geochronologic Investigation of Gümüşhane and Rize Granitic Plutons and Their Comparison]. Dissertation thesis, İstanbul Technical University (in Turkish with English abstract, unpublished)

Cook NJ, Chryssoulis SL (1990) Concentrations of invisible gold in the common sulphides. Can Mineral 28:1–16

Cook NJ, Ciobanu CL, Pring A, Skinner W, Shimizu M, Danyushevsky L, Saini-Eidukat B, Melcher F (2009) Trace and minor elements in sphalerite: a LA-ICPMS study. Geochim Cosmochim Acta 73(16):4761–4791

Cooke DR, Simmons SF (2000) Characteristics and genesis of epithermal gold deposits. Rev Econ Geol 13:221–244

Corbett GJ, Leach TM (1998) Southwest Pacific Rim gold-copper systems: structure, alteration and mineralisation. Soc Econ Geol Spec Publ 6:236

Criss RE, Taylor HP (1983) An $^{18}O/^{16}O$ and D/H study of tertiary hydrothermal systems in the southern half of the Idaho batholith. GSA Bull 94:640–663

Czamanske GK (1974) The FeS content of sphalerite along the chalcopyrite-pyrite-bornite sulphur fugacity buffer. Econ Geol 69:1328–1334

Dag N (1993) Fluid inclusion study on Narlica prospect. Eurogold, Unpublished company report, p 1–11

Delaloye M, Çoğulu E, Chessex R (1972) Etude géochronometrique des massifs cristallins de Rize et de Gümüşhane, Pontides Orientales (Turquie). Arch Sci Phys Nat 25(Supplement 7): 43–52

Dilek Y, Thy P, Hacker B, Grundvig S (1999) Structure and petrology of Tauride ophiolites and mafic dike intrusions (Turkey): implications for the Neo-Tethyan ocean. GSA Bull 111:1192–1216

Dilek Y, Imamverdiyev N, Altunkaynak S (2010) Geochemistry and tectonics of Cenozoic volcanism in the Lesser Caucasus (Azerbaijan) and the peri-Arabian region: collision-induced mantle dynamics and its magmatic fingerprint. Int Geol Rev 52(4–6):536–578

Dirik K, Göncüoğlu MC (1996) Neotectonic characteristics of Central Anatolia. Int Geol Rev 38:807–817

Dokuz A (2011) A slab detachment and delamination model for the generation of Carboniferous high-potassium I-type magmatism in the Eastern Pontides, NE Turkey: the Köse composite pluton. Gondwana Res 19:926–944

Dönmez M, Akçay AE, Genç SC, Acar S (2005) Middle-Upper Eocene volcanism and marine ignimbrites in Biga Peninsula. Bull Mineral Res Exp 131:49–61 (in Turkish)
Dora OÖ, Candan O, Kaya O, Koralay E, Dürr S (2001) Revision of the so-called "leptite-gneisses" in the Menderes Massif: a supracrustal metasedimentary origin. Int J Earth Sci 89(4):836–851
Ebert S (2004) Ovacik Normandy gold mine, Turkey. Unpublished company report, Normandy, pp 1–18
Einaudi MT, Hedenquist JW, İnan EE (2003) Sulfidation state of fluids in active and extinct hydrothermal systems: transitions from porphyry to epithermal precious metal deposits. In: Simmons SF (ed) Sulfidation state of hydrothermal fluids. Soc Econ Geol Spec Publ 10:285–314
Elsenheimer D, Valley JW (1992) In situ oxygen isotope analysis of feldspar and quartz by Nd:YAG laser microprobe. Chem Geol 101:21–42
Emre Ö, Duman TY, Özalp S, Elmacı H, Olgun Ş, Şaroğlu F (2013) 1/1.125.000 scaled active faults map of Turkey. General Directorate of Mineral Research and Exploration, Sp Publ Series-30, Ankara-Turkey
Ercan T, Satır M, Steinitz G, Dora A, Sarıfakioğlu E, Adis C, Walter HJ, Yıldırım T (1995) Features of tertiary volcanism observed at Biga Peninsula and Gökçeada, Tavsan Islands. Bull Mineral Res Exp 117:55–86 (in Turkish with English abstract)
Ercan T, Türkecan A, Guillou H, Satır M, Sevin D, Saroğlu F (1998) Features of the tertiary volcanism around the Sea of Marmara. Bull Mineral Res Exp 120:97–118
Erkül F (2010) Tectonic significance of synextensional ductile shear zones within the early Miocene Alaçamdağ granites, northwestern Turkey. Geol Mag 147(4):611–637
Erkül F, Helvacı C, Sözbilir H (2005) Stratigraphy and geochronology of the Early Miocene volcanic units in the Bigadiç Borate Basin, Western Turkey. Turk J Earth Sci 14:227–253
Eyüboğlu Y, Santosh M, Yi K, Tüysüz N, Korkmaz S, Dudas FO, Akaryalı E, Bektaş O (2014) The Eastern Black Sea-type volcanogenic massive sulphide deposits: geochemistry, zircon U-Pb geochronology and an overview of the geodynamics of ore genesis. Ore Geol Rev 59:29–54
Fayon AK, Whitney DL, Tessier C, Carver JI, Dilek Y (2001) Effects of plate convergence obliquity on timing and mechanisms of exhumation of a mid-crustal terrain, the Central Anatolian Crystalline Complex. Earth Planet Sci Lett 192:191–205
Fleet ME, Mumin AH (1997) Gold-bearing arsenian pyrite and marcasite and arsenopyrite from Carlin Trend gold deposits and laboratory synthesis. Am Mineral 82:182–193
Gedikoğlu A (1978) Harşit Granit Karmaşığı ve Çevre Kayaçları [Harşit Granite Complex and its Country Rocks (Giresun-Doğankent)]. PhD thesis, Karadeniz Technical University, Trabzon (in Turkish with English abstract, unpublished)
Genna A, Jébrak M, Marcoux E, Milési JP (1996) Genesis of cockade breccias in the tectonic evolution of the Cirotan epithermal gold system, West Java. Can J Earth Sci 33:93–102
Giles DL (1974) Geology and mineralisation of the ulutaş copper–molybdenum prospect, mineral exploration in two areas. UNDP Technical Report, 6, MTA, Ankara (unpublished)
Görür N, Oktay FY, Seymen I, Şengör AMC (1984) Paleotectonic evolution of Tuz Gölü Basin complex, central Turkey. In: Dixon JE, Robertson AHF (eds) The geological evolution of the Eastern Mediterranean. Geol Soc Lond Spec Publ 17:81–96
Görür N, Tüysüz O, Şengör AMC (1998) Tectonic evolution of the central Anatolian basins. Int Geol Rev 40:831–850
Gülmez F, Genç SC, Keskin M, Tüysüz O (2013) A post-collision slab-breakoff model for the origin of the Middle Eocene magmatic rocks of the Armutlu-Almacık belt, NW Turkey and its regional implications. In: Robertson AHF, Parlak O, Ünlügenç UC (eds) Geological development of Anatolia and the Easternmost Mediterranean Region. Geol Soci Lond Spec Publ 372:107–139
Gulyuz N, Shipton Z, Gulyuz E, Lord R, Kaymakci N, Kuscu İ (2017) Gold grade distribution within an epithermal quartz vein system, Kestanelik, NW Turkey: implications for gold exploration. In: 19th EGU General Assembly, EGU2017, 23–28 April 2017, Vienna, Austria, p 1210
Hasözbek A, Satır M, Erdoğan B, Akay E, Siebel W (2010) Early Miocene post-collisional magmatism in NW Turkey: geochemical and geochronological constraints. Int Geol Rev 53(9):1098–1119

Heald P, Foley NK, Hayba DO (1987) Comparative anatomy of volcanic-hosted epithermal deposits: acid-sulphate and adularia-sericite types. Econ Geol 82:1–26
Hedenquist JW, Izawa E, Arribas A Jr, White NC (1996) Epithermal gold deposits: styles, characteristics, and exploration. Poster Booklet Resour Geol Spec Publ 1:17 (with translations to Spanish, French, Japanese, and Chinese)
Hedenquist JW, Arribas A Jr, Gonzalez-Urien E (2000) Exploration for epithermal gold deposits. Rev Econ Geol 13:245–277
Henley RW (1985) The geothermal framework of epithermal deposits. Rev Econ Geol 2(l):–24
Henley RW (1990) Ore transport and deposition in epithermal environments. Univ West Aust Geol Dept Publ 23:51–69
Hobbs BE (1985) The geological significance of microfabric analysis. In: Wenk HR (ed) Preferred orientation in deformed metals and rocks: an introduction to modern texture analysis. Academic, Orlando, pp 463–479
İlbeyli N (2005) Mineralogical–geochemical constraints on intrusives in central Anatolia, Turkey: tectono-magmatic evolution and characteristics of mantle source. Geol Mag 142:187–207
İlbeyli N (2008) Geochemical characteristics of the Şebinkarahisar granitoids in the Eastern Pontides, northeast Turkey: petrogenesis and tectonic implications. Int Geol Rev 50:563–582
İlbeyli N, Pearce JA, Thirwall MF, Mitchell JG (2004) Petrogenesis of collision-related plutonics in Central Anatolia, Turkey. Lithos 72:163–182
Işık V, Tekeli O (2001) Late orogenic crustal extension in the northern Menderes massif (western Turkey): evidence for metamorphic core complex formation. Int J Earth Sci 89(4):757–765
JICA (1986) The Republic of Turkey report on the cooperative mineral exploration of Gümüşhane area, consolidated report. Japanese International Cooperation Agency, Metal Mining Agency of Japan
Kadıoğlu YK, Güleç N (1996) Mafic microgranular enclaves and interaction between felsic and mafic magmas in the Ağaçören Intrusive Suite: evidence from petrographic features and mineral chemistry. Int Geol Rev 3(8):854–867
Kadıoğlu YK, Dilek Y, Güleç N, Foland KA (2003) Tectonomagmatic evolution of bimodal plutons in the central Anatolian crystalline complex, Turkey. J Geol 111:671–690
Kadıoğlu YK, Dilek Y, Foland KA (2006) Slab breakoff and syncollisional origin of the Late Cretaceous magmatism in the Central Anatolian Crystalline Complex, Turkey. In: Dilek Y, Pavlides S (eds) Postcollisional tectonics and magmatism in the Mediterranean Region and Asia. GSA Spec Pap 409:381–415
Karacık Z, Yılmaz Y, Pearce JA (2007) The Dikili-Çandarlı volcanics, Western Turkey: magmatic interactions as recorded by petrographic and geochemical features. Turk J Earth Sci 16:493–522
Karakaya MÇ, Karakaya N, Temel A (2001) Kaolin occurrences in Erenler Dağı volcanics, southwest Konya Province, Turkey. Int Geol Rev 43/8:711–722
Karslı O, Chen B, Aydın F, Şen C (2007) Geochemical and Sr-Nd-Pb isotopic compositions of the Eocene Dölek and Sarıçiçek Plutons, Eastern Turkey: implications for magma interaction in the genesis of high-K calc-alkaline granitoids in a post-collision extensional setting. Lithos 98:67–96
Karslı O, Dokuz A, Uysal I, Aydin F, Kandemir R, Wijbrans J (2010) Generation of the Early Cenozoic adakitic volcanism by partial melting of mafic lower crust, Eastern Turkey: implications for crustal thickening to delamination. Lithos 114:109–120
Karslı O, Ketenci M, Uysal İ, Dokuz A, Aydın F, Chen B, Kandemir R, Wijbrans J (2011) Adakite-like granitoid porphyries in the Eastern Pontides, NE Turkey: potential parental melts and geodynamic implications. Lithos 127:354–372
Karslı O, Caran Ş, Dokuz A, Çoban H, Chen B, Kandemir R (2012) A-type granitoids from the Eastern Pontides, NE Turkey: records for generation of hybrid A-type rocks in a subduction-related environment. Tectonophysics 530–531:208–224
Kaygusuz A, Aydinçakır E (2009) Mineralogy, whole-rock and Sr–Nd isotope geochemistry of mafic microgranular enclaves in Cretaceous Dagbasi granitoids, Eastern Pontides, NE Turkey: evidence of magma mixing, mingling and chemical equilibration. Chem Erde 69:247–277

Kaygusuz A, Siebel W, Şen C, Satir M (2008) Petrochemistry and petrology of I-type granitoids in an arc setting: the composite Torul pluton, Eastern Pontides, NE Turkey. Int J Earth Sci 97:739–764

Kaygusuz A, Chen B, Aslan Z, Siebel W, Şen C (2009) U-Pb zircon SHRIMP ages, geochemical and Sr-Nd isotopic compositions of the early cretaceous I-type Sarıosman Pluton, Eastern Pontides, NE Turkey. Turk J Earth Sci 18:549–581

Kaygusuz A, Arslan M, Siebel W, Sipahi F, İlbeyli N (2012) Geochronological evidence and tectonic significance of Carboniferous magmatism in the southwest Trabzon area, eastern Pontides, Turkey. Int Geol Rev 54(15):1776–1800

Ketin İ (1966) Tectonic units of Anatolia (Asia Minor). Bull Mineral Res Exp 66:23–34

Koçyiğit A, Beyhan A (1998) New intracontinental transcurrent structure: the Central Anatolian fault zone, Turkey. Tectonophysics 284(3–4):317–336

Köksal S, Romer RL, Göncüoğlu M, Toksoy-Köksal F (2004) Timing of postcollisional H-type to A-type granitic magmatism: U–Pb titanite ages from the Alpine central Anatolian granitoids (Turkey). Int J Earth Sci 93:974–989

Konak N, Okay AI, Hakyemez HY (2009) Tectonics and stratigraphy of the eastern Pontides: field Trip guide Book. 2nd International Symposium on the Geology of the Black Sea Region, Ankara, p 120

Köprübaşı N, Şen C, Kaygusuz A (2000) Doğu Pontid adayayı granitoyidlerin karşılaştırılmalı petrografik ve kimyasal özellikleri [Comparative petrographical and chemical features of the eastern Pontide arc granitoid]. Uygulamalı Yerbilimleri 1:111–120 (in Turkish with English abstract)

Kürkçüoğlu B (2010) Geochemistry and petrogenesis of basaltic rocks from the Develidağ volcanic complex, Central Anatolia, Turkey. Asian J Earth Sci 37:42–51

Kürkçüoğlu B, Furman T, Hanan B (2008) Geochemistry of postcollisional mafic lavas from the North Anatolian Fault zone, Northwestern Turkey. Lithos 101:416–434

Kuşcu İ, Gençalioğlu-Kuşcu G, Tosdal RM, Ullrich T, Friedman R (2010) Magmatism in the southeastern Anatolian orogenic belt: transition from arc to post-collisional setting in an evolving orogen. In: Sosson M, Kaymakçı N, Stephenson RA, Bergerat F, Starostenko V (eds) Sedimentary basin tectonics from the Black Sea and Caucasus to the Arabian Platform. Geol Soc Lond Spec Publ 340:437–460

Large R, Danyushevsky L, Hollit C, Maslennikov V, Meffre S, Gilbert S, Bull S, Scott R, Emsbo P, Thomas H, Singh B, Foster J (2009) Gold and trace element zonation in pyrite using a laser imaging technique: implications for the timing of gold in orogenic and Carlin-style sediment-hosted deposits. Econ Geol 104:635–668

Larson PB, Taylor HP (1986) $^{18}O/^{16}O$ relationships in hydrothermally altered rocks from the Lake City caldera, San Juan Mountains, Colorado. J Volcanol Geothermal Res 30:47–82

Larson PB, Zimmerman BS (1991) Variations in δ18O values, water/rock ratios, and water flux in the Rico paleothermal anomaly, southwest Colorado. Geochem Soc Spec Publ 3:463–469

Lefebvre C (2011) The tectonics of the Central Anatolian Crystalline Complex: a structural, metamorphic and paleomagnetic study. Utrecht Univ Utrecht Stud Earth Sci 3:1–147

Lindgren W (1933) Mineral deposits, 4th edn. McGraw-Hill, New York, p 930

Maslennikov VV, Maslennikova SP, Large RR, Danyushevskiy LV (2009) Study of trace element zonation in vent chimneys from the Silurian Yaman-Kasy volcanic-hosted massive sulphide deposit (Southern Urals, Russia) using laser ablation-inductively coupled plasma mass spectrometry (LA-ICPMS). Econ Geol 104:1111–1141

Mattey D, Macpherson C (1993) High-precision oxygen isotope microanalysis of ferromagnesian minerals by laser-fluorination. Chem Geol 105:305–318

Mauk JL, Hoskin PWO, Seal II RR (1998) Morphology of pyrite and marcasite at the Golden Cross mine, New Zealand. In: Arehart GB, Hulston JR (eds) Water–rock interaction, Balkema, Rotterdam 9:557–560

McKenzie DP (1972) Active tectonics of the Mediterranean region. Geophys J R Astron Soc 30(2):109–185

Meijers MJM, Kaymakci N, Van Hinsbergen DJJ, Langereis CG, Stephenson RA, Hippolyte J-C (2010) Late Cretaceous to Paleocene oroclinal bending in the central Pontides (Turkey). Tectonics 29:TC4016

Moore WJ, Mckee EH, Akıncı Ö (1980) Chemistry and chronology of plutonic rocks in the Pontide mountains, northern Turkey. Symposium of European Copper Deposits, Belgrade, pp 209–216

MTA (1993a) Türkiye Altın ve Gümüş Envanteri [Gold and silver inventory of Turkey]. MTA Publication no.198 (in Turkish)

MTA (1993b) Türkiye Kurşun-Çinko envanteri [Lead-zinc inventory of Turkey]. MTA Publication no. 199, p 94 (in Turkish)

Okay AI, Şahintürk Ö (1997) Geology of the Eastern Pontides. In: Robinson AG (ed) Regional and petroleum geology of the Black Sea and surrounding Region. Am Assoc Pet Geol Mem 68:291–310

Okay AI, Tüysüz O (1999) Tethyan sutures of northern Turkey. In: Durand B, Jolivet L, Horvath L, Serranne M (eds) The Mediterranean Basins: tertiary extension within the Alpine orogeny. Geol Soci Lond Spec Publ 156:475–515

Okay AI, Siyako M, Burkan KA (1991) Geology and tectonic evolution of the Biga Peninsula. Bull Tech Univ İstanbul 44:191–255

Okay AI, Satır M, Maluski H, Siyako M, Monie P, Metzger R, Akyüz S, Yin A (1996) Paleo- and Neo-Tethyan events in Northwestern Turkey: geologic and geochronologic constraints. In: Harrison M (ed) Tectonics of Asia. Cambridge University Press, Cambridge, MA, pp 420–441

Önal A, Boztuğ D, Kürüm S, Harlavan Y, Arehart GB, Arslan M (2005) K–Ar age determination, whole-rock and oxygen isotope geochemistry of the postcollisional Bizmişen and Çaltı plutons, SW Erzincan, Eastern Central Anatolia, Turkey. Geol J 40:457–476

Orgun Y, Gultekin AH, Onal A (2005) Geology, mineralogy and fluid inclusion data from the Arapucan Pb-Zn-cu-ag deposit, Canakkale, Turkey. J Asian Earth Sci 25:629–642

Oygür V (1997) Anatomy of an epithermal mineralisation: Mumcu (Balıkesir-Sındırgı), inner-Western Anatolia, Turkey. Bull Mineral Res Exp 119:29–39

Oyman T, Minareci F, Piskin O (2003) Efemcukuru B-rich epithermal gold deposit (İzmir, Turkey). Ore Geol Rev 23:35–53

Oyman T, Ciabonu CL, Cook NJ, Danyushevsky L (2010) The Efemçukuru gold deposit, western Turkey: petrography and invisible gold in arsenian pyrite. IAGOD Symposium 2010, Giant Ore Deposits Down-Under, Adelaide- Australia

Özdemir S (2011) Çanakkale-Balcılar polimetal Cevherleşmesi Oluşumunun incelenmesi. Master's Thesis, Ankara University, pp 110 (unpublished)

Özen Y, Arık F (2015) S, O and Pb isotopic evidence on the origin of the İnkaya (Simav-Kütahya) Cu–Pb–Zn–(Ag) Prospect, NW Turkey. Ore Geol Rev 70:262–280

Özgenç İ, İlbeyli N (2008) Petrogenesis of the Late Cenozoic Eğrigöz pluton in western Anatolia, Turkey: implications for magma genesis and crustal processes. Int Geol Rev 50(4):375–391

Özpınar Y, Kılıç M, Avşar M, Sarı R, Küçükefe Ş, Agnerian H, Doygun Z, Yenigün K (2012) Anew assessment of the Kısacık gold mineralisation (Ayvacık-Çanakkale NW Anatolia). Rom J Earth Sci 86(2):111–116

Pals DW, Spry PG, Chryssoulis SL (2003) Invisible gold and tellurium in arsenic-rich pyrite from the Emperor gold deposit, Fiji; implications for gold distribution and deposition. Econ Geol 98:479–493

Parlak O, Karaoğlan F, Rızaoğlu T, Klötzli U, Koller F, Billor Z (2013) U–Pb and ^{40}Ar–^{39}Ar geochronology of the ophiolites and granitoids from the Tauride belt: implications for the evolution of the Inner Tauride suture. J Geodyn 65:22–37

Pasquarè G, Poli S, Vezzoli L, Zanchi A (1988) Continental arc volcanism and tectonic setting in Central Anatolia, Turkey. Tectonophysics 146:217–230

Phillips WJ (1972) Hydraulic fracturing and mineralisation. J Geol Soc Lond 128:337–359

Pirajno F (2009) Hydrothermal processes and mineral systems. Springer, Berlin, p 1250

Pourteau A, Candan O, Oberhänsli R (2010) High-pressure metasediments in central Turkey: constraints on the Neotethyan closure history. Tectonics 29:TC5004

Repstock A, Voudouris P, Kolitsch U (2015) New occurrences of watanabeite, colusite, "arsenosulvanite" and Cu-excess tetrahedrite-tennantite at the Pefka high-sulphidation epithermal deposit, northeastern Greece. Neu Jb Mineral Abh 192:135–149

Rice SP, Robertson AHF, Ustaömer T (2006) Late Cretaceous–Early Cenozoic tectonic evolution of the Eurasian active margin in the Central and Eastern Pontides, northern Turkey. Geol Soc Lond Spec Publ 260:413–445

Rice SP, Robertson AHF, Ustaömer T, İnan N, Tasli K (2009) Late Cretaceous–Early Eocene tectonic development of the Tethyan suture zone in the Erzincan area, Eastern Pontides, Turkey. Geol Mag 146:567–590

Richards JP (2015) Tectonic, magmatic, and metallogenic evolution of the Tethyan orogen: from subduction to collision. Ore Geol Rev 70:323–345

Ring U, Collins AS (2005) U-Pb SIMS dating of synkinematic granites; timing of core-complex formation in the northern Anatolide Belt of western Turkey. J Geol Soc 162(2):289–298

Robertson AHF, Parlak O, Ustaömer T (2009) Melange genesis and ophiolite emplacement related to subduction of the northern margin of the Tauride-Anatolide continent, central and western Turkey. In: Van Hinsbergen DJJ, Edwards MA, Govers R (eds) Collision and collapse at the Africa-Arabia-Eurasia subduction zone. Geol Soc Lond Spec Publ 311:9–66

Ross K (2013a) Petrographic report on the TV tower project, Turkey Pilot Gold 87 (unpublished)

Ross K (2013b) Petrographic report on samples from the TV tower project, Biga Peninsula, Turkey. Pilot Gold, Inc, p 84 (unpublished)

Şahin Demir Ç, Uçurum A (2016) Geology-mineralogy and isotope (O-D, S, Cu and Ar/Ar) geochemistry of Sisorta high sulphidation epithermal gold deposit (Koyulhisar-Sivas). Geol Bull Turk 59(1):87–114 (In Turkish with English abstract)

Scott S, Barnes H (1971) Sphalerite geothermometry and geobarometry. Econ Geol 66:653–669

Şener AK, Menteş B, Sarı R, Saygılı A, Tufan V (2006a) Geological synthesis of epithermal gold deposits in the Sındırgı district, Balıkesir Province, Western Turkey. In: Cook NJ, Özgenç İ, Oyman T (eds) Au-Ag-Te-Se deposits. Proceedings of 2006 Workshop of IGCP-486, İzmir, Turkey, pp 148–153

Şener AK, Tufan V, Sarı R, Kaplan EH (2006b) Sındırgı Gold Project. Galata Madencilik, Turkey Company Unpublished Report, pp 1–20

Şengör AMC (1979) The North Anatolian transform fault: its age, offset and tectonic significance. J Geol Soc Am 136:269–282

Şengör AMC, Yılmaz Y (1981) Tethyan evolution of Turkey: a plate tectonic approach. Tectonophysics 75:181–241

Şengör AMC, Satır M, Akkok R (1984) Timing of tectonic events in the Menderes Massif, western Turkey: implications for tectonic evolution and evidence for pan-African basement in Turkey. Tectonics 3:693–707

Sha P (1993) Geochemistry and genesis of sediment-hosted disseminated gold mineralisation at the Gold Quarry mine, Nevada. PhD thesis, University of Alabama, Tuscaloosa

Sharp ZD (1990) A laser-based microanalytical method for the in situ determination of oxygen isotope ratios of silicates and oxides. Geochim Cosmochim Acta 54:1353–1357

Shikazono W (1974) Physicochemical environment and mechanism of volcanic hydrothermal ore deposition in Japan, with special reference to oxygen fugacity. Univ Tokyo Fac Sci J 19:27–56

Shikazono W (2003) Geochemical and tectonic evolution of arc-backarc hydrothermal systems: implication for the origin of Kuroko and epithermal vein-type mineralisations and the global geochemical cycle, Developments in Geochemistry, 8. Elsevier, London

Sillitoe RH (1985) Ore-related breccias in volcanoplutonic arcs. Econ Geol 80:1467–1514

Sillitoe RH (2012) Copper provinces. Soc Econ Geol Spec Publ 16:1–18

Sillitoe RH, Hedenquist JW (2003) Linkages between volcanotectonic settings, ore-fluid compositions, and epithermal precious-metal deposits. In: Simmons SF, Graham IJ (eds) Volcanic, geothermal, and ore-forming fluids: rulers and witnesses of processes within the earth. Soc Econ Geol Spec Publ 10:315–343

Simmons SF, Christenson BW (1994) Origins of calcite in a boiling geothermal system. Am J Sci 294:361–400

Simon G, Kesler SE, Chryssoulis SL (1999) Geochemistry and textures of gold-bearing arsenian pyrite, Twin Creeks, Nevada; implications for deposition of gold in Carlin-type deposits. Econ Geol 94:405–421

Siyako M, Burkan KA, Okay AI (1989) Tertiary geology and hydrocarbon potential of the Biga and Gelibolu Peninsula. TAPG Bull 1–3:183–199

Smith MT, Lepore WA, İncekaraoğlu T, Shabestari P, Boran H, Raabe K (2014) Küçükdağ: a new, high sulphidation epithermal Au-Ag-Cu deposit at the TV Tower property in Western Turkey. Econ Geol 109:1501–1511

Sung YH, Brugger J, Ciobanu CL, Pring A, Skinner W, Nugus M (2009) Invisible gold in arsenian pyrite and arsenopyrite from a multistage Archaean gold deposit: Sunrise Dam, Eastern Goldfields Province, Western Australia. Mineral Depos 44:765–791

Taner MF (1977) Etude géologique et pétrographique de la région de Güneyce-İkizdere, située au sud de Rize (Pontides orientales, Turquie). PhD thesis, Université de Geneve (unpublished)

Taylor HP (1979) Oxygen and hydrogen isotope relationships in hydrothermal mineral deposits. In: Barnes HL (ed) Geochemistry of hydrothermal ore deposits, 2nd edn. Wiley, New York, pp 236–277

Taylor R (2009) Ore textures: recognition and interpretation. Springer-Verlag, Berlin, p 287

Tezer EB (2006) Balıkesir–Ayvalık İlçesi Kubaşlar Altın Oluşumunun Maden Jeolojisi. [Ore geology of the Kubaşlar (Balıkesir-Ayvalık) gold formation]. Master's thesis, Ankara University (In Turkish, unpublished), p 70

Thomas H, Large R, Bull SW, Maslennikov V, Berry RF, Fraser R, Froud S, Moye R (2011) Pyrite and pyrrhotite texture and composition in sediments, laminated quartz veins, and reefs at Bendigo Gold Mine, Australia: insight for ore genesis. Econ Geol 106:1–31

Thomson SN, Ring U (2006) Thermochronologic evaluation of postcollision extension in the Anatolide Orogen, western Turkey. Tectonics 25:TC3005

Toprak V (1998) Vent distribution and its relation to regional tectonics, Capadocian Volcanics, Turkey. J Volcanol Geotherm Res 85:67–77

Toprak V, Göncüoğlu MC (1993) Keçiboyduran-Melendiz Fayı ve bölgesel anlamı (Orta Anadolu). [Keçiboyduran-Melendiz Fault (Central Anatolia) and its regional geological significance]. Haçet Univ Yerbilimleri 16:55–65 (in Turkish)

Topuz G, Altherr R, Kalt A, Satır M, Werner O, Schwarz WH (2004) Aluminous granulites from the Pulur complex, NE Turkey: a case of partial melting, efficient melt extraction and crystallisation. Lithos 72:183–207

Topuz G, Altherr R, Schwarz WH, Siebel W, Satır M, Dokuz A (2005) Post-collisional plutonizm with adakite-like signatures: the Eocene Saraycık granodiorite (Eastern Pontides, Turkey). Contrib Mineral Petrol 150:441–455

Topuz G, Altherr R, Schwarz WH, Dokuz A, Meyer HP (2007) Variscan amphibolite-facies rocks from the Kurtog˘lu metamorphic complex. Gümüşhane area, Eastern Pontides, Turkey. Int J Earth Sci 96:861–873

Topuz G, Altherr R, Siebel W, Schwarz WH, Zack T, Hasözbek A, Barth M, Satır M, Şen C (2010) Carboniferous high-potassium I-type granitoid magmatism in the Eastern Pontides: the Gümüşhane pluton (NE Turkey). Lithos 116:92–110

Topuz G, Okay AI, Altherr R, Schwarz WH, Siebel W, Zack T, Satır M, Şen C (2011) Post-collisional adakite-like magmatism in the Ağvanis Massif and implications for the evolution of the Eocene magmatism in the Eastern Pontides (NE Turkey). Lithos 125:131–150

Türeli TK (1991) Geology, petrography and geochemistry of Ekecikdağ plutonic rocks (Aksaray region – Central Anatolia). PhD thesis, (Unpublished) Middle Eastern Technical University (METU), Ankara, p 194

Tüysüz O, Dellaloğlu AA, Terzioğlu N (1995) A magmatic belt within the Neo-Tethyan suture zone and its role in the tectonic evolution of northern Turkey. Tectonophysics 243(1–2):173–191

Ünal E (2010) Genetic investigation and comparison of Kartaldağ and Madendağ epithermal gold mineralisation in Çanakkale-region. Master's thesis, Middle East Technical University (Unpublished), p 181

Ünal-İmer E, Güleç N, Kuşcu İ, Fallick AE (2013) Genetic investigation and comparison of Kartaldağ and Madendağ epithermal gold deposits in Çanakkale, NW Turkey. Ore Geol Rev 53:204–222

Ustaömer T, Robertson AFH (1997) Tectonic-sedimentary evolution of the north Tethyan margin in the Central Pontides of northern Turkey. In: Robinson AG (ed) Regional and petroleum geology of the Black Sea and surrounding Region. Mem Am Assoc Pet Geol 68:255–290

Ustaömer T, Robertson AFH (2010) Late Palaeozoic–early Cenozoic tectonic development of the Eastern Pontides (Artvin area), Turkey: stages of closure of Tethys along the southern margin of Eurasia. Geol Soc Lond Spec Publ 340:281–327

Van Hinsbergen DJJ, Maffione M, Plunder A, Kaymakcı N, Ganerød M, Hendriks BWH, Corfu F, Gürer D, de Gelder GINO, Peter K, PcPhee PJ, Brouwer FM, Advokaat El Vissers RLM (2016) Tectonic evolution and paleogeography of the Kırşehir Block and the Central Anatolian Ophiolites, Turkey. Tectonics 35:983–1014

Vural A (2006) Bayramiç (Çanakkale) ve çevresinin altın zenginleşmelerinin araştırılması. [Investigation of gold enrichments in Bayramiç (Çanakkale) and its surroundings]. PhD thesis, Ankara University, p 267 (In Turkish, unpublished)

Watanabe M, Soeda A (1981) Distribution of polytype contents of molybdenite from Japan and possible controlling factor in polytypism. Neues Jb Mineral Abh 141:258–279

Wells JD, Mullens TE (1973) Gold-bearing arsenian pyrite determined by microprobe analysis, Cortez and Carlin Gold mines, Nevada. Econ Geol 68:187–201

White NC, Hedenquist JW (1990) Epithermal environments and styles of mineralisation: variations and their causes, and guidelines for exploration. In: Hedenquist JW, White NC, Siddeley G (eds) Epithermal gold mineralisation of the circum-pacific: geology, geochemistry, origin and exploration. J Geochem Explor 36:445–474

Whitney DL, Dilek Y (1998) Metamorphism during Alpine crustal thickening and extension of Central Anatolia, Turkey: the Niğde Massif core complex. J Petrol 39:1385–1403

Whitney DL, Hamilton MA (2004) Timing of high-grade metamorphism in central Turkey and the assembly of Anatolia. J Geol Soc 161:823–828

Whitney DL, Teyssier C, Dilek Y, Fayon AK (2001) Metamorphism of the Central Anatolian Crystalline Complex, Turkey: influence of orogen-normal collision vs. wrench dominated tectonics on P–T–t paths. J Met Geol 19:411–432

Whitney DL, Teyssier C, Fayon AK, Hamilton MA, Heizler M (2003) Tectonic controls on metamorphism, partial melting, and intrusion: timing and duration of regional metamorphism and magmatism in the Niğde Massif, Turkey. Tectonophysics 376:37–60

Winderbaum L, Ciobanu CL, Cook NJ, Paul M, Metcalfe A, Gilbert S (2012) Multivariate analysis of an LA-ICP-MS trace element dataset for pyrite. Math Geosci 44:823–842

Yalçınkaya N (2010) Koru Köyü (Lapseki-Çanakkale) Pb-Zn-Ag Yatağının, Jeolojik, Mineralojik ve Jeokimyasal İncelenmesi. [Geological, Mineralogical and Geochemical Investigation of the Koru (Lapseki-Çanakkale) Pb-Zn-Ag Deposit]. Master's thesis, Çanakkale Onsekiz Mart University, p 181 (In Turkish, unpublished)

Yavuz H (2013) Kaymaz (Eskişehir) Listvenitik Altın Yatağı'nın Özellikleri ve Kökenine Bir Yaklaşım [Properties of Kaymaz listvenitic gold deposit and an approach to genesis of Kaymaz (Eskişehir) gold deposit genesis]. MSc thesis, Dokuz Eylül University, İzmir, Turkey, p 110 (In Turkish, unpublished)

Ye L, Cook NJ, Ciobanu CL, Liu YP, Zhang Q, Liu TG, Gao W, Yang YL, Danyushevskiy L (2011) Trace and minor elements in sphalerite from base metal deposits in South China: a LA-ICPMS study. Ore Geol Rev 39:188–217

Yiğit O (2009) Mineral deposits of Turkey in relation to Tethyan metallogeny: implications for future mineral exploration. Econ Geol 104:19–51

Yiğit O (2012) A prospective sector in the Tethyan Metallogenic Belt: geology and geochronology of mineral deposits in the Biga Peninsula, NW Turkey. Ore Geol Rev 46:118–148

Yılmaz H (1992) Turkey Regional Project. EuroGold, Unpublished company report, p 1–20

Yılmaz S, Boztuğ D (1996) Space and time relations of three plutonic phases in the Eastern Pontides, Turkey. Int Geol Rev 38:935–956

Yılmaz Y, Tüysüz O, Yiğitbaş E, Genç SC, Şengör AMC (1997) Geology and tectonics of the Pontides. In: Robinson AG (eds) Regional and petroleum geology of the Black Sea and surrounding region. Am Assoc Pet Geol Memoir 68:183–226

Yılmaz A, Adamia S, Chabukiani A, Chkhotua T, Erdoğan K, Tuzcu S, Karabıyıkoğlu M (2000) Structural correlation of the southern Transcaucasus (Georgia) –eastern Pontides (Turkey). In: Bozkurt E, Winchester JA, Piper JDA (eds) Tectonics and magmatism in Turkey and surrounding area. Geol Soc Lond Spec Publ 173:171–182

Yılmaz H, Oyman T, Arehart GB, Çolakoğlu AR, Billor Z (2007) Low-sulphidation type Au-Ag mineralisation at Bergama, İzmir, Turkey. Ore Geol Rev 32:81–124

Yılmaz H, Oyman T, Sönmez FN, Arehart GB, Billor Z (2010) Intermediate sulphidation epithermal gold-base metal deposits in tertiary subaerial volcanic rocks, Şahinli/Tespih Dere (Lapseki/Western Turkey). Ore Geol Rev 37:236–258

Yılmaz H, Sönmez FN, Akay E, Şener AK, Tufan ST (2013) Low-sulphidation epithermal Au-Ag mineralisation in the Sındırgı District, Balıkesir Province, Turkey. Turk J Earth Sci 22:485–522

Yılmaz-Şahin S (2005) Transition from arc- to post-collision extensional setting revealed by K-Ar dating and petrology: an example from the granitoids of the Eastern Pontide Igneous Terrane, Araklı-Trabzon, NE Turkey. Geol J 40:425–440

Young ED, Coutts DW, Kapitan D (1998) UV laser ablation and irm-GCMS microanalysis of $^{18}O/^{16}O$ and $^{17}O/^{16}O$ with application to calcium-alluminium-rich inclusion from Allende meteorite. Geochim Cosmochim Acta 62:3161–3168

Zhao HX, Frimmel HE, Jiang SY, Dai BZ (2011) LA-ICP-MS trace element analysis of pyrite from the Xiaoqinling gold district, China: implications for ore genesis. Ore Geol Rev 43:142–153

Zheng Y, Zhang L, Chen Y, Hollings P, Chen H (2013) Metamorphosed Pb–Zn–(Ag) ores of the Keketale VMS deposit, NW China: evidence from ore textures, fluid inclusions, geochronology and pyrite compositions. Ore Geol Rev 54:167–180

Zhu Y, An F, Tan J (2011) Geochemistry of hydrothermal gold deposits: a review. Geosci Front 2(3):367–374